DRAFT

NOAA Technical Memorandum NOS ORCA-65

ALOHA™ (Areal Locations of Hazardous Atmospheres) 5.0
THEORETICAL DESCRIPTION

R. Michael Reynolds

Seattle, Washington 98115
August 1992

noaa NATIONAL OCEANIC AND ATMOSPHERIC ADMINISTRATION

DRAFT

NOTICE

Mention of a commercial company or product does not constitute an endorsement by the Hazardous Materials Response and Assessment Division, NOAA. Use of information from this publication concerning proprietary products or the tests of such products for publicity or advertising purposes is not authorized. ALOHA™, a trademark of the U.S. government, was developed by NOAA and the U.S. Environmental Protection Agency.

Contribution No. HMRAD 92-5 from NOAA/Hazardous Materials Response and Assessment Division

EXECUTIVE SUMMARY

A complete technical description of the ALOHA 5.0 gas plume model is provided. ALOHA is designed for use on site at accidental chemical spills when evacuation information is needed rapidly. That was its original conception and it is our continuing goal. ALOHA is also useful for contingency planning. The user can create and save customized scenarios with known chemicals, storage facilities, and locale information and keep these on hand in hard copy and disk files.

A myriad of separate complex models covering aspects of gas or liquid release, evaporation, and dispersion, including the special case of heavier-than-air gases is unified into a single, user-friendly computer presentation with the smallest number of parameterizations possible. Reducing the user input interface to the minimal set while maintaining a high degree of accuracy and usefulness is the major achievement of ALOHA.

The ALOHA air dispersion model has been compared to three similar models and to field programs. Whenever significant deviations are found, care is taken to ensure that all deviations of ALOHA's estimates from predictions made by similar models are the result of intended differences in algorithms. The model is being further verified against field data, and more complete sensitivity analyses of the model are in preparation.

Contents

List of Figures

List of Tables

Chapter 1

Introduction

1.1 ALOHA Defined

ALOHA (Areal Locations of Hazardous Atmospheres) is a computer program that takes operator and/or instrumentation input data and provides estimates of the dispersion of gas from accidental spills. The output estimates are designed for rapid user assimilation and make liberal use of graphics. The air model is approximate by necessity and its usefulness is entirely dependent on user interpretation of inputs and outputs.

ALOHA originated as an in-house tool to aid in response situations. In its original format it was based on a simple model—a continuous point source with a Gaussian plume distribution (Turner, 1970). It has evolved over the years into a tool used for a wide range of response, planning, and academic purposes. It is distributed worldwide to thousands of users in government and industry (in the USA by the National Safety Council). ALOHA is a tool that can be used during emergency situations and, as such, must meet certain criteria:

- **Operates on common computers.** The model must run quickly on small computers (PC or Macintosh) which are transportable and affordable for most users. The algorithms and physics represent a compromise between accuracy and speed so that good results are available quickly enough to be of immediate use.
- **User friendly.** The program must be clear and easy to use so less experienced responders can use it during high-pressure situations with minimal chance of error.
- **Reliable.** The user interface is designed to minimize operator error. The program checks and cross-checks all entries before proceeding to solutions. Any detected or suspected misapplications are announced and if input error is not physically possible or is improbable, the program demands correction.

ALOHA 5.0 is a significant improvement to the ALOHA package. It is a time-dependent model that treats neutral or heavy gases and a variety of time-dependent sources including broken pipes, leaking tanks, and evaporating puddles. It incorporates modern theories of evaporation, non-boiling or boiling, from puddles which can change in size depending on a balance between the evaporation rate and the rate of material entering the puddle.

A very important advancement made by ALOHA 5.0 (over previous versions) is the ability to model the dispersion of heavy gases which form collapsing clouds and spread by gravitational

forces as they are dispersed by wind and atmospheric turbulence. Heavier-than-air gas dispersion is a complex interaction of atmospheric turbulence, entrainment, advection, and gravitational spreading.

1.2 About This Document

This report summarizes the technical background on which ALOHA 5.0 is based. It is not an exhaustive review of the theory of atmospheric diffusion, although selected classical references are cited. The discussion concentrates only on the physical descriptions and theory related to ALOHA. Equations are presented as they are used in the software code. Details of menu structure, data entry, and programming are covered elsewhere. For detailed information on the use of ALOHA see the user manual (NOAA et al., 1990a).

1.3 What ALOHA 5.0 Does and Does Not Do

ALOHA 5.0 has the following attributes:

- **Rapid deployment.** It provides a first-response user with an additional tool for describing the behavior of a chemical gas in the event of an accidental release.
- **Quality Control.** Significant effort has been put into checking user inputs for reasonableness and for providing guidance on how to select input correctly. Numerous warnings and help messages appear on the screen throughout the model.
- **Useable accuracy.** Even though approximations are necessary, every effort is made to ensure that the result is as accurate as possible. When compared to the results from sophisticated, specialized models or field measurements, ALOHA generally will deviate in a conservative direction, (i.e. predict higher concentrations and larger affected areas).
- **Contingency planning.** ALOHA 5.0 can be used for site characterization of industrial settings. Dimensions of permanent tanks, pipes, and other fixtures can be described and saved as text or ALOHA-runnable files. Different accident scenarios can then be played to derive worst-case possibilities.
- **Neutral or heavy gas models.** ALOHA 5.0 is able to model heavy gases and neutral gases.
- **Pressurized and refrigerated tank releases.** ALOHA 5.0 will model the emission of gas from pressurized tanks or refrigerated tanks with liquified gases. Flashing (sudden change from liquid to gas inside the tank), choked flow (blocking of the gas in an exit nozzle), and pooling of the cryogenic liquid are considered.

ALOHA must be compact and fast and, as a result, cannot do everything. The emergency scene first responder is the target audience of ALOHA and hence the model does not address regional and/or air quality issues. The following is a list of the major limitations that presently exist in ALOHA 5.0.

- **Topography.** Topographic effects and mesoscale weather are not included in the model. The earth is assumed to be flat and the mean wind speed and direction are assumed to be constant everywhere.

- **Radioactivity.** ALOHA 5.0 is not suitable for radioactive emissions.

- **Buoyant gases.** Gases from a burning source have an initial positive buoyancy which is not explicitly handled by ALOHA 5.0. Care must be used when applying ALOHA to burning sources or stack gas emissions. One should expect significant differences between the plume's behavior from ground-level sources and its behavior from elevated sources as was reported by Smith (1984) and Fox (1984).

- **Low-level background.** ALOHA 5.0 is not intended to treat chronic, low-level (fugitive) emissions. The maximum duration of a source release in ALOHA 5.0 is one hour.

- **Near-field.** ALOHA does not consider the near-field region, including the effects of momentum jets. Considerable information on eddy size and turbulent intensity is required to model this region properly. As a result, ALOHA refuses to provide plume information for distances less than approximately 10 m. If a puddle on the ground is larger than 10 m, then the plume is not drawn over the puddle. If the plume footprint is shorter than 50 m, it is not displayed.

- **Liquids in pipes.** Only pressurized gases in pipes are covered by the current version of ALOHA.

1.4 ALOHA 5.0 Input

To be of maximum use, ALOHA requires a minimal amount of information which the user can enter easily with the help of an extensive graphical interface.

The setup of ALOHA 5.0 proceeds along the following lines:

1. **Geographic location and time.** Location is used to calculate incoming solar radiation, and elevation is used to calculate ambient air pressure. Time can be either manually specified or taken from the computer's internal clock.

2. **Site Definition.** Information about a particular building of interest (location relative to the plume, number of stories, air exchange rate, surroundings) is used to predict indoor concentrations and doses.

3. **Chemical Definition.** Chemical selection (Sec. 1.5) determines all physical and chemical properties of the material under study. The chemical selection is a major part of the ALOHA software. Users can operate ALOHA from the larger CAMEO™ software after a chemical has been selected or they can use ALOHA independently. In either case, ALOHA uses information in its resident library. Users may modify the library by adding new chemicals or additional property information for existing chemicals. Chemical selection is discussed in detail in the user manual (NOAA, 1990b) and is outlined in Sec. 1.5 below.

4. **Atmospheric Data.** The atmospheric parameters of interest to ALOHA 5.0 are (a) stability class, (b) inversion height, (c) wind speed, (d) wind direction, (e) air temperature, (f) ground roughness, (g) cloudiness, and (h) humidity. If a SAM (Station for Atmospheric Measurements) is connected, then wind speed, wind direction, standard deviation of wind direction (and thus stability class), and air temperature are updated automatically in real time.

5. **Source Definition.** The source can be one of the following types:

   (a) **Direct.** The proposed source is defined as a point release with the following parameters: (a) release type: a continuous or instantaneous release, (b) release amount: either release rate if it is continuous or the size of release (mass[1] or volume) if it is instantaneous, and (c) source height (permitted only for neutral gases).

   (b) **Puddle.** If the spill is a puddle of evaporating liquid on the ground, the required data are: (a) puddle area, (b) puddle volume (or depth or mass), (c) ground temperature (air temperature is the default value if ground temperature is unknown), (d) ground type, and (e) puddle temperature.

   (c) **Tank.** Product in a tank may be a gas, a liquid, or a liquified gas. If it is a liquefied gas, it can be either compressed at ambient temperature or cooled at ambient pressure. The latter case is called cryogenic. Liquefied gases may change state in the tank as pressure drops, on exit from the tank by forming an aerosol spray, or by boiling on the ground. All three cases might occur during one accident. If the flow rate out of the tank exceeds puddle evaporation rate, the puddle will grow in area. In the case of a pressurized liquid release, flow may be entirely a gas or aerosol, with no puddle formed (ALOHA's concept of two-phase flow).

   The parameters required for a tank solution are (a) tank shape (cylinder, or sphere), (b) tank dimensions, (c) hole shape and size, (d) hole location, (e) amount of contents in the tank, and if the tank contents are a gas (f) internal gas pressure.

   (d) **Pipe.** ALOHA treats only cases of gas pipeline releases. Pipes may be very long, connected to a very large source, or of finite length and unconnected to a source. Users must enter information about (a) pipe length, (b) diameter, (c) pressure, (d) temperature, and (e) must indicate whether the inner pipe surface is rough or smooth.

6. **Computation Type.** ALOHA 5.0 will compute atmospheric gas dispersion in one of two user-selected methods. ALOHA will determine which method to use based on the chemical and volume spilled, or the user may select the most appropriate method.

   (a) **Neutral Gas.** This is the standard of a passive contaminant that does not alter the dynamic behavior of the air.

   (b) **Heavy Gas.** If a pollutant that is more dense than the air is released at ground level, it will spread under the influence of gravity as it is advected and dispersed by the atmospheric turbulence.

[1] In the input display, "mass" and "weight" are used interchangeably according to user familiarity. Thus weight in pounds and mass in kilograms are called "mass" in the menus. ALOHA keeps track of these and converts all input to mass in kilograms for internal computations.

1.5 The ALOHA Chemical Database

The rate at which a substance is released into the air and its subsequent airborne transport depend on a number of physical properties specific to that substance. The physical properties required to compute release rates and trajectories for approximately 700 pure chemical substances are included in the data file, ChemLib (Table 1.1). For about half the chemicals, only the minimum number of properties needed to compute direct releases of neutrally buoyant gases are included in the database. However, property values for chemicals present in the database as well as for those not present can be modified or added to the database using the ChemManager application.

Table 1.1: Chemical properties included in the ALOHA database that are currently used in ALOHA computations, along with the sources of these data. The last five properties listed are described by formula in the DIPPR database; the ALOHA database contains the code for the DIPPR database formula, minimum and maximum temperatures for which the formula is valid, and the coefficients in the formula.

Chemical name	CAMEO
NOAA number†	CAMEO
CAS Registry number	CAMEO
IDLH value	CAMEO
TLV value	CAMEO
Molecular weight	CAMEO
Critical temperature	DIPPR
Critical pressure	DIPPR
Critical volume	DIPPR
Freezing point	DIPPR
Normal boiling point	DIPPR
Vapor pressure	CAMEO
Reference temperature for vapor pressure	CAMEO
Density of the liquid phase	DIPPR
Vapor pressure	DIPPR
Heat of vaporization	DIPPR
Heat capacity (constant pressure) of the liquid phase	DIPPR
Heat capacity (constant pressure) of the vapor phase	DIPPR

† The NOAA number is a unique number assigned to each substance by the developers of CAMEO.

Only pure chemical substances (no mixtures or solutions) are included in the database. The chemicals are a subset of the substances found in the CAMEO 3.0 chemical database (NOAA, 1990b) which, in turn, includes the substances found in (i) *Chemical Hazard Response Information System* (CHRIS) (U.S. Coast Guard, 1985), (ii) Emergency Response Guide Book (U.S. Dept. of Transportation, 1984), (iii) Chemical Profiles (EPA, 1986), and (iv) Emergency Handling of Hazardous Materials in Surface Transportation (Am. Assoc. of Railroads, 1986). Substances that are not included in the ALOHA database include mixtures, chemicals with very low vapor pressures, and chemicals for which essential data were unavailable or inconsistent. It was intended that the ALOHA database include the chemicals most commonly involved in accidental releases.

The chemicals included in the ALOHA database are indexed by common names; these names are consistent with those found in CAMEO. In general, no attempt was made to index chemicals by synonyms or unique identifiers, though the Chemical Abstract Service Registry Number (CAS Number) is included in the data for each chemical. When difficulties arise,

CAMEO can be used to help the user find the appropriate chemical in the database.

Data used in the database were extracted from two sources: the CAMEO 3.0 chemical database (NOAA, 1990b), and the electronic version of Physical and Thermodynamic Properties of Pure Chemicals: Data Compilation (Daubert and Danner, 1989), a database created by the Design Institute for Physical Property Data (DIPPR). The DIPPR database contains the values for 25 properties at a single reference temperature. An additional 13 properties are described by formulas that yield the property value as a function of temperature; only some of the properties in the DIPPR database are included in the ALOHA database.

In addition, a number of data fields in the database contain no numerical data. These fields are reserved for data that are not currently used but might be used in future versions of ALOHA. In some cases the fields are reserved for properties that are also described by DIPPR formula:

> IDLH TIME, %IDLH, TLV time, TLV %, User designated LOC (level of concern), LOC units, LOC time, LOC %, Vapor density, Reference temperature for vapor density, Liquid density, Reference temperature for liquid density, Specific gravity, Reference temperature for specific gravity, Heat of formation, Reference temperature for heat of formation, Surface tension, Reference temperature for surface tension, Heat of vaporization, Reference temperature for heat of vaporization, Heat capacity at constant pressure, Reference temperature for heat capacity, Heat capacity at constant volume, Reference temperature for heat capacity, Kinematic viscosity of liquid phase, Reference temperature for kinematic viscosity of liquid phase, Kinematic viscosity of vapor phase, Reference temperature for kinematic viscosity of vapor phase, Molecular gas diffusivity, Reference temperature for molecular gas diffusivity, Thermal Diffusivity, Reference temperature for thermal diffusivity.

1.6 ALOHA Output

ALOHA provides five different output "windows." The windows can be arranged as tiles or stacks typical of the Macintosh computer[2] Output windows can be clipped and pasted into documents or they may be saved for later reference. The user manual (NOAA, 1990) provides complete information on the setup and manipulation of the output windows.

ALOHA 5.0 offers the following output options:

- **Text summary.** The text summary is a recap of the setup information and chemical properties based on input information. Source strength and dispersion information are also summarized in this window once computations have been made.

- **Dispersion footprint.** The footprint is a plan view of the area in which the concentration exceeds a specified "level of concern." Often called the "dead canary footprint" after the practice of using a canary in a cage as an indicator of poisonous gases in mines, the footprint covers the area on which the concentration exceeds the prescribed concentration level at any time within the hour following initiation of a release.

  A dashed line which surrounds the footprint defines the possible error in footprint direction due to inability to adjust for changes in wind direction. The dashed line area will vary depending on the selected atmospheric stability. (These lines are sometimes called the "ladybug lines.")

[2]Versions of ALOHA and CAMEO that operate on DOS computers in the Windows™ environment are in the final stages of development.

- **Concentration vs. time.** This plot tells the user the amount of chemical present at a specific location. Two curves are drawn in this plot. The first curve represents the concentration of chemical in the air outside the building. The second curve represents the concentrations inside the building as described in Chapter 5. The graph is drawn only for the first sixty minutes after the start of the release.

- **Dose vs. time.** This plot shows the accumulated amount of chemical to which a person at the spot might be exposed. The dose graph has two curves for outside and inside conditions as for concentration plots. Like the concentration graph, it displays the dose accumulated during the hour after the start of the release.

- **Source strength vs. time.** This plot tells how rapidly the chemical is being released to the atmosphere. For an instantaneous spill, ALOHA assumes all the chemical is released in the first minute of the release. For time-dependent sources (also called "unsteady" and "variable" sources), the source plots will show one to five different release levels.

1.7 Dose and Exposure

The definition of these basic terms is not well founded (Singh et al., 1989; Wilson, 1991). Most scientists agree that **exposure** is the measurement of contaminant in ambient air and it is the product of concentration and time. (And thus the quantity of exposure depends on the units used.) **Dose** is defined as the accumulated amount of chemical that actually reaches the body or target organisms within the body. ALOHA uses the following equation for dose:

$$D = \int_0^t c(t')^n \, dt' \tag{1.1}$$

where D is the dose, $c(t)$ is the concentration at the location of the observer, which could be inside or outside a structure, t is the current time since the beginning of the spill, and n is an exponent that can be adjusted for different chemicals and organisms. As an example, Singh, et al. (1989) define **fatality risk** for exposure to a constant chlorine concentration, c as $c^{2.75}t$ where c is expressed in units of mg m^{-3} and t in min.

From the discussion above, exposure is the dose from (1.1) with n set to one. ALOHA allows the user to adjust n to any desired value, but it is recommended that the user use $n = 1$ unless there is a specific reason for using a different value.

An example of the differences between concentration and dose is given in Figure 1.1. The value of n in this example is one, so dose and exposure are identical. Note that the units of dose are written as (ppm, min) representing the chosen units for concentration and time.

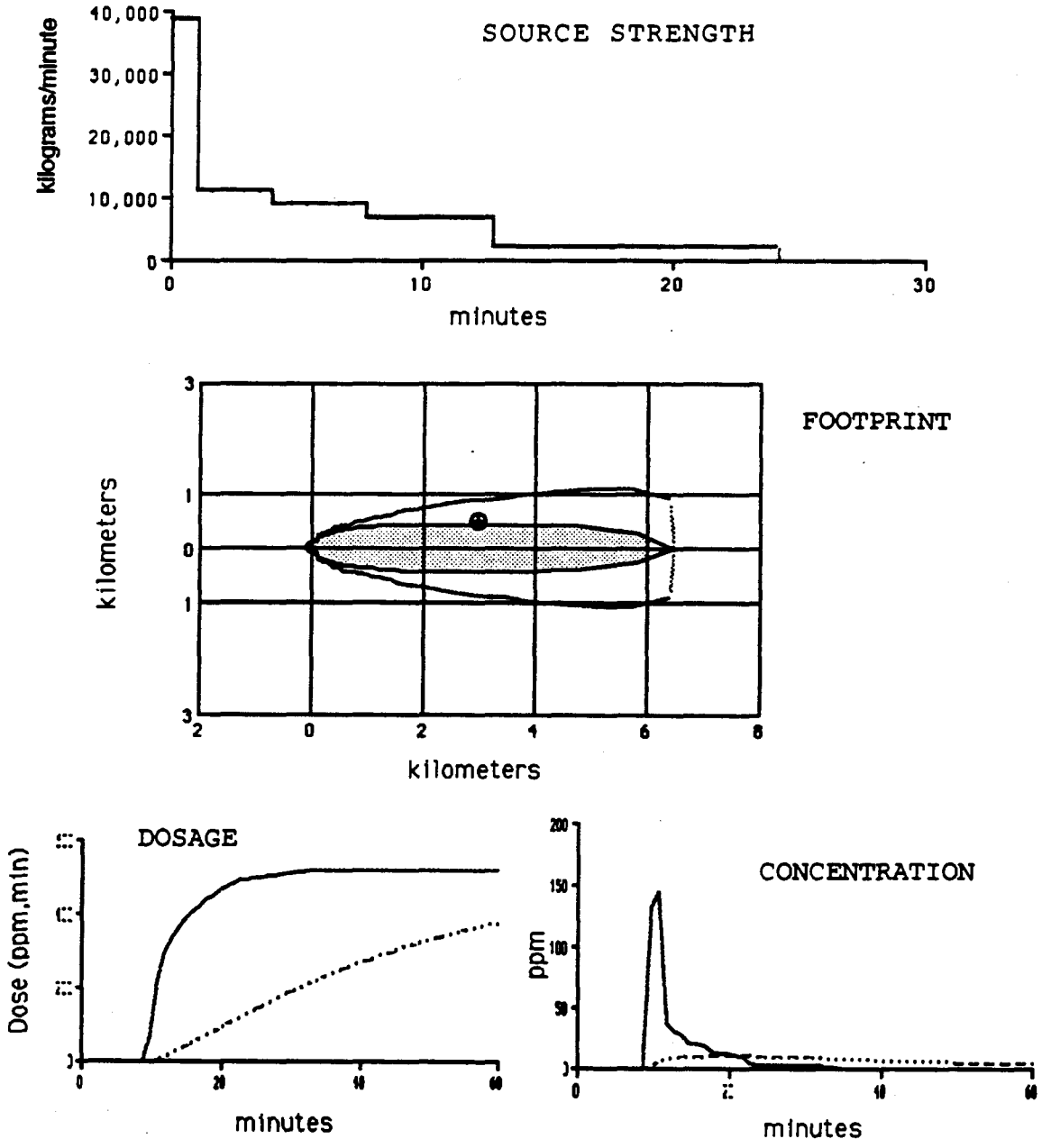

Figure 1.1: Examples of ALOHA 5.0 output products for the case of a spill of liquid anhydrous ammonia. The terms "dosage" and "dose" are identical. The text description of the scenario is given in Figure 1.2 below.

SITE DATA INFORMATION:
Location: SEATTLE, WASHINGTON
Building Air Exchanges Per Hour: 1.67 (Sheltered single storied)
Date & Time: Using internal Macintosh clock

CHEMICAL INFORMATION:
Chemical Name: AMMONIA, ANHYDROUS Molecular Weight: 17.03 kg/kmol
TLV-TWA: 25.00 ppm IDLH: 500.00 ppm
Footprint Level of Concern: 500 ppm
Boiling Point: -33.43° Celsius
Vapor Pressure at Ambient Temperature: greater than 1 atm
Ambient Saturation Concentration: 1,000,000 ppm or 100.0%

ATMOSPHERIC INFORMATION:(MANUAL INPUT OF DATA)
Wind: 10 meters/sec from 125° true No Inversion Height
Stability Class: D Air Temperature: 20° Celsius
Relative Humidity: 75% Ground Roughness: Open country
Cloud Cover: 3 tenths

SOURCE STRENGTH INFORMATION:
Liquid leak from hole in vertical cylindrical tank selected
Tank Diameter: 10 meters Tank Length: 5 meters
Tank Volume: 393 cubic meters
Internal Temperature: 20° Celsius
Chemical Mass in Tank: 501,262 pounds Tank is 95% full
Circular Opening Diameter: 30 centimeters
Opening is 1.10 meters from tank bottom
Release Duration: 24 minutes
Max Computed Release Rate: 79,100 kilograms/min
Max Average Sustained Release Rate: 38,700 kilograms/min
(averaged over a minute or more)
Total Amount Released: 171,000 kilograms
Note: The release was a two phase flow.

FOOTPRINT INFORMATION:
Model Run: Heavy Gas
User specified LOC: equals IDLH (500 ppm)
Max Threat Zone for LOC: 6.5 kilometers
For more detailed information check the Time Dependent
Conc/Dose information at specific locations.

TIME DEPENDENT INFORMATION:
Concentration/Dose Estimates at the point:
Downwind: 3.0 kilometers
Off Centerline: 500 meters
Max Concentration:
Outdoor: 144 ppm
Indoor: 10.4 ppm
Max Dose:
Outdoor: 517 (ppm,min)
Indoor: 375 (ppm,min)
Note: Indoor graphs are shown with a dotted line.

Figure 1.2: Examples of ALOHA 5.0 output text summary for the example spill of anhydrous ammonia. (The screen layout might vary for different applications.)

Chapter 2

Source Algorithms

2.1 General Comments

ALOHA 5.0 allows the user a choice of several accident scenarios, then uses an appropriate source algorithm to inject material into the air over a limited time. The source emission time may vary between limits of one minute to one hour. A flat, homogeneous earth is assumed. For purposes of solar radiation and day/night decisions, time is fixed at the moment the leak begins.

ALOHA 5.0 provides for the following source options (Figure 2.1):

- **Direct.** The user selects this option when dealing with an (a) instantaneous or (b) continuous release of material from a point source.
- **Puddle.** This option is selected when the source is a liquid puddle of constant radius. The liquid can be either (a) normal evaporating liquid, or (b) boiling (includes cryogenic LNG).
- **Tank.** This option is selected when the source is a horizontal or vertical cylinder, or a spherical tank at ground level with a single hole[1]. The tank initially contains a gas, a liquid, or a liquefied gas. The contents can change phase as a result of temperature and/or pressure changes.
- **Pipe.** This option is selected when the source is a pressurized pipe containing gas with a single hole at ground level.

2.2 Direct

Direct injection of a gas is the simplest of all algorithms, and the most hypothetical. The direct source is a point release and can be either a continuous emission of rate Q ($\mathrm{kg\,s^{-1}}$) or an instantaneous release of total mass, M (kg).

The following data must be provided for a direct release: (a) type: instantaneous or continuous release, (b) total mass, M, or the mass flow rate, Q, and (c) source height.

[1]For tanks and pipes the hole height is assumed to be close enough to the ground that for dispersion algorithms, ground-release equations apply.

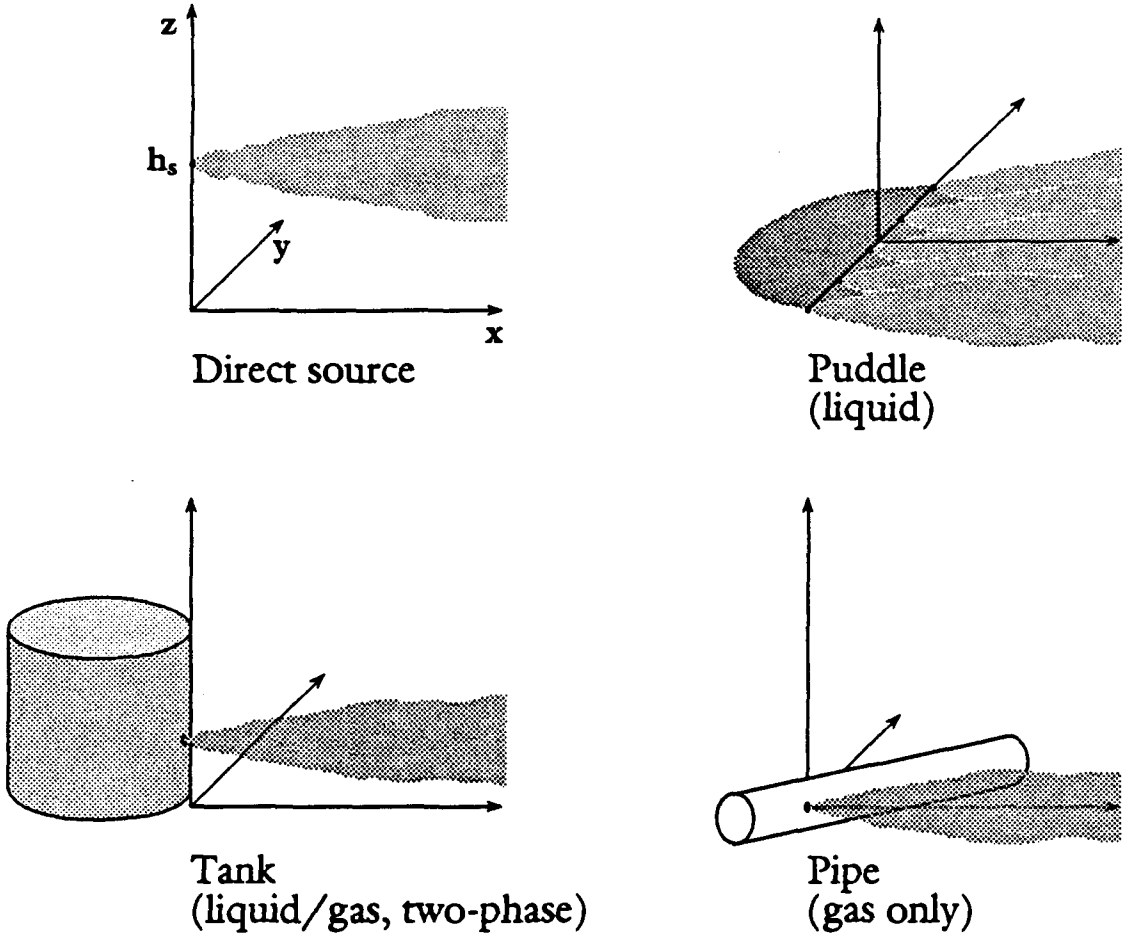

Figure 2.1: Four different types of sources in ALOHA 5.0. (a) Direct: a continuous or instantaneous gas source is injected at height h_s. (b) An evaporating puddle (approximated as a five-element line source) occurs at ground level when liquid is spilled onto the ground faster than it evaporates (or boils off). (c) A tank can emit gas, liquid, or aerosol spray. (d) A pipe: ALOHA treats only cases of pressurized gas.

The direct input is the only ALOHA option that allows the release height to be above the ground level. If the Gaussian dispersion model is selected (Chapter 3) and $h_s > 0$, then the reflection equations (3.4) and (3.5) account for the non-zero source height.

In the case of an instantaneous release of gas, the entire release is assumed to have occurred uniformly over over the smallest ALOHA time period. If M is the total mass released, then the release rate is given by

$$Q(t) = \begin{cases} M/\delta t & 0 < t < \delta t \\ 0 & \text{otherwise} \end{cases} \tag{2.1}$$

where δt is the ALOHA minimum time step, 1 minute. In the continuous case, Q is constant for one hour.

2.3 Puddle

With the "Puddle" option, we model evaporation from an instantaneously formed liquid puddle of fixed radius, r_p. The puddle temperature can change, but its radius is constant. As evaporation removes material the puddle only grows thinner. The "Tank" option (Sec. 2.4) allows material to spill into the puddle, and in this case the puddle radius may increase.

ALOHA 5.0 asks the user to specify details about the puddle then, depending on whether or not the puddle is boiling, selects the correct algorithm to compute gas evaporation rate. Input parameters are:

1. **Puddle area.** The puddle area may be estimated visually. Because different analytical models assume round or square puddles to simplify the complexity of the solutions, ALOHA converts puddle area to equivalent radius or side dimension as necessary.

2. **Puddle volume.** The user must enter the volume of the puddle. Alternatively, ALOHA can compute volume from (a) mean puddle depth, or (b) mass of spilled material.

3. **Ground type.** Ground type is used for estimating the heat flux into the puddle from the ground. Ground type can be designated as concrete, sandy, moist, or a default type. The porosity of the soil is not a consideration, and ALOHA does not consider penetration of the liquid into the soil.

4. **Initial ground temperature.** The initial ground temperature is assumed to be uniform. The temperature profile changes with time as heat is transferred to/from the puddle.

5. **Initial puddle temperature.** The initial puddle temperature is assumed to be uniform throughout the puddle. The maximum allowable temperature is the boiling point of the chemical.

2.3.1 Puddle Energy Balance

The areal averaged evaporative flux from a puddle, $E(t)$, with units of ($\mathrm{kg\,m^{-2}\,s^{-1}}$), when multiplied by the area becomes the plume source term, $Q(t)$. ALOHA uses an energy balance

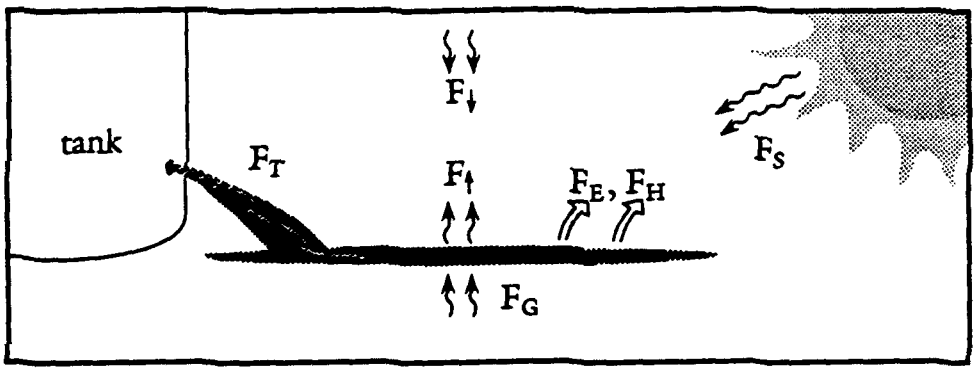

Figure 2.2: Schematic of a puddle and the different heat fluxes that contribute to the heat budget.

algorithm to compute $E(t)$:

$$\frac{du(t)}{dt} = \frac{1}{\rho_p d_p(t)} [F_S + F_\downarrow + F_\uparrow + F_G + F_H + F_E] \tag{2.2}$$

where $u(t)$ is the internal energy per unit mass, $\rho_p(t)$ is the puddle mean density, $d_p(t)$ is the puddle thickness, F_S is the net short-wave solar flux into the puddle, $F_\downarrow$ is the longwave radiation flux down from the atmosphere, $F_\uparrow(t)$ is the longwave radiation flux upwards into the atmosphere, $F_G(t)$ is the heat exchanged with the ground by molecular thermal conduction, $F_H(t)$ is the sensible heat flux from the atmosphere, and $F_E(t)$ is the heat lost from the puddle due to evaporation. The units of each term in brackets are $\mathrm{W\,m^{-2}}$. Positive values of energy signify heat transfer into the puddle. Negative values signify heat loss. Time varying terms which are re-computed on each time step are denoted by the parenthesis, (t). When a tank spills liquid into the puddle, an additional heat flux, $F_T(t)$, must be included (Sec. 2.4.2).

The heat budget method for predicting evaporation and puddle temperature has been used over the past ten or more years. Briscoe and Shaw (1980) modeled a cryogenic puddle by considering F_G to be the only important term for cryogenic liquids such as liquid natural gas (LNG). Kawamura and Mackay (1985, 1987) treated ordinary evaporating liquids and included F_S, $F_\downarrow$, $F_\uparrow$, F_H, and F_G.

Non-Boiling Liquid

At the outset of the puddle computation, the boiling point of the liquid, T_B, is compared to the initial ground temperature, $T_G(0)$. If $T_B > T_G(0)$ the liquid is non-boiling, and the evaporation rate is determined from the temperature of the puddle. The sum of all the heat fluxes will either increase or decrease the internal energy of the puddle, and the change in temperature of the puddle is proportional to the change in internal energy,

$$\frac{dT_p(t)}{dt} \approx \frac{1}{\rho_p c_{pl} d_p} \sum \text{fluxes} \tag{2.3}$$

where $T_p(t)$ is the puddle temperature, and c_{pl} is the mean specific heat of the puddle liquid. All variables are assumed to be uniform over the extent of the puddle.

In some cases with high fluxes and a chemical with a low boiling point, it is possible for the temperature of the puddle to rise until $T_p = T_B$. In this case, the liquid begins to boil and ALOHA switches to the boiling algorithm. Once a chemical begins to boil, we assume it continues to boil until either all the mass has evaporated or the time exceeds the one-hour limit.

Boiling Liquid

When T_B is less than the ground temperature, the material boils on the ground and $T_p = T_B$. The vapor pressure is equal to the atmospheric pressure, and the evaporative flux, $F_E(t)$, balances (2.3) with dT_p/dt equal to zero.

When the boiling point of the liquid is very low, as in LNG at −161°C, the liquid is termed **cryogenic** and F_G can be up to 10^4 $W\,m^{-2}$, up to two orders of magnitude greater then the other terms in (2.2). In non-cryogenic, boiling cases (e.g. butane with $T_B = -.5$°C) the other fluxes can be equally important and must be considered. ALOHA considers all heat flux terms even though some may be negligible in comparison with the ground flux.

2.3.2 Puddle Temperature and Reference Heights

The puddle **skin temperature,** $T_{skin}(x,y,t)$, the temperature of the liquid in the surface microlayer exposed to the atmosphere, determines the heat exchanges with the atmosphere. The **bulk temperature,** $T_b(x,y,t)$, is an average of the temperature over the depth of the puddle. The **puddle temperature,** $T_p(t)$, is an average temperature over the entire vertical and horizontal extent of the puddle. ALOHA assumes that the puddle is completely mixed at all times, with no horizontal variation and $T_{skin} = T_b = T_p$. In actuality, the skin and bulk temperatures are different; Kawamura and MacKay (1985, 1987) measured T_{skin} values as much as 5–6°C less than T_b.

The atmospheric profiles of wind and temperature upwind of the puddle are assumed to be stationary (not changing in time) and horizontally homogenious. For most terrains, above 2 m, the air temperature changes slowly with height (we neglect adiabatic expansion for these heights). The **standard air temperature,** T_a, is defined as the mean temperature at the **screen height** of 1–2 m. The mean wind speed, $U(z)$, has a logarithmic vertical structure. The **standard wind speed,** U_{10}, is defined to be an average wind (10–30 minute average) at a height of 10 m. ALOHA uses wind and temperature measurements at 2 m height and averages for five minutes. The errors resulting from these approximations are negligible.

2.3.3 Solar Radiation, F_S

The flux of solar shortwave radiation at the top of the atmosphere (the solar constant) is 1367 $W\,m^{-2}$. Approximately 17–20% of it is absorbed by the clear atmosphere, and clouds act to reflect and absorb it further. In a review of solar radiation measurements (Frouin et al., 1989), the maximum, ground-level, downward flux for continental and maritime situations varied from 1090 to 1130 $W\,m^{-2}$, an atmospheric transmittance of 80–83%.

ALOHA follows the formulation of Raphael (1962), and the equation for solar flux incident

on a flat level surface is

$$F_S = \begin{cases} 1111(1 - 0.0071C_I^2)\,(\sin\phi_S - 0.1) & \sin(\phi_S) > 0.1 \\ 0 & \text{otherwise} \end{cases} \tag{2.4}$$

where C_I is the cloudiness index on a scale of ($0 \leq C_I \leq 10$) and ϕ_S is the solar altitude.

ϕ_S is a function of the latitude, θ, the longitude, λ, the sun's declination angle, δ_S, the sun hour angle h_S, the hour of the day in GMT, Z, and the Julian day, J.

$$\delta_S = 23.49 \sin\left(2\pi \frac{J - 80}{365}\right) \quad \text{degrees} \tag{2.5}$$

$$h_S = 15.011\,(Z - 12) - \lambda \quad \text{degrees} \tag{2.6}$$

$$\sin\phi_S = \sin(\theta)\sin(\delta_S) + \cos(\theta)\cos(\delta_S)\cos(h_S) \tag{2.7}$$

where δ_S in (2.7) is in radians.

A fraction of the flux reaching the ground is reflected back into the atmosphere. Equation (2.4) accounts for this by an overall reduction of incident irradiance by 9–11%. For example, when the sun is overhead, (2.4) yields a maximum flux of 1000 $\mathrm{W\,m^{-2}}$ for an atmospheric transmittance of 73.2% which is about 9% less than has been measured. Ground albedo varies with the surface and with solar angle, but worldwide intercomparisons of daily insolation in marine and continental sites suggest that a global daily average surface albedo of 8% is reasonable. There is a small observed increase in reflectivity for low sun angles, but the solar input is very small at these angles. Data reviewed by Raphael (1962) indicate that, "for engineering purposes," the reflectivity of the surface is independent of wind speed and atmospheric turbidity, including clouds.

Global location and universal time are required for the calculation of F_S. ALOHA contains a lookup table of θ and λ. The date and time of day can be the computer internal time or a user-designated time. ALOHA computes F_S one time at the beginning of the spill. The error in computed evaporation with this approximation is usually less than a few percent with the worst case being in the morning and late afternon when the $\sin(\phi_S)$ makes the most rapid change over one hour.

2.3.4 Longwave Radiation, $F_\uparrow$ and $F_\downarrow$

The temperature difference between the puddle liquid and the atmosphere results in a net loss or gain of energy by longwave radiation. The magnitude of the longwave flux in either direction is approximately 400 $\mathrm{W\,m^{-2}}$, and the net difference is about 10% of that. Exchanges are based on the Stefan-Boltzman radiation law. The longwave radiation upwards from the surface of the puddle is given by

$$F_\uparrow = -\varepsilon\sigma T_{skin}^4 \tag{2.8}$$

where ε is the puddle emissivity, σ is the Stefan-Boltzman constant ($\sigma = 5.67 \times 10^{-8} \mathrm{W\,m^{-2}\,K^{-4}}$), and T_{skin} is the surface temperature of the puddle (K). The negative sign accounts for the fact that the positive direction of heat flow is into the puddle. As discussed in Sec. 2.3.2, ALOHA uses only one temperature, T_p, and assumes $T_p \approx T_{skin}$.

The longwave radiation downwards from the atmosphere into the puddle can be expressed by the equation

$$F_{\downarrow} = (1 - r)B\sigma T_a^4 \tag{2.9}$$

where r is the surface reflectivity to longwavé radiation, B is the atmospheric radiation factor, and T_a is the temperature of the air (K). These are all constant terms and $F_{\downarrow}$ is constant for each scenario.

The emissivity of many chemicals is not readily available, so the approximate value for water, $\epsilon = 0.97$, is used in all cases. Likewise, r is set to 0.03, the value for water. The atmospheric radiation factor is calculated as a function of the cloud cover and humidity using the empirical formulas of Thibodeaux (1979);

$$B = a + be_v \tag{2.10}$$

where a and b are constants dependent on the cloud cover (Table 2.1), and e_v is the vapor pressure of water (Pa).

Table 2.1: Radiation factor coefficients for different cloud index values.

C_f:	0	1	2	3	4	5	6	7	8	9	10
a:	.74	.75	.76	.77	.783	.793	.80	.81	.82	.84	.87
$b \times 10^6$:	44.3	44.3	44.3	42.2	40.7	40.5	39.9	38.4	35.4	31.0	26.6

The atmospheric water vapor pressure is computed to within 0.001 Pa by

$$e_v = 99.89\frac{\mathrm{RH}}{100}\exp\left(21.66 - \frac{5431.3}{T_a}\right) \tag{2.11}$$

where T_a is the standard air temperature (K) and RH is the relative humidity (%). Typically, $0.8 < B < 0.9$.

2.3.5 Heat Exchange from the Ground, F_G

The heat exchange with the ground, F_G, is an important contribution to the budget for cryogenic spills where puddle-ground temperature differences are large and the temperature in the puddle is constant at T_B. All heat exchanges with the atmosphere depend on the skin temperature, but these are small in the case of cryogenic boiling and the error from the skin/bulk approximation is likewise small. **Ground temperature** is difficult to define, but it is needed to initialize ALOHA. Variations in the surface heat fluxes result in a temperature profile that propagates downward into the soil with phase shift and attenuation that depend on the period of the variations (Figure 2.3). The effective depth of penetration for seasonal variations is several meters while for diurnal variations it is about 0.5 m (Arya, 1988, p39). Thus we expect that in cases of extreme solar heating the temperature profile in the ground changes very quickly in the top few centimeters and more slowly below that.

The ALOHA ground flux algorithm assumes that the initial ground temperature profile is constant and it uses that temperature to calculate an error function solution. When the profile is not constant, the question of which temperature to choose is difficult and some experience

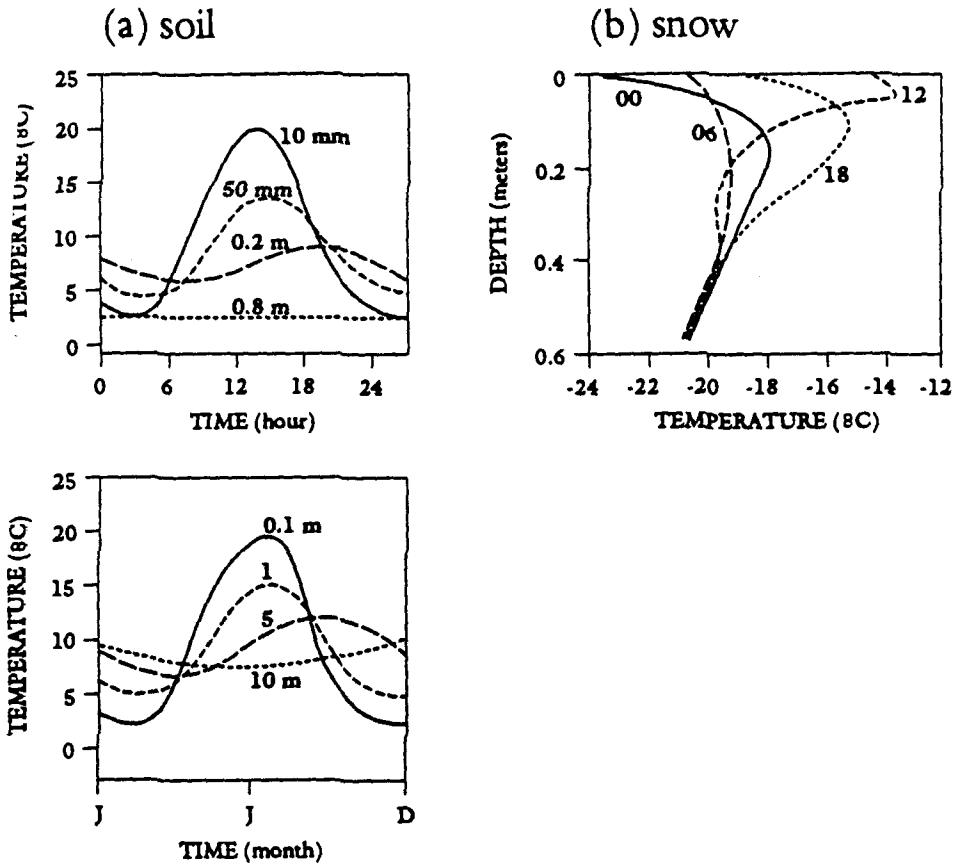

Figure 2.3: Examples of the variation of ground temperature with depth and time. (a) The cycles of soil temperature for daily and annual periods. (b) Variations in the temperature in snow over a day. (after Oke, 1978).

and care must be exercised in choosing it. Again, for cryogenic cases, the temperature difference is large (typically 100 K), and errors in estimating T_G have minimal impact on the soultion.

The ground is considered to be a semi-infinite solid with initially constant temperature, T_G, whose surface is maintained at temperature T_B beginning from zero time. Because $T_B \ll T_G$ for any reasonable choice of initial ground temperature, errors due to initial puddle non-uniformity are small. The initial boundary-value problem solution for F_G is provided by the methods of Carslaw and Jaeger (1959, p60).

$$F_G(t) = \frac{\chi \alpha_G}{\sqrt{\pi \kappa_G}} \left(\frac{T_G - T_B}{\sqrt{t}} \right) \tag{2.12}$$

where T_G is the initial ground bulk temperature (K), χ is the ground roughness conversion factor (≈ 3), α_G is the ground thermal conductivity ($\mathrm{W\,m^{-1}\,K^{-1}}$), κ_G is the ground thermal diffusivity ($\mathrm{m^2\,s^{-1}}$), and t is the elapsed time of the spill, e.g., the time the liquid has been on the ground[2]. Equation (2.12) predicts that after a period of time, the flux to or from the ground will become

[2]Ground flux is the only time-dependent term in which the initial time of the spill is of crucial importance. The source zero time is coincident with the time the liquid came in contact with the ground.

Table 2.2: Thermal properties of natural materials. (From Oke, 1978, p38)

Material	Remarks	ρ (kg m^{-3} $\times 10^3$)	c_p Specific heat (J kg^{-1} K^{-1} $\times 10^3$)	C Heat capacity (J m^{-3} K^{-1} $\times 10^6$)	α_G Thermal conductivity (W m^{-1} K^{-1})	κ_G Thermal diffusivity (m^2 s^{-1} $\times 10^{-6}$)
Sandy soil (40% pore space)	Dry	1.60	0.80	1.28	0.30	0.24
	Saturated	2.00	1.48	2.96	2.20	0.74
Clay soil (40% pore space)	Dry	1.60	0.89	1.42	0.25	0.18
	Saturated	2.00	1.55	3.10	1.58	0.51
Peat soil (80% pore space)	Dry	0.30	1.92	0.58	0.06	0.10
	Saturated	1.10	3.65	4.02	0.50	0.12
Snow	Fresh	0.10	2.09	0.21	0.08	0.10
	Old	0.48	2.09	0.84	0.42	0.40
Ice	0°C, pure	0.92	2.10	1.93	2.24	1.16
Water*	4°C,still	1.00	4.18	4.18	0.57	0.14
Air*	10°C,still	0.0012	1.01	0.0012	0.025	20.50
	Turbulent	0.0012	1.01	0.0012	≈ 125	$\approx 10^7$

* Depends on temperature.

negligible as the temperature in the ground near the surface becomes constant with depth at the surface temperature, T_B. Typical values of α_G and κ_G are found in (Table 2.2).

The ground roughness term, χ, was introduced by Briscoe and Shaw (1980). A constant value of 3 gives good agreement between theoretical predictions and experiments with cryogenic LNG. ALOHA retains this correction for all cases.

The treatment of the soil constants is resolved by grouping the first right-hand terms of (2.12) into a single constant, c_1. In S.I. units,

$$c_1 = \frac{\chi \alpha_G}{\sqrt{\pi \kappa_G}} = \begin{cases} 2398 & \text{default} \\ 988 & \text{sandy, dry soil} \\ 1723 & \text{sandy, moist soil} \\ 2414 & \text{concrete} \end{cases} \tag{2.13}$$

Table 2.2 compares the variations in heat capacities, molecular conductivities and specific heats for various types of ground material and for air and water. Selection of ground type can have pronounced effects on the evaporation, especially in cryogenic situations.

When the puddle is non-boiling, (2.12) is retained in the model computation, but for reasons given in Sec. 2.3.2, we substitute puddle surface temperature, $T_p(t)$, for T_B. As the temperature difference between the puddle and the ground decreases, the flux decreases.

2.3.6 Evaporation and Latent Heat Flux, F_E and F_H

Latent (evaporative) and sensible heat transfer, F_E and F_H respectively, are both computed from a model by Brighton (1985, 1990). Very close to the liquid-air interface, vapor is transferred through molecular exchanges in the same manner that heat and momentum are transferred. Most transfer takes place within a few molecular free path lengths of the surface. The Brighton

method uses a boundary layer approximation to an advection-diffusion equation in which cross wind variations are neglected over the length of the evaporating pool. For mathematical simplicity, the standard logarithmic profile of wind just above the surface is approximated by a power-law profile. The puddle is approximated as a rectangle with downwind length, D_p. A dimensionless mass transfer coefficient, j, is defined such that the evaporation mass flux is

$$\frac{E(x,t)}{\rho_{cs} u_*} = j\left(\frac{x}{z_0}, \frac{D_p}{z_0}, Re_0, Sc, Sc_T\right) \tag{2.14}$$

where $E(x,t)$ is the evaporation rate, ρ_{cs} is the contaminant saturation vapor concentration in air, u_* is the friction velocity, x is the distance in the downwind direction, z_0 is the puddle roughness length, D_p is the puddle downwind expanse ($0 \le x \le D_p$), Re_0 is the roughness Reynolds number, Sc is the laminar Schmidt number, and Sc_T is the turbulent Schmidt number.

The **roughness Reynolds number** is a measure of surface stress in the boundary layer flow.

$$Re_0 = u_* z_0 / \nu \tag{2.15}$$

where ν is the molecular kinematic viscosity of the air ($m^2 s^{-1}$).

The **laminar Schmidt number** is the ratio of ν to the molecular diffusivity of the gas,

$$Sc = \nu / \kappa_g \tag{2.16}$$

where κ_g is the diffusivity of the contaminant in the air-contaminant mixture ($m^2 s^{-1}$).

The **turbulent Schmidt number** is, by analogy,

$$Sc_T = K / K_E \tag{2.17}$$

where K is the turbulent eddy viscosity and K_E is the eddy diffusivity. K and K_E are much greater than any of the molecular coefficients and thus apply to the turbulent transfer of momentum, vapor, and other gas constituents.

Brighton defines a dimensionless coordinate system

$$X = \frac{nk^2 x}{Sc_T z_1} \tag{2.18}$$

$$Z = \frac{z}{z_1} \tag{2.19}$$

where n is the power of the wind profile term, and is selected so that the power-law profile matches the log profile at a height z_1, and k is the von Kármán constant (taken as 0.4). The **matching height**, z_1, and **matching wind speed**, U_1, are related to the neutral wind profile (see Sec. 4.3.2, page 67) by

$$z_1 = z_0 e^{1/n} \tag{2.20}$$

$$U_1 = \frac{u_*}{k} \ln \frac{z_1}{z_0} \tag{2.21}$$

In the case of an evaporating pool of limited fetch, the matching conditions represent the height and the downwind convective velocity of the center of mass of the vapor plume (Hunt

and Weber, 1979). Hence, n, U_1, and z_1 are all slowly varying functions of distance, which are taken to be constant for a given puddle.

Brighton's analytical, steady-state solution for $j(X)$ is given in the form

$$j(X) = \frac{k}{Sc_T}(1+n)\,G(e^{\Lambda}X) \tag{2.22}$$

where

$$\Lambda = \frac{1}{n} + 1 + 2\ln(1+n) - 2\gamma_e + \frac{k}{Sc_T}(1+n)f(Sc) \tag{2.23}$$

and γ_e is Euler's constant (= 0.577). The form of $f(Sc)$ depends on Re_0.

$$f(Sc) = \begin{cases} \left(3.85Sc^{\frac{1}{3}} - 1.3\right)^2 + \frac{Sc_T}{k}\ln(0.13Sc) & Re_0 < 0.13\text{: smooth} \\ 7.3Re_0^{\frac{1}{4}}\sqrt{Sc} - 5Sc_T & Re_0 > 2\text{: rough} \end{cases} \tag{2.24}$$

For values of $0.13 \le Re_0 \le 2$, $f(Sc)$ is estimated by a straight-line interpolation between the two extremes.

The function $G(\xi)$ where $\xi = e^{\Lambda}X$ is given by

$$G(\xi) = \int_0^{\infty} \frac{e^{-p\xi}}{p(\ln^2 p + \pi^2)}\,dp \tag{2.25}$$

Puddle-Average Evaporation

$E(x,t)$ varies from the windward to the leeward edge of the puddle. The mean dimensionless evaporation rate, $\bar{\jmath}$, is the integral of $j(X)$ over the range of $0 < X < X_1$ where X_1 is X evaluated at $x = D_p$.

$$\begin{aligned} \bar{\jmath} &= \frac{1}{X_1}\int_0^{X_1} j(X)\,dX \\ &\approx \frac{k}{Sc_T}(1+n)\left[\frac{1}{2} - \frac{1}{\pi}\arctan\left(\frac{\ln\left(e^{\Lambda}X_1\right)}{\pi}\right)\right. \\ &\quad \left. + \frac{1-\gamma_e}{\ln^2\left(e^{\Lambda}X_1\right)+\pi^2} + \frac{\left(1+(1-\gamma_e)^2+\frac{1}{6}\pi^2\right)\ln\left(e^{\Lambda}X_1\right)}{\left(\ln^2\left(e^{\Lambda}X_1\right)+\pi^2\right)^2}\right] \end{aligned} \tag{2.26}$$

Brighton argues that one may use a constant value of $X_1 = 9.68$ for a reasonable approximation. However, ALOHA 5.0 computes the dimensionless downwind distance with D_p set to the puddle diameter.

$\bar{\jmath}$ is corrected for the pertubation of the boundary-layer flow by the evaporating liquid. This correction can be important for volatile chemicals.

$$\bar{\jmath}_c = -\bar{\jmath}\frac{P_a}{e_{cs}}\ln\left(1 - \frac{e_{cs}}{P_a}\right) \tag{2.27}$$

where e_{cs} is the chemical vapor pressure and P_a is the ambient pressure.

Computational Approximations

To compute Re_0 in (2.15), the friction velocity is computed from an equation from Deacon (1973) for neutral conditions over the ocean

$$u_* = 0.03 U_{z'} \left(\frac{10}{z'}\right)^n \tag{2.28}$$

The standard height for wind measurement is 10 m, and (2.28) agrees with the rule of thumb that $u_* \approx 3\%\ U_{10}$. As discussed in Sec. 2.3.2, ALOHA uses measurements at 2 m without correction and the errors introduced are negligible. A constant value of $z_0 = 0.0004$ m is a reasonable value for a liquid puddle (Brutsaert, 1982, pg. 114), see Table 3.4 (page 53).

The Schmidt number in (2.16) requires the molecular diffusivity of the chemical in air, κ_g. This quantity is often unknown and, unless explicitly defined by the user, is taken to be proportional to the diffusivity of water vapor in air, κ_v, and is given by Graham's Law (Thibodeaux, 1979)

$$\kappa_g = \kappa_v \sqrt{\frac{\mathrm{M}_v}{\mathrm{M}_c}} \tag{2.29}$$

where M_v is the molecular weight of water (18), and M_c is the molecular weight of the chemical. κ_v is set to $2.39 \times 10^{-5}\ \mathrm{m^2\,s^{-1}}$, which is its value for water at 8°C.

It is assumed that the chemical concentration in the air is low and hence does not affect the viscosity or the diffusivity of water vapor or heat. Hence, the values for ν, κ_v, and κ_a as functions of temperature are computed for uncontaminated air.

A constant value, $Sc_T = 0.85$, is used for (2.17). This matches measurements by Fackrell and Robins (1982) and it satisfies Brighton's requirement for matching logarithmic concentrations near the surface.

Evaluation of (2.18) for the non-dimensional distance, X_1, requires the power-law exponent, n, k, and the matching height, z_1. Representative values of n for the Pasquill stability classes (Table 3.1, page 49) are

St Class	n	z_1
A	0.108	4.20
B	0.112	3.02
C	0.120	1.67
D	0.142	0.46
E	0.203	0.055
F	0.253	0.020

The matching height is computed by (2.20) with known $z_0 = 0.0004m$ and n.

The vapor correction in (2.27) requires the chemical vapor pressure, which is computed by the Reidel method (Perry et al., 1984, pg 3-274).

$$e_{cs} = P_c \exp\left(A - BT_r^{-1} + C \ln T_r + DT_r^6\right) \tag{2.30}$$

where T_r is the reduced temperature (T_p/T_c), T_p is the puddle temperature (assumed equal to the skin temperature), T_c is the critical temperature, P_c is the critical pressure, and

$$A = -35Q \tag{2.31}$$

$$B = -36Q \tag{2.32}$$

$$C = 42Q + \alpha_c \tag{2.33}$$

$$D = -Q \tag{2.34}$$

$$Q = 0.0838(3.758 - \alpha_c) \tag{2.35}$$

$$\alpha_c = \frac{0.315\psi - \ln(P_s/P_c)}{0.0838\psi - \ln(T_{rb})} \tag{2.36}$$

$$\psi = -35 + 36T_{rb}^{-1} + 42\ln T_{rb} - T_{rb}^{6} \tag{2.37}$$

where P_s is the standard pressure[3] of 1 atm, $T_{rb} = T_{nb}/T_c$ is the reduced temperature at normal boiling point, and T_{nb} is the **normal boiling point**, the temperature when $e_{cs} = P_s$.

The gas density at the interface (saturation concentration) is computed with the ideal gas relationship,

$$\rho_g = \frac{M_w e_{cs}}{RT_p} \tag{2.38}$$

where R is the universal gas constant ($= 8314\ \mathrm{Pa\,m^3\,kmol^{-1}\,K^{-1}}$) and the evaporating material is assumed to be at the puddle temperature (actually at the skin temperature, see Sec. 2.3.2).

Latent Heat Flux

Equations (2.26) to (2.29) can be used to compute the puddle-mean evaporation rate, $\overline{E}$. The latent heat flux is computed from the equation

$$F_E = L_c\overline{E} \tag{2.39}$$

where L_c is the heat of evaporation for the chemical at the puddle temperature ($\mathrm{J\,kg^{-1}}$). L_c is computed using the DIPPR equations from the ALOHA data base (Sec. 1.5).

Sensible Heat Flux

The sensible heat flux is the heat directly transferred to or from the atmosphere as a result of the temperature differences at the air-liquid interface.

$$F_H = \rho_a c_{pa} C_H u_*(T_a - T_p) \tag{2.40}$$

where C_H is the sensible transfer coefficient given by

$$C_H = \jmath_c\left(\frac{Sc}{Pr}\right)^{2/3} \tag{2.41}$$

[3]**Standard pressure is defined as 1 atm and standard ambient pressure is 10^5 Pa (1 bar). The term standard temperature and pressure (STP) means 0°C and 1 atm. The term standard ambient temperature and pressure (SATP) means 25°C and 1 bar. Finally, the normal boiling point is the boiling point at 1 atm (standard pressure) and the standard boiling point is the boiling point temperature at 1 bar. (Atkins, 1990, p133).**

Pr the Prandtl number, is a measure of the relative effectiveness of diffusion of momentum and heat. Its molecular form is

$$Pr = \nu/\kappa_a \tag{2.42}$$

$Pr \approx 0.7$ for air and other diatomic gases, and is nearly independent of temperature.

The specific heat of the air, c_{pa}, is assumed constant at 1004 $J\,kg^{-1}\,K^{-1}$. The thermal diffusivity of the air ($m^2\,s^{-1}$) is estimated from the table of physical properties for dry air at atmospheric pressure (Thibodeaux, 1979)

$$\kappa_a = -1.85 \times 10^{-5} + 1.4 \times 10^{-7} T_a \tag{2.43}$$

where T_a is the ambient air temperature (K).

The density of the air ($kg\,m^{-3}$) is computed as

$$\rho_a = 2.42 - 0.0041 T_a \tag{2.44}$$

An Example from an Evaporating Pool Experiment

Kawamura and Mackay (1985) made measurements of evaporation from small dishes of different chemicals in a variety of wind and heating conditions. One case, Experiment #1, used toluene in an insulated pan ($F_G = 0$) and the following conditions:

Chemical	toluene
Date/time	17 Sep 1984, 13–14 EST
Averaging time	1 hour
Pool area	0.657 m^2
Pool depth	0.023 m
Weather	sunny, clear
T_a	21.3 °C
U_{10}	3.9 $m\,s^{-1}$
T_p(final)	30.3°C
T_{skin}(final)	23.7°C
Evap Rate	4.49 ($kg\,m^{-2}\,hr^{-1}$)

Figure 2.4 shows the relative importance of the different heat flux terms and the computed evaporation rates. ALOHA-calculated values for individual heat fluxes (positive for heat into the puddle) over time are shown in the left-hand figure: Solar flux, F_S, is computed once and is constant during the time period; downward and upperward longwave radiation, $F_\downarrow$ and $F_\uparrow$ respectively, are large terms with a small difference; heat flux, F_H, starts at zero (we assume that, initially, $T_p = T_a$) then goes negative as the puddle cools, and evaporation, F_E is a large negative term. The right-hand figure shows the resultant evaporation rate in the 1300 EST curve: the evaporation quickly rises to about 4.8 $kg\,m^{-2}\,hr^{-1}$ and stays there until all the liquid has evaporated at 65 minutes. Within one-half hour, the solution has settled to a constant evaporation rate. The measured evaporation rate for Experiment 1 of 4.49 $kg\,m^{-2}\,hr^{-1}$ compares well with this calculation.

Solar radiation has a pronounced effect on the evaporation rate as seen from a comparison run at midnight (in the right panel of the figure). The 00 EST curve is the same calculation

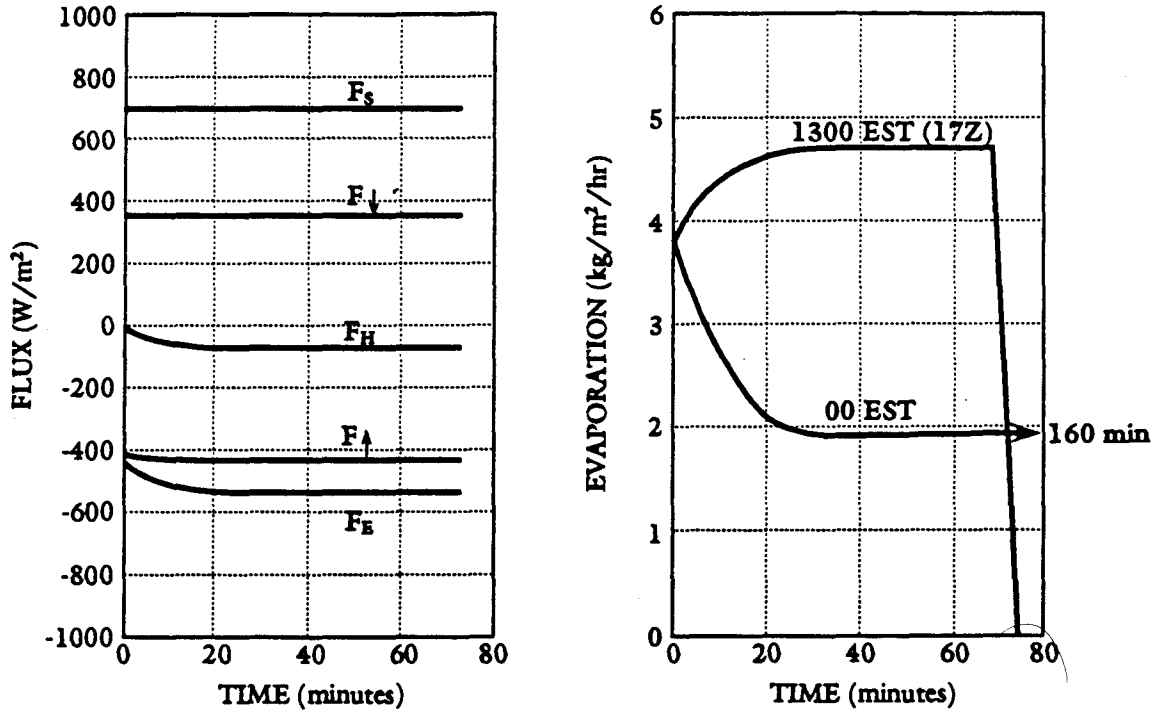

Figure 2.4: Example of the puddle model for Experiment #1 from Kawamura and Mackay (1985).

without solar radiation. The steady state is reached in about the same time, but the evaporation rate is much less and the time to evaporate all the liquid is now 160 min. With all other parameters the same, the absence of solar heating leads to a reduction in evaporation by a factor of 2.7 and a corresponding increase in depletion time from 65 to 160 minutes. In both cases the time to reach steady state is about the same.

2.3.7 Computation Notes

The puddle area is approximated as a rectangle (Figure 2.5). The depth of the puddle is uniform, d_p. The puddle temperature, T_p, is assumed to be uniform. For purposes of computing evaporation, the puddle's downwind extent is the same as its width; see (2.14) and discussion. Five *equal* point sources are assumed. The sources are located with relation to the puddle as shown and the strength of each one is $\overline{E}/5$. The placement of the point sources as shown in the figure produces a more reasonable and intuitively satisfying footprint, especially very near the puddle.

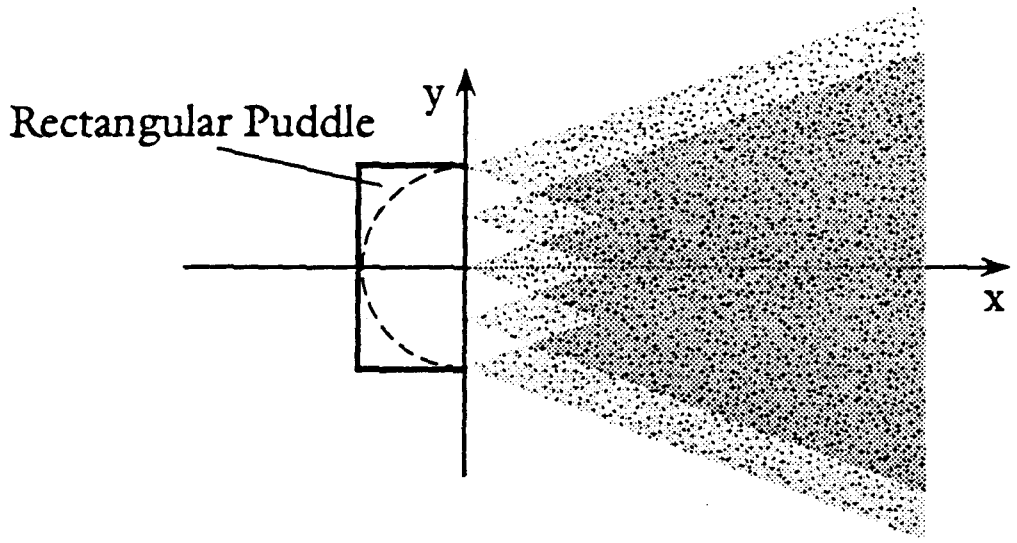

Figure 2.5: Sketch of a simple puddle. The puddle is approximated as five equal point sources with the placement shown.

2.4 Tank

2.4.1 General Comments

ALOHA 5.0 has algorithms to predict the outflow rate and duration of leaks from damaged chemical storage and transportation tanks. A few parameters are essential to running the tank model. The **tank geometry** is essential and ALOHA allows the following types of tanks:(**a**) horizontal cylinder, (**b**) vertical cylinder, and (**c**) sphere. The tank volume can be derived from available information on the tank geometry (height, diameter, etc.). For example, if the user provides values for height and diameter of a cylindrical tank, ALOHA will compute tank volume, V_t.

The user must specify the **chemical state** of the contents: (**a**) liquid, (**b**) gas, or (**c**) unknown. At the same time he/she must specify the the **temperature**, T_t, of the contents of the tank. ALOHA contains a library of the physical and thermodynamic properties ofcommon chemicals and will verify user input.

The **total mass** of material in the tank is specified directly or calculated from other known quantities. If a liquid is selected, liquid volume, V_l, and the volume of the gas-filled void above the liquid, are derived from the input information. The user must either provide (**a**) mass (see footnote on page 4) of liquid if it is known or (**b**) the volume of liquid. Volume can be derived from a guess at either the liquid level or percent full. If a gas is selected, then the user must provide either (**a**) gas pressure, P_t, or (**b**) mass (weight) of gas, M_g. If the state is unknown, the user must provide the mass (weight) of material in the tank and ALOHA will then compute the state of the chemical based on volume and temperature.

Finally, the **hole** geometry, area, and location are defined. The following holes are allowed: (**a**) circular (diameter $= 2r_h$), (**b**) horizontal rectangular hole (width$= \zeta_w$, height$= \zeta_h$), and (**c**) a short spout or pipe whose cross-section agrees with the circle/rectangle dimensions. Examples of damaged containers are given in Figure 2.6.

After verifying the user input for physical/thermodynamic consistency, the model begins

with either all gas, or a liquid with a vapor head space in the tank. In the case of a liquid, the hole can be either above or below the liquid surface. The hole location is crucial in determining the outcome of the spill. The source algorithm computes time step intervals such that 1% of the initial mass in the tank exits in any one time step. At the beginning of each time step, the conditions in the tank are analyzed and one of the following conditions is selected:

1. **Liquid Output.** The tank contains liquid below its normal boiling point and the hole is below the liquid surface. The pressure and temperature in the liquid are such that liquid emerges from the hole and a puddle is formed.
   (a) **Evaporating puddle.** The liquid emerges as liquid and its boiling point is above the temperature of the ground.
   (b) **Boiling puddle (cryogenic).** The liquid boiling point is below the ground temperature so it will boil on the ground. When the boiling point is sufficiently low such that heat flux from the ground dominates all other heat sources, the puddle is called cryogenic (see page 14).
2. **Two-Phase Output.** If the pressure in the gas void at the top of the tank drops below the vapor pressure of the chemical, bubbles begin to form in the liquid. This process is called **flashing,** and a two-phase fluid, a mixture of gas and liquid, can emerge from the tank. Two-phase mixtures behave like non-ideal gases. Outside the tank, a small amount ($\approx$ 20 to 25%) immediately goes to the gaseous phase (flashes) and the remainder forms a liquid aerosol. Depending on the density of the aerosol, the Gaussian or the heavy-gas dispersion models may be recommended. The computation of mass flow depends on whether the hole occurs on the tank wall or in a valve or pipe connected to the tank.
   (a) **Simple hole.** ALOHA simplifies the flashing process by assuming that the liquid instantly becomes a homogeneous foam with gas-like properties and with uniform density. The foam leaves the tank as an aerosol spray.
   (b) **Short Spout.** Occasionally, as with relief valves, the leak occurs at a spout and it is possible for aerosols to be formed in the spout. The solution is not dependent on spout length. ALOHA 5.0 treats this situation in an approximate manner.
3. **Gas Output.** If the tank is filled with gas, the pressure of the gas and the leak hole size are important in determining the behavior of the exiting gas. A spout can cause choked flow.
   (a) **Subsonic flow.** For large holes and/or low tank-ambient pressure difference, the gas leaves the tank at speeds below the velocity of sound.
   (b) **Supersonic flow.** At high enough pressures and small holes, the gas exits at speeds above the speed of sound for that gas. The mass flux through the hole reaches a maximum amount regardless of increased pressure differential. This inhibited flow situation is called **choked flow.**

Constant values are given to parameters to which the model is insensitive. The following assumptions are made by ALOHA 5.0:

1. Tank walls are 1-cm-thick steel.
2. Only one chemical is in the tank. No multi-component cases are considered.

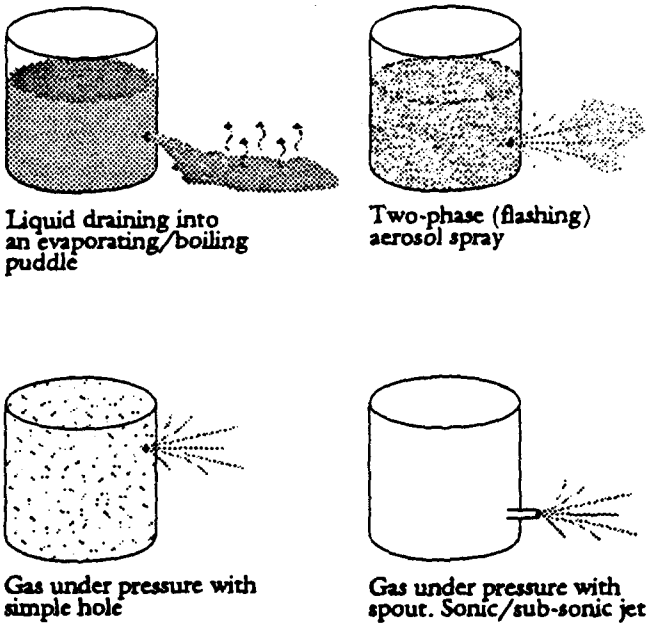

Figure 2.6: Examples of leaking containers and the types of leaks that can occur. A liquid spill can form a puddle, but if flashing occurs, the liquid will go directly to gas. The presence of a spout at the hole can cause significantly different behavour.

3. There is only one hole in the tank and it can be described either as a circle or as a rectangle. The area of the hole is used to compute an equivalent circular hole.

4. If the tank contains a chemical that is a gas at ambient conditions but is stored as a liquid, then it is stored either (a) refrigerated at ambient pressure and at its boiling point temperature ($T_t = T_B(P_a)$) or (b) it is compressed at ambient temperature just sufficiently to form a liquid ($T_B(P_l) = T_a$). The former case results in a boiling puddle and the latter case results in an aerosol formation as P_l drops steadily as material leaves the hole.

5. The transition from liquid to two-phase foam occurs instantly to a uniform mixture.

2.4.2 Liquid Leaks

When the material in the tank is a liquid and its temperature is below the boiling point at the tank pressure, it emerges from the tank as a liquid. The liquid forms a puddle on the ground.

Inside the Tank

The mass flow of the emerging liquid is given by Bernoulli's equation

$$Q_T(t) = C_{dis} A_f \sqrt{2\,(P_h - P_a)\,\rho_l} \tag{2.45}$$

where $A_f(t)$ is the flow area, C_{dis} is the discharge coefficient, $P_h(t)$ is the pressure of the liquid in the tank at hole depth, P_a is the ambient barometric pressure, and $\rho_l(t)$ is the density of the liquid in the tank. The density is assumed to be uniform. C_{dis} is assumed to be constant at

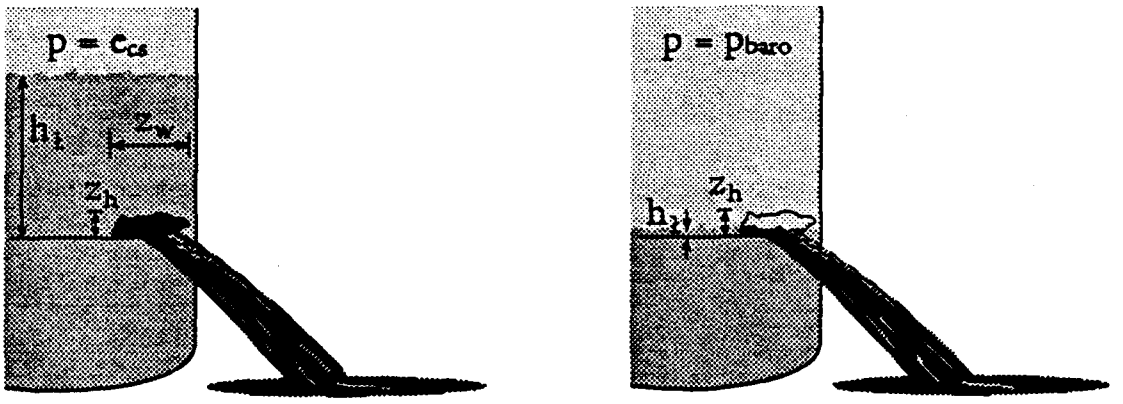

(a) surface above hole (b) surface intersects hole

Figure 2.7: Detail of a rectangular hole showing the effective flow area for the case of (a) the liquid surface is above the hole and (b) the liquid level intersects the hole.

0.61 (Belore and Buist, 1986). The flow area depends on whether the liquid surface intersects the hole (Figure 2.7).

For the two cases, the flow area is computed by

$$\frac{A_f(t)}{A_h} = \begin{cases} 1 & \text{surface above hole} \\ h_l/\zeta_h & \text{surface intersects hole} \end{cases} \tag{2.46}$$

where A_h is the area of the actual hole, $h_l(t)$ is the height of the liquid above the bottom of the hole, and ζ_h is the height of the hole (diameter in the case of a round hole).

When the hole is below the liquid surface, $P_h(t)$, is the sum of the pressure in the gas void at the top of the tank and that exerted by the column of liquid above the bottom of the hole.

$$P_h(t) = \begin{cases} e_{cs} + h_l \rho_l g & \text{surface above hole} \\ p_a + h_l \rho_l g & \text{surface intersects hole} \end{cases} \tag{2.47}$$

where $e_{cs}(t)$ is the saturated vapor pressure of the chemical and is assumed to be the pressure in the void, and g is the acceleration of gravity. The sequence of pressure drop, evaporation, and temperature change is assumed to occur rapidly at each time step, so that for a new time step the vapor in the void has a new temperature and a pressure equal to e_{cs}. As h_l decreases, P_h will decrease. P_h will decrease until it is less than P_a and the flow will stop until an air bubble is ingested back into the tank. This will reduce the vacuum and allow flow to continue in a series of gushes. To simulate this process, when P_h reaches $1.01P_a$ it is held constant to that value.

The temperature of the liquid in the tank is changed by (a) evaporation into the vapor space and (b) heat transfer through the tank walls. Change in the total internal energy of the liquid by evaporation and heat transfer is given by

$$\frac{dU_l}{dt} = Q_e L_c + F_{Hw} A_{tw} \tag{2.48}$$

where U_l is the total internal energy of the liquid, Q_e is the rate of total mass evaporated into the vapor space, L_c is the heat of vaporization, F_{Hw} is the heat input through the walls, and A_{tw} is the area of the side walls of the tank.

To approximate Q_e ($\mathrm{kg\,s^{-1}}$) it is assumed that enough liquid evaporates to maintain the gas at its vapor pressure. The perfect gas law then gives

$$Q_e(t) = Q_T \frac{\rho_v}{\rho_l - \rho_v} \tag{2.49}$$

where $\rho_v(t)$ is the density of the vapor, and $\rho_l(t)$ is the density of the liquid.

F_{Hw} ($\mathrm{W\ m^{-2}}$) is given by

$$F_{Hw} = \frac{\alpha_w V_l (T_a - T_t)}{\delta_w V_t} \tag{2.50}$$

where α_w is the conductivity for heat of the wall material (assume steel) ($\mathrm{W\,m^{-2}\,K^{-1}}$), V_l is the volume of liquid in the tank, T_a is the ambient temperature in the air, T_t is the temperature of the vapor and liquid in the tank, δ_w is the wall thickness (assume 1 cm), and V_t is the total volume of the tank. The heat transferred to the gas portion of the tank is negligible because of the small heat capacity of the gas compared to the liquid.

The temperature change is computed for a time step, Δt. From (2.48)–(2.50),

$$\Delta T = \frac{\mathrm{d}U_l/\mathrm{d}t}{\rho_l c_{pl} V_l} \Delta t \tag{2.51}$$

At each time step the temperature is re-computed. The mass change (1%) and the temperature are used in equations (2.45)–(2.47) to compute a new value for Q_T and the new time step Δt is computed until either one hour has passed or the tank is empty.

Puddle Growth Outside the Tank

If liquid pours into the puddle faster than the puddle evaporates, it will thicken and spread under the influence of gravity. A puddle radius is recomputed at each time step, based on the mass flow into the puddle, Q_T, and the loss of mass from the puddle due to evaporation, Q_E. When $Q_T > Q_E$, a concentric ring grows around the periphery of the existing puddle so that for the new time step

$$\Delta r_p = \frac{1}{r_p} \sqrt{\frac{2gM_p}{\pi \rho_l}} \Delta t \tag{2.52}$$

where M_p is the new computed mass of the puddle (kg), g is the acceleration of gravity (9.808 $\mathrm{m\,s^{-2}}$), r_p is the previous puddle radius, ρ_l is the density of the liquid in the puddle ($\mathrm{kg\,m^{-3}}$), and Δt is the time step (sec). The factor of 2 is used by Briscoe and Shaw (1980) to account for the inertia of the liquid which is equal to only a fraction of the inertia of the whole liquid-pool mass moving with the acceleration of its leading edge.

The puddle area is not allowed to shrink. The puddle will continue to grow according to (2.52) and will become thinner. When the layer depth shrinks to 0.5 cm, puddle growth will

stop and the puddle will continue to grow thinner at constant radius until it has completely evaporated or the one-hour time cutoff occurs.

For computation of heat transfer from the ground (boiling/cryogenic case), the heat transfer in each ring is a function of the length of time that the ring has been on the ground. A generalization on (2.12) for a spreading puddle is

$$F_G = \frac{1}{A_p}\left[c_1(T_G - T_B)\sum_{i=1}^{N}\frac{2\pi\overline{r_i}(r_i - r_{i-1})}{\sqrt{t-\tau_i}}\right] \tag{2.53}$$

where A_p is the area of the puddle at time t, c_1 is defined in (2.13), $\overline{r_i}$ is the mean radius of the ith concentric ring, r_i is the outer radius of the ith ring, and τ_i is the time the ring was placed on the ground ($\tau_i < t$). F_G varies over the puddle, but an average is computed by dividing the total heat transfer by the puddle area.

Tank Heat Flux to the Puddle

The puddle energy balance, (2.2), has an additional term when the tank deposits liquid into the puddle. The change in temperature of the puddle during one time step is approximated by

$$\Delta T_p = \left[\frac{1}{\rho_p c_{pl} d_p}\sum \text{Fluxes} + \frac{(T_t - T_p)Q_T}{M_p}\right]\Delta t \tag{2.54}$$

where ΔT_p is the change in the puddle temperature during time step Δt, T_t is the temperature of the fluid coming out of the tank, T_p is the puddle temperature, Q_T is the computed mass flow out of the hole, and M_p is the puddle mass.

When the puddle is boiling, $\Delta T_p = 0$ and the evaporative flux is calculated to balance the right-hand side.

Time Scales

Typically, the time it takes for all the liquid to drain from a tank is much less than the time required to evaporate the puddle that forms. Because of the different time scales, the output from the tank model is fit in a least-squares sense to the function

$$Q_T \doteq A_t\left(1 - \frac{t}{t_c}\right)^{1/2} + B_t\left(1 - \frac{t}{t_c}\right) \tag{2.55}$$

where Q_T is the liquid flow rate ($\mathrm{kg\,s^{-1}}$), A_t and B_t are curve fit parameters, and t_c is the time when the leak stops. This then defines a continuous source function for the puddle at all times for $0 < t \leq t_c$. The liquid coming from the tank is assumed to have constant temperature and density based on the average of the beginning and end values from the tank model.

2.4.3 Two-Phase Conditions

Rare, but major and dangerous chemical releases are usually related to overpressure and venting in connection with runaway chemical reactions and/or accidental breaches in vessel pipe works

containing toxic and flammable liquids. The realization that most emergency releases involve high momentum two-phase discharges, even in cases of controlled releases, has led to increased interest in modeling such jet releases.

Many substances that are gases under normal conditions of temperature and pressure are stored at ambient temperature in tanks under sufficiently high pressures to liquify them. A rupture of a liquified gas tank leads to a release of a mixture of liquid droplets and gas. This type of release is referred to as **two-phase flow**. If temperature and pressure conditions indicate that the tank contents consist of a gas liquified by pressure, the Source Module[4] computes the release rate using a two-phase flow algorithm. Two-phase conditions are assumed to persist until the end of the source computation.

In the two-phase case, a mixture of gas and liquid aerosols are released. ALOHA assumes that all expelled liquid is quickly evaporated from the aerosol cloud and no puddle is formed. The chemical is assumed to be either already a gas or an aerosol which evaporates before hitting the ground (Britter and McQuaid, 1988; personal communication, 1989). The evaporative heat loss can result in a vapor cloud which is substantially cooler than the initial liquid-vapor mixture.

Two different algorithms are used for pressurized two-phase flow depending on whether the leak is a simple hole in the tank or is at the end of a short length of pipe. Most theory for the latter case comes from studies of controlled releases from relief valves. A relief valve leak can be approximated as a short pipe with leak area A_h. In the absence of frictional losses, flashing flows through ducts are generally choked, and in many applications the critical pressure can be approximated by the vapor pressure corresponding to the temperature in the tank (Fauske and Epstein, 1988).

The ALOHA algorithm for two-phase flow only considers a round hole with area, A_h. In the case of a rectangular hole (Figure 2.7),

$$A_h = \pi \zeta_w^2 / 4 \tag{2.56}$$

The **stagnation pressure**, referred to in literature of two-phase flow, is taken to be identical to the pressure at the hole as described by (2.47).

Simple Hole

Flow from a simple hole in the wall of the tank is governed by Bernoulli's equation in the form of (2.45) but modified by an effective height and density of the gas-liquid mixture.

$$Q_T(t) = A_h C_{dis} \sqrt{2 \left(P_{eff} - P_a\right) \rho_{eff}} \tag{2.57}$$

where C_{dis} is the discharge coefficient ($= 0.61$), $P_{eff}(t)$ is the effective hole pressure, P_a is the ambient pressure, and $\rho_{eff}(t)$ is the effective density of the mixture in the tank.

The quality[5] of the mixture in the tank is computed from

$$\chi_0(t) = \frac{e_{cs} \left(v_g - v_l\right) c_{pl} T_t}{L_c^2} \tag{2.58}$$

[4]The "Source Module" is the software that determines the source term for the dispersion calculations.

[5]Quality is defined as the mass of the vapor divided by the mass of the mixture.

and the effective specific volume ($\rho_{eff} = 1/v_{eff}$) is given by

$$v_{eff} = \chi_0(v_g - v_l) + v_l \tag{2.59}$$

where v_g is the specific volume of the gas phase ($m^3\,kg^{-1}$), v_l is the specific volume of the liquid phase ($m^3\,kg^{-1}$), T_t is the temperature in the tank (K), and L_c is the heat of vaporization of the liquid ($J\,kg^{-1}$). The computed values of v_{eff} and the known mass in the tank are used along with the tank geometry to compute h_{eff} and then P_{eff} from (2.47).

Two-Phase Flow from a Short Pipe

A simplified form of the **homogeneous nonequilibrium model** was developed by Fauske and Epstein (1988) to compute the release rate of a two-phase mixture from a short pipe or duct (Henry and Fauske 1971, Fauske 1985). Fauske and Epstein's homogeneous nonequilibrium model has been demonstrated to predict two-phase release rates through pipes or ducts between 0 and 10 cm in length. The mass flux through a short pipe is described by the following expression,

$$Q_T(t) = \frac{A_h L_c}{v_g - v_l}\sqrt{\frac{1}{N_F T_t\, c_{pl}}} \tag{2.60}$$

where $Q_T(t)$ is the mass flux from the pipe ($kg\,s^{-1}$), L_c is the heat of vaporization ($J\,kg^{-1}$), T_t is the temperature of the fluid (K), c_{pl} is the heat capacity of the fluid ($J\,kg^{-1}\,K^{-1}$), and the term N_F is given by the equation

$$N_F = \frac{v_l L_c^2}{2(P_{eff} - P_a)\, C_{dis}^2 (v_g - v_l)^2\, T_t\, c_{pl}} + \frac{l_p}{l_e} \tag{2.61}$$

where l_p is the length of the pipe (m), and $l_e = 0.1$ m.

Longer Pipes and the Homogeneous Equilibrium Model

As l_p approaches 0.1 m, the homogeneous nonequilibrium model approximately reduces to the **homogeneous equilibrium model** (Leung, 1986; also Fauske and Epstein 1988),

$$Q_T(t) = \frac{A_h F L_c}{(v_g - v_l)\sqrt{T_t c_{pl}}} \tag{2.62}$$

where F is the frictional flow reduction factor based on the length-to-diameter ratio.

The homogeneous equilibrium model predicts that two-phase releases through pipes exceeding 0.1 m are generally choked and mass release rates decrease only slightly with increasing pipe length. Mass release rates are independent of the quality of the effluent. In the event that the effluent entering the pipe is a pure liquid and is at a pressure equal to its vapor pressure, flashing is assumed to occur in the pipe resulting in choked flow.

Valve failures and releases through relief valves can also be modeled using the homogeneous nonequilibrium model with the pipe length set to 0.1 m. Huff (1985) states that the homogeneous equilibrium model is an appropriate model for typical valve geometries. The DIERS Project

Manual also recognizes the homogeneous equilibrium model as a method of computing release rates through safety valves and rupture disks (Fisher et al. 1989). These conclusions can also be applied to the homogeneous nonequilibrium model since it predicts only slightly higher release rates than the homogeneous equilibrium model.

ALOHA Approximations

Certain assumptions and limitations are inherent in the homogeneous nonequilibrium model as it is used in ALOHA:

- All two-phase releases are described either as releases through an orifice in the tank wall, or through a 10-cm pipe. Since the discharge rate decreases slowly with increasing pipe length beyond 10 cm, the homogeneous nonequilibrium model yields slightly overestimated values of the flow rate through longer pipes.
- The homogeneous nonequilibrium model is limited to two-phase flow that is predominantly liquid. The following expression describes the maximum value of quality for which the model is valid,

$$\chi_{max} = \frac{P_h(v_g - v_l)T_t\, c_{pl}}{L_c^2} \tag{2.63}$$

  where P_h is the pressure of the liquid at the hole, and χ_{max} is the maximum value for which the homogeneous nonequilibrium model is valid.
- A liquid stored at its normal boiling point forms a homogeneous two-phase mixture that is in thermodynamic phase equilibrium. This is an essential condition in the homogeneous nonequilibrium model. This assumption also simplifies the task of computing the fluid level in the tank during the release, since the two-phase fluid is always assumed to fill the tank unless the maximum quality is exceeded (see (2.64) below).

For a hole, the homogeneous nonequilibrium model with a zero pipelength reduces to the Bernoulli equation, (2.57). Regardless of whether the leak is above or below the initial level of the liquid, the density of the effluent is approximated by the density of the liquid phase. This approximation results in an overestimate of the release rate when the hole is above the liquid level, since the actual density of the two-phase effluent would be less than that of the pure liquid. The pressure driving the orifice flow is computed from the sum of the vapor pressure of the liquid in the tank and the approximate hydrostatic pressure. In order to estimate the hydrostatic pressure, a working assumption is made that, when conditions are conducive to a two-phase release, the tank contents form a uniform two-phase mixture that either fills the tank or reaches the maximum quality for which the homogeneous nonequilibrium model is valid (χ_{max}).

Releases through short pipes or valves are computed using the homogeneous nonequilibrium model with the 0.1 m pipe length. The mass release rate depends on neither driving pressure nor the quality of the fluid entering the pipe. As in the case of a hole in the tank wall, a working assumption is made that when conditions are conducive to a two-phase release, the tank contents form a uniform two-phase mixture. As long as the hole is located below the calculated level of the two-phase fluid in the tank, the calculated release rate is independent of the location of the leak.

The Expelled Aerosol

For all two-phase releases, the mixture that is expelled from the tank continues to flash-boil adiabatically as an aerosol until its temperature reaches its boiling point. The quality of the resulting aerosol is calculated using an equation for isenthalpic (constant enthalpy) expansion,

$$\chi_0 = \frac{c_{pl}(T_t - T_B)}{L_m} \tag{2.64}$$

where T_B = boiling point of the liquid, L_m is the latent heat of vaporization, and χ_0 is the maximum quality for which the homogeneous nonequilibrium model is valid.

The above treatment is used to compute the mass release rate as a function of instantaneous conditions (i.e. the mass of chemical in the tank from the temperature of the tank). The total release is divided into one hundred time steps; the duration of a step is sufficient to allow one percent of the mass to be released. The time duration is found by dividing one percent of the mass by the instantaneous release rate.

After each time step, parameters are computed to describe the conditions in the tank. The temperature is computed by assuming that the tank walls are 1-cm thick steel and the mixture is cooled by evaporation, and the pressure is set equal to the vapor pressure of the liquid at this temperature. The temperature is held equal to or above the boiling point. The mass released, the density, and temperature are computed for each time step.

2.4.4 Gas Leaks

ALOHA 5.0 incorporates some of the algorithms used in the computer model "LEAKR" described by Belore and Buist (1986). Flow can be either subsonic or supersonic depending on three ratios. The first is the ratio of atmospheric pressure to tank pressure,

$$R_P = P_a/P_t \tag{2.65}$$

During initialization, the user provides the temperature of the gas, T_t, and either the pressure or the mass (weight). A virial equation of state is used to compute the other properties of the gas.

$$P_t = \frac{ZRT_t}{V_m} \tag{2.66}$$

where V_m is the molar specific volume of the gas, Z is the compression factor given by

$$Z = \frac{1}{1 - \frac{B'}{V_m}} - \frac{A'}{RT_t^{3/2} V_m \left(1 + \frac{B'}{V_m}\right)} \tag{2.67}$$

where

$$A' = 0.4278 \left(\frac{R^2 T_c^{5/2}}{P_c}\right), \text{ and} \tag{2.68}$$

$$B' = 0.0867 R \left(\frac{T_c}{P_c}\right) \tag{2.69}$$

R is the universal gas constant ($= 8.314$ J mole^{-1} K^{-1}), T_c is the gas critical temperature, V_m is the molar volume, and P_c is the gas critical pressure. Equations (2.66)–(2.69) can be solved iteratively to determine P_t and V_m. If the mass of the gas is known, then V_m can be computed directly from molecular weight and tank volume and P_t is computed from (2.66). If the pressure is input, V_m must be computed iteratively.

The second important parameter is the hole-to-tank length scale ratio given by

$$\beta_c = L_h / L_t \tag{2.70}$$

where

$$L_h = \begin{cases} 2r_h & \text{round hole} \\ \sqrt{\zeta_w \zeta_h} & \text{rectangular hole} \end{cases} \tag{2.71}$$

$$L_t = \begin{cases} 2r_t & \text{spherical tank} \\ 2r_t & \text{cylindrical tank} \end{cases} \tag{2.72}$$

The third important variable is the **critical pressure ratio**, R_c, whose form depends on β_c.

$$R_c = \left(\frac{2}{\gamma+1}\right)^{\frac{\gamma}{\gamma-1}} \qquad \beta_c > 0.2 \quad \text{(big hole)} \tag{2.73}$$

$$R_c^{\frac{1-\gamma}{\gamma}} + \frac{\gamma-1}{2}\beta_c^4 R_c^2 = \frac{\gamma+1}{2} \qquad \beta_c \leq 0.2 \quad \text{(small hole)} \tag{2.74}$$

Choked Flow

If $R_P \leq R_c$ the flow is at the speed of sound and is usually **choked**, indicating that further reduction of downstream pressure does not change the flow rate appreciably. The mass flow rate is given by

$$Q(t) = C_{dis} A_h \sqrt{\rho_g(t)\, P_t(t)\, \gamma \left(\frac{2}{\gamma+1}\right)^{\frac{\gamma+1}{\gamma-1}}} \tag{2.75}$$

where C_{dis} is introduced in (2.45).

Unchoked Flow

When $R_P > R_c$ the flow is subsonic and the mass flow is given by

$$Q(t) = C_{dis} A_h \sqrt{2\rho_g P_t \frac{\gamma}{\gamma-1}\left(\left(\frac{P_a}{P_t}\right)^{2/\gamma} - \left(\frac{P_a}{P_t}\right)^{(\gamma+1)/\gamma}\right)} \tag{2.76}$$

As gas leaves the tank the temperature drops by adiabatic expansion.

$$T_t' = T_t \left(\frac{P_t}{P_t'}\right)^{\frac{1-\gamma}{\gamma}} \tag{2.77}$$

Calculations have shown that heat flux through the tank walls adds little to this effect. Detailed discussions on the relationship between choked and unchoked flow is given by Shapiro (1953) and Blevins (1985). This relationship as applied to hazard analysis is discussed by Hanna and Strimaitis (1989).

2.5 Pipe

2.5.1 General Comments

Only pure gas releases from pipe ruptures are considered by ALOHA 5.0. The gas pipe releases are based on modifications made by Wilson (1979, 1981a) to the model developed by Bell (1978). A key assumption in the theory is that the process is almost entirely isothermal at temperature, T_g. Measurements show that heat transfer to the moving gas through the pipe walls maintains an almost isothermal condition throughout the length of the pipe except for the last 200 hole diameters. Within 200 diameters of the hole, the flow is assumed to be adiabatic because of the large acceleration near the end of the pipe.

2.5.2 Theory

Wilson showed that an exponential was the correct solution of an isothermal, quasi-steady state pipe flow, and that the release of gases from a finite length of pipe can be approximated by a double exponential of the form

$$Q(t) = \frac{Q_0}{(1+\alpha)}\left(e^{-t/\alpha^2\beta} + \alpha e^{-t/\beta}\right) \tag{2.78}$$

where $Q(t)$ is the rate of mass discharge per unit time, Q_0 is the initial mass flow at the time of the rupture, α is a non-dimensional mass conservation factor, and β is the release rate time constant.

The pressure in most pipelines will be much greater than ambient pressure. Therefore, Q_0 is calculated assuming a choked flow condition as in (2.75) where for a pipe, $C_{dis} = 1$ and the internal pressure, temperature and gas constant at the time of rupture are known:

$$Q_0 = P_0 A_h \sqrt{\frac{\gamma}{R_g T_g}\Gamma^{-1}} \tag{2.79}$$

where

$$\gamma = \frac{C_p}{C_v} = 1 + \frac{R_g}{C_v} \tag{2.80}$$

$$\Gamma = \left(\frac{\gamma+1}{2}\right)^{\frac{\gamma+1}{\gamma-1}} \tag{2.81}$$

P_0 is the initial pipe pressure, R_g is the gas constant for 1 kg of the gas, A_h is the rupture area, and T_g is the gas temperature.

The time constant, β, is computed by the equation (Wilson, 1989):

$$\beta = \frac{2}{3}\tau_p K_F \Gamma^{3/2} K_H^{-3}\left[\left(1 + \frac{K_H^2}{K_F\Gamma}\right)^{3/2} - 1\right] \tag{2.82}$$

where

$$\begin{aligned} \tau_p &= L_p/c \\ K_F &= d_p/(\gamma\mu L_p) \\ K_H &= A_h/A_p \end{aligned}$$

L_p is the length of the pipe, c is the speed of sound in the pipe, d_p is the pipe diameter, μ is the Darcy-Weisbach friction factor, A_p is the cross-section area of the pipe, and A_h is the area of the hole. The speed of sound for an isothermal pipe is

$$c = \sqrt{\gamma R_g T_g} \tag{2.83}$$

The friction factor is computed by Blevins (1985) as

$$\mu = \frac{0.25}{(0.57 - \log(\varepsilon/d_p))^2} \tag{2.84}$$

where the roughness coefficient, ε, is set to 0.0001 m for normal conditions and is increased to 0.002 m for rough pipe conditions. For typical pipe conditions, $0.01 < \mu < 0.02$.

Equation (2.82) can be simplified for small- and large-hole conditions respectively. Typically, $1.1 < \gamma < 1.8$ and thus $4 \times 10^{-6} < \Gamma < 0.7$. When $K_H^2/K_F\Gamma$ is small, the pipe can be treated like a long isothermal storage tank. A Taylor's approximation of the form $(1+a)^{3/2} - 1 \approx 3a/2$, where $K_H^2/K_F\Gamma = a \ll 1$, is used and (2.82) becomes

$$\beta \approx \tau_p K_H^{-1} \Gamma^{1/2} \qquad \text{(small hole)} \tag{2.85}$$

A hole is considered to be large if $(K_H^2/K_F\Gamma) > 30$ and (2.82) reduces to

$$\beta \approx \frac{2}{3}\tau_p K_F^{-1/2} \qquad \text{(large hole)} \tag{2.86}$$

The total mass in the pipeline, M_T, is calculated as

$$M_T = \frac{P_0 A_p L_p}{R_g T_g} \tag{2.87}$$

and the mass conservation factor is

$$\alpha = \frac{M_T}{\beta Q_0} \tag{2.88}$$

β, α, and c are functions of the temperature of the gas at the hole (exit temperature). For each time step, the exit temperature must be re-evaluated by the methods described below. Adiabatic decompression of the gas within 200 diameters of the hole is assumed. Beyond 200 diameters of the hole, the flow is approximately isothermal with frictional heating and adibatic cooling in near balance. The exit temperature of the current time step is given by

$$T_f = T_g \left(\frac{P_a}{P_{ia}}\right)^{(\gamma-1)/\gamma} \tag{2.89}$$

where T_g is the exit temperature at the previous step, P_a is the ambient air pressure, and P_{ia} is the pressure at the isothermal-adiabatic interface,

$$P_{ia} = Qc/A_p \tag{2.90}$$

At the isothermal-adiabatic interface, for steady-state conditions, the model assumes an infinite reservoir attached to a finite length of pipe with the hole the same size as the pipe. For this case, the flow rate is calculated as

$$Q = A_p \rho_{ia} v_{ia} \tag{2.91}$$

where v_{ia} is the velocity of the gas at the isothermal-adiabatic interface, and ρ_{ia} is the density at the interface. Choked flow is assumed and leads to the relationships

$$v_{ia} = c/\gamma \tag{2.92}$$

$$\rho_{ia} = \rho_r P_{ia}/P_r \tag{2.93}$$

where the subscript r refers to the reservoir. A non-linear equation for the velocity of the gas out of the reservoir must be solved to find a value for P_{ia} to be used in the above equation. If $\mathcal{M}$ is the Mach number (ratio of discharge speed to the speed of sound), the equation for isothermal pipe flow is (Blevins, 1985)

$$\int_0^{L_p} \frac{\mu}{d_p} \mathrm{d}L = \int_{\mathcal{M}^2}^{1/\gamma} \left(\frac{1-\gamma\mathcal{M}^2}{\gamma\mathcal{M}^4} \right) \mathrm{d}\mathcal{M}^2 \tag{2.94}$$

where the approximation has been made that the length of the pipe where isothermal flow predominates is much larger than the part where adiabatic flow occurs, so that the upper limit of the left-hand integral is set to be the whole length of the pipe. Equation 2.94 can be integrated to give

$$K_F^{-1} = \frac{c^2 - \gamma v_{ir}^2}{\gamma v_{ir}^2} - \frac{c^2 - \gamma v_{ia}^2}{\gamma v_{ia}^2} + 2 \ln \left(\frac{v_{ir}}{v_{ia}} \right) \tag{2.95}$$

where v_{ir} is the gas velocity at the reservoir-pipe interface.

Using the above equations for v_{ir}, P_{ia} is estimated from the relationship

$$P_{ia} = \left(\frac{v_{ir}}{v_{ia}} \right) \left(P_r - \frac{1}{2} \rho_r v_{ir}^2 \right) \tag{2.96}$$

2.5.3 Computational Notes

Equation 2.95 is solved by using a bracketing and weighted bisection method of iteration where the weights are inversely proportional to the residual error.

The pipe release algorithm computes an array of gas release rates at different times. As in other source routines, the length of the time interval varies such that equal amounts of mass are released in each time step. If n is the total number of time steps, then each new time step is found from the previous one by using a Newton-Raphson iteration scheme to find the roots of the equation.

$$F(t_{i+1}) = \frac{M_T}{n} - \int_{t_i}^{t_{i+1}} Q(t) \mathrm{d}t \tag{2.97}$$

where t_i is the previous time and t_{i+1} is the new time. Minimum time interval is 60 seconds and the release is terminated if it extends beyond one hour.

Mathematical Symbols

A	intermediate variable in Reidel method for computation of e_{cs} (none)
A'	intermediate parameter in the computation of the compression factor (none)
A_f	flow area for liquid in a leaking tank (m^2)
A_h	area of the hole in a leaking tank (m^2)
A_p	area of a pipe cross-section (m^2)
A_t	curve fit parameter for matching the tank discharge time to the puddle evaporation time (none)
	area of a puddle (m^2)
A_{tw}	area of the side walls of a tank through which heat can flow (m^2)
B	longwave radiation factor (none)
	intermediate variable in Reidel method for computation of e_{cs} (none)
B'	intermediate parameter in the computation of the compression factor (none)
B_t	curve fit parameter for matching the tank discharge time to the puddle evaporation time (none)
C	concentration ($kg\,m^{-3}$)
	intermediate variable in Reidel method for computation of e_{cs} (none)
C_{dis}	discharge coefficient, = 0.61 for fluid from a tank (none)
C_H	bulk heat transfer parameter (none)
c	sonic velocity in a gas ($m\,s^{-1}$)
c_{pa}	specific heat at constant pressure for air ($J\,kg^{-1}\,K^{-1}$)
c_{pl}	specific heat of the liquid in a tank ($J\,kg^{-1}\,K^{-1}$)
c_1	$\chi\kappa/\sqrt{\pi\alpha}$ ($W\,K^{-1}\,s^{-0.5}$)
D	intermediate variable in Reidel method for computation of e_{cs} (none)
D_p	puddle along-wind length (m)
d_p	puddle depth (m)
	pipe diameter (m)
e_{cs}	chemical saturation vapor pressure (Pa)
E	evaporation rate per unit area ($kg\,s^{-1}\,m^{-2}$)
$\overline{E}$	mean evaporation over an entire puddle ($kg\,s^{-1}\,m^{-2}$)
E_{Aj}	evaporation rate per unit area in the jth concentric ring ($kg\,s^{-1}\,m^{-2}$)
F	friction factor in the homogenious equilibrium model (none)
F_E	heat flux by evaporation ($W\,m^{-2}$)
F_{Hw}	tank wall heat flux ($W\,m^{-2}$)
F_M	mass flux ($kgm^{-2}\,s^{-1}$)
F_S	heat flux from solar radiation ($W\,m^{-2}$)
$F_\uparrow$	longwave radiation upwards ($W\,m^{-2}$)
$F_\downarrow$	longwave radiation downward ($W\,m^{-2}$)
F_G	heat conduction to the ground ($W\,m^{-2}$)
F_H	sensible heat flux ($W\,m^{-2}$)
G	intermediate parameter in the Brighton evaporation model (none)
g	acceleration of gravity ($m\,s^{-2}$)
H_w	total heat transfer through a tank wall ($J\,s^{-1}$)
h	the hour of the day (hr)
h_l	height of liquid above the bottom of a hole in a tank (m)
h_S	solar hour angle (radians)
h_s	source height for a direct release (m)
J	Julian Day (day)
j	non-dimensional evaporation rate (none)
$\overline{j}$	non-dimensional evaporation rate averaged over the length of the puddle (none)
$\overline{j}_c$	$\overline{j}$ corrected for vapor pressure (none)
K	turbulent viscosity ($m^2\ s^{-1}$)
K_E	turbulent diffusivity of vapor ($m^2\ s^{-1}$)
K_F	pipe friction parameter, see (2.83) (none)
K_H	ratio of pipe hole area to cross-section area (none)
K_M	turbulent diffusivity of mass ($m^2\ s^{-1}$)
k	von Kàrmàn constant (0.4)
L_c	heat of vaporization for a chemical ($J\,kg^{-1}$)
L_h	characteristic length for a tank hole (m)
L_m	heat of vaporization for an aerosol ($J\,kg^{-1}$)
L_t	characteristic scale length for a tank (m)
L_w	heat of vaporization for water into air ($J\,kg^{-1}$)
L_p	length of a pipe (m)
l_e	reference spout length (0.1 m)
l_p	pipe or spout length (m)
M	total mass released from a source (kg)
M_c	molecular weight of a chemical (kg)
M_g	mass of gas in a tank (kg)
M_P	total mass of gas in a pipe (kg)
M_p	total mass of a puddle (kg)
M_T	total mass in a tank (kg)
M_w	molecular weight of water (kg)
m	total puddle mass (kg)
N_F	friction factor in the homogenious nonequilibrium model (none)
n	exponent in power-law wind profile (none)
	number of time steps in a pipe source computation (none)
P_a	ambient pressure at ground level (Pa)
P_C	critical pressure for a substance (Pa)
P_{eff}	effective hole pressure during two-phase flow (Pa)
P_h	pressure of liquid in a tank at the hole (Pa)
P_{ia}	pipe pressure at the isothermal-adiabatic interface (Pa)
P_{ir}	pipe pressure at the isothermal-reservoir interface (Pa)
P_l	pressure of liquefied gas at ambient temperature (Pa)
P_0	initial pressure in a pipe (Pa)
P_S	standard pressure (Pa)

Mathematical Symbols (cont.)

P_t	pressure of the gas in a tank (Pa)
Q	source emission strength ($kg\,s^{-1}$)
	intermediate variable in Reidel method for computation of e_{cs} (none)
Q_e	tank void evaporative mass flow ($kg\,s^{-1}$)
Q_E	puddle evaporative mass flow ($kg\,s^{-1}$)
Q_P	rate of mass discharge from a pipe ($kg\,s^{-1}$)
Q_T	rate of mass discharge from a tank ($kg\,s^{-1}$)
Q_0	initial rate of mass discharge ($kg\,s^{-1}$)
R	universal gas constant (8314 Pa m^3 $kmol^{-1}$ K^{-1})
R_c	critical pressure ratio for computation of gas release from a tank (none)
R_g	gas constant (Pa $m^3\,kg^{-1}\,K^{-1}$)
R_{e0}	roughness Reynolds Number (none)
R_P	ratio of atmospheric pressure to tank pressure (none)
RH	relative humidity (%)
r	puddle surface reflectance to longwave radiation (none)
r_i	radius of the puddle at time step i (m)
r_h	radius of a circular hole in a tank (m)
r_p	radius of the puddle (m)
Sc	Schmidt number for a chemical in air (none)
Sc_T	turbulent Schmidt number for a chemical in air (none)
T_a	air temperature (K)
T_B	boiling point of a liquid (K)
T_b	bulk temperature of a puddle (K)
T_C	critical temperature for a substance (K)
T_f	exit temperature of gas from a pipe (K)
T_G	temperature of the ground (K)
T_g	initial gas temperature in a pipe (K)
T_p	puddle temperature (K)
T_r	reduced temperature for a substance (K)
T_{nb}	normal boiling point of a chemical (K)
T_{rB}	reduced temperature for a substance at its boiling point (K)
T_{skin}	skin temperature for a puddle of liquid (K)
T_t	temperature in the tank (K)
T_t'	exit temperature of a gas from a tank (K)
T_z	temperature of the ground at depth, z (K)
t	time since the start of the discharge (s)
t_c	time when a tank leak stops (s)
U	mean wind speed in the x direction ($m\,s^{-1}$)
U_1	reference U at height z_1 ($m\,s^{-1}$)
U_l	total internal energy of a liquid in a tank (J)
U_{10}	mean wind speed at a height of 10 m ($m\,s^{-1}$)
u	internal energy per unit mass ($J\,kg^{-1}$)
u_*	friction velocity of a turbulent boundary layer ($m\,s^{-1}$)
V_t	volume of the tank (m^3)
V_l	volume of liquid in a tank (m^3)
V_m	molar specific volume of a gas ($m^3\,mole^{-1}$)
v_{eff}	effective specific volume of a two-phase mixture ($m^3\,kg^{-1}$)
v_{ia}	gas velocity at isothermal-adiabatic interface in a pipe ($m\,s^{-1}$)
v_{ir}	gas velocity at isothermal-reservoir interface in a pipe ($m\,s^{-1}$)
X	nondimensional distance from the leading edge of the puddle (none)
x	the horizontal distance downstream (m)
y	the horizontal distance perpendicular to the plume axis (m)
Z	hour in GMT (hrs)
	compression factor for a non-ideal gas (none)
z	vertical distance above the ground (m)
z_0	the turbulent roughness length (m)
z_1	matching height in the Brighton eveporation model (m)
α	gas pipe mass flow conservation factor (none)
α_c	intermediate variable in Reidel method for computation of e_{cs} (none)
α_G	ground thermal conductivity (W m^{-1} K^{-1})
α_w	conductivity of the tank walls (W m^{-1} K^{-1})
β	gas pipe release time constant (sec)
β_c	ratio of tank hole size to tank size (none)
Δr_p	puddle radius change in a time step (m)
ΔT	temperature change over one time step (K)
ΔT_p	puddle temperature change over one time step (K)
Δt	time step in the source software calculations (s)
δ_h	height of a hole in a tank or pipe (m)
δ_S	the solar declination angle (radians)
δt	minimum time step (1 min)
δ_w	width of a hole in a tank or pipe (m)
	thickness of the tank wall (m)
κ_a	molecular thermal diffusivity of air ($m^2\,s^{-1}$)
κ_G	ground diffusivity ($m^2 s^{-1}$)
κ_g	molecular diffusivity of a gas in air ($m^2\,s^{-2}$)
κ_v	molecular diffusivity of water vapor in air ($m^2\,s^{-2}$)
ϵ	pipe roughness factor (m)
ε	puddle emissivity (none)
Γ	Adiabatic compression factor, see (2.80) (none)

Mathematical Symbols (cont.)

γ	ratio of specific heats (none)
γ_e	Euler's constant (0.577)
χ	ground roughness conversion factor (none)
χ_0	quality of a two-phase mixture in a tank (none)
χ_{max}	maximum quality for validity of the homogenious nonequilibrium model (none)
Λ	intermediate parameter in Brighton evaporation model (none)
λ	longitude (deg)
$\mathcal{M}$	Mach number of discharged gas from a pipe (none)
μ	Darcy-Weisbach friction factor (none)
ν	molecular kinematic viscosity ($m^2 s^{-1}$)
ϕ_S	solar altitude, angle above the horizon (radians)
ψ	intermediate variable in Reidel method for computation of e_{cs} (none)
ρ_a	density of air at standard pressure ($kg\,m^{-3}$)
ρ_{cs}	gas density for a saturated gas in a mixture ($kg\,m^{-3}$)
ρ_{eff}	effective density of a two-phase mixture in a tank ($kg\,m^{-3}$)
ρ_g	density of the gas in a pipe ($kg\,m^{-3}$) density of the gas in a tank void area ($kg\,m^{-3}$)
ρ_{ia}	pipe gas density at the isothermal-adiabatic interface ($kg\,m^{-3}$)
ρ_l	density of liquid in a tank ($kg\,m^{-3}$)
ρ_p	puddle liquid density ($kg\,m^{-3}$)
σ	Stefan-Boltzman constant (5.67×10^{-8} W m^{-2} K^{-4})
θ	latitude (deg)
τ_i	length of time of the ith time step (s)
τ_p	intermediate parameter in pipe gas emission algorithm (s)
ζ_h	height of a rectangular hole in a tank or pipe (m)
ζ_w	width of a rectangular hole in a tank or pipe (m)

Chapter 3

Neutral Gas Dispersion

3.1 General Description

Neutral gases do not alter the density of the ambient air, and thus have no affect on air flow. Known as passive contaminants, field studies have shown that neutral gases disperse such that their concentration distributions fit well to Gaussian (bell-shaped) curves. Models that use this distribution are called Gaussian plume models. Earlier versions of ALOHA used only the Gaussian plume model.

The classical Gaussian plume is a steady-state model that requires a continuous release of contaminant (Figure 3.1). The **ensemble average** (i.e. probabilistic) plume shape is approximated by time averages sufficient to smooth the effects of plume meandering. The equation for the Gaussian plume is a function only of the mean wind speed (assumed constant) and the cross wind and vertical standard deviations ($\sigma_y(x)$ and $\sigma_z(x)$). The standard deviations are referred to as the **dispersion parameters**, and many field studies are aimed at developing reasonable empirical methods relating the dispersion parameters to actual boundary-layer turbulence.

ALOHA restricts itself to cases most likely to be encountered during accidental spill situations. It computes pollutant concentrations only for observers at ground level ($z = 0$) and, with the exception of **Direct Input**, only treats ground-level sources. Plume interaction with the ground and an inversion, if one exists, are included.

ALOHA 5.0 is a significant improvement over earlier versions. It is a time-dependent model and uses a modified form of the Gaussian plume. The source is considered to be a contiguous group of one to five short-duration injections of contaminant. Each injection travels and disperses much like a Gaussian plume, with the exception that its forward and leading edges diffuse upstream and downstream under the action of the turbulent mixing and vertical shear. We call each of these independent plume segments **clouds**[1]. Figure 3.7 shows gas clouds as they are advected downwind and disperse in three directions. The clouds are shown as non-contiguous puffs so the x-spreading can be seen easily. Puffs have been treated theoretically in the literature, and any emission of gas, whether continuous or of finite duration, can be considered to be a superposition of a number of puffs.

[1] A puff is the name given to an instantaneous release of gas from a point source. A cloud is the result of a release of limited duration. In the limit of zero duration, a cloud becomes a puff.

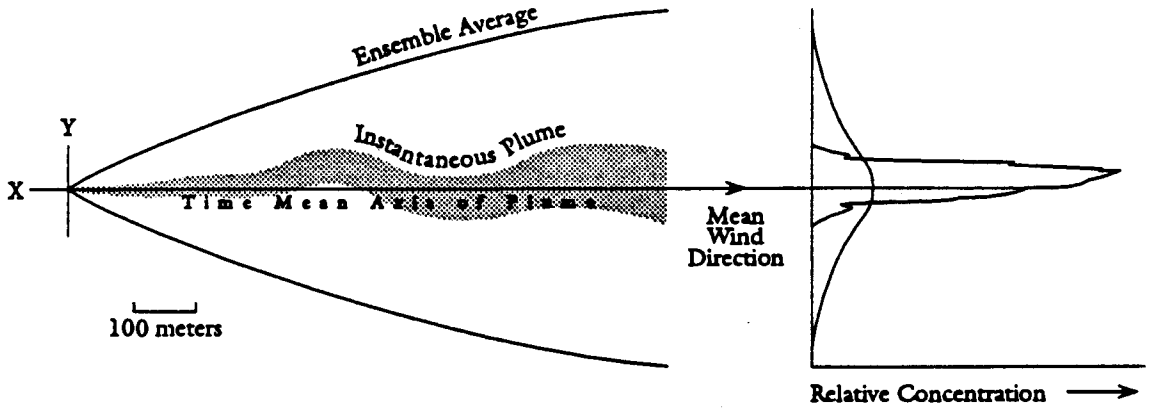

Figure 3.1: Plan view of a continuous Gaussian plume. As the gas is carried by the wind it meanders with the larger eddies and disperses in all three directions from the smaller-scale eddies. The ensemble concentration average is predicted by dispersion theory. Actual concentrations may exceed predicted values by a considerable amount. The averaging time should be (a) long enough to filter out the effect of the longest turbulent eddies and (b) short enough that the mean values are constant. In most instances, 5–30 minutes is an appropriate averaging time. (adapted from Beals, 1971, page 18)

3.2 Continuous Source

We begin with a complete description of the classical Gaussian plume. The interested reader is directed to Sutton (1932), Beals (1971), Briggs (1973), Hanna et al.(1982), and Pasquill and Smith (1983).

The Gaussian model of plume dispersion, although having many shortcomings, has the following advantages for the ALOHA effort:

- It produces results that agree reasonably well with experimental data.
- It is conceptually easy to understand.
- The mathematics are relatively easy to perform with medium-scale computing power.
- It is consistent with the statistical nature of turbulence.
- It is used extensively in dispersion modeling and is generally accepted as a good tool.
- It requires only a few, easily understood parameters and so is "user-friendly" to less-skilled users.

3.2.1 Elevated Source

The general expression for the Gaussian plume treats a point source located at $x = y = 0$ and $z = h_s$, where h_s is the source height. ALOHA concentrates almost exclusively on ground

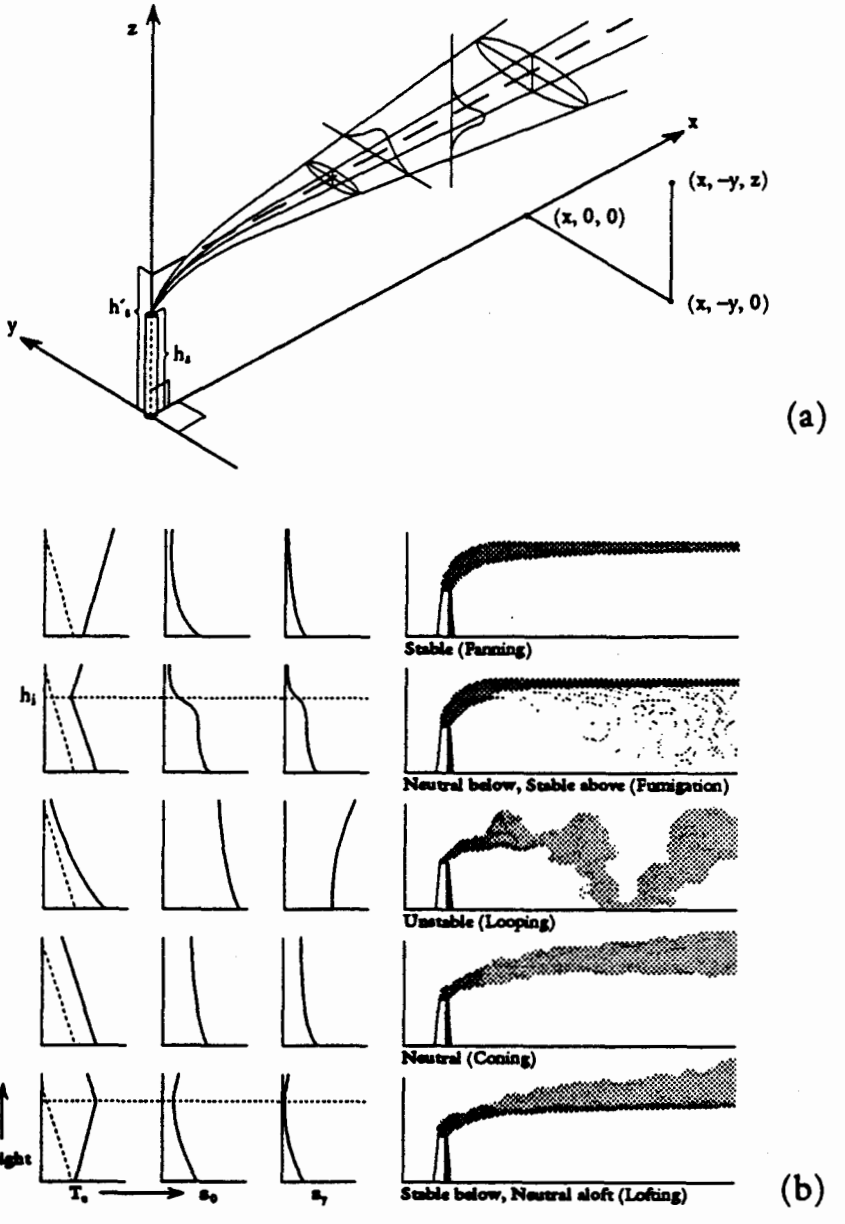

Figure 3.2: Buoyant gas dispersion from a stack is not treated by ALOHA although the direct source option allows the user to specify an effective release height, h'_s. The plume will disperse normally until it interacts with the ground and/or a capping inversion. Shown are the source height, h_s, the effective height in the case of lofting, h'_s, and the inversion height in the case of an unstable boundary layer, h_i. ALOHA does not treat buoyant emissions directly, and it does not allow penetration of an inversion.

releases where $h_s = 0$, and is not intended to be applied to stack releases, in which buoyant rise may be important. The case of $h_s > 0$ is allowed only in the direct release option (Figure 3.2 and Sec. 2.2). The source strength, Q, is the mass of material released per unit time. The time-averaged wind speed, U, is uniform everywhere. The contaminant concentration, $C(x, y, z)$, is given by

$$C(x,y,z) = \frac{Q}{2\pi\sigma_y\sigma_z U} \exp\left[-\frac{1}{2}\left(\frac{y}{\sigma_y}\right)^2\right] \left\{\exp\left[-\frac{1}{2}\left(\frac{z-h_s}{\sigma_z}\right)^2\right] + \exp\left[-\frac{1}{2}\left(\frac{z+h_s}{\sigma_z}\right)^2\right]\right\} \quad (3.1)$$

where $\sigma_y(x)$ is the standard deviation of C in the cross-wind direction and $\sigma_z(x)$ is the standard deviation of $C(x, y, z)$ in the vertical direction. These dispersion parameters are functions only of the downwind direction, x. The z-dependent terms model the trapping effect of the ground by proposing a mirror source at a distance h_s beneath the ground.

An alternate way of writing (3.1) is to segment the y, and z dependent terms. In this way the contribution of dispersion in each direction can be treated separately. This formulation is easier to implement in a numerical model and is followed by ALOHA.

$$C(x,y,z) = \frac{Q}{U} g_y(x,y)\, g_z(x,z) \quad (3.2)$$

where

$$g_y(x,y) = \frac{1}{\sqrt{2\pi}\sigma_y(x)} \exp\left[-\frac{1}{2}\left(\frac{y}{\sigma_y(x)}\right)^2\right] \quad (3.3)$$

$$g_z(x,z) = \frac{1}{\sqrt{2\pi}\sigma_z(x)} \left\{\exp\left[-\frac{1}{2}\left(\frac{z-h_s}{\sigma_z(x)}\right)^2\right] + \exp\left[-\frac{1}{2}\left(\frac{z+h_s}{\sigma_z(x)}\right)^2\right]\right\} \quad (3.4)$$

The estimation of the dispersion parameters is described in Sec. 3.3 below.

3.2.2 Modeling a Capping Inversion

Figure 3.2(b) shows the behavior of a gas emission into five different types of boundary layers. The temperature profiles define the boundary layer stability which can be stable, neutral, or unstable. The dashed line represents the temperature gradient in a neutral atmosphere when cooling from adiabatic expansion dominates. The uppermost case is a stable boundary layer when the temperature gradient is greater than the adiabatic gradient and turbulent mixing is minimal as is evidenced by the small values for σ_x and σ_y.

The next-to-the-top case is typical for a low capping inversion. This case usually occurs in the morning over land as the sun heats the ground and causes turbulent mixing of the air up to a height, h_i. Above h_i the air is stable. Buoyant plumes rise from the surface and are contained by the stable inversion layer. In the process, stable air is entrained from above causing the layer to grow[2]. The effect of the inversion can be quite complex and simplifications must be made. We assumed that the inversion completely blocks any vertical diffusion above h_i, and the ground and inversion surfaces act as a pair of reflecting surfaces. Equation (3.4) is extended in a similar

[2]Highly buoyant plumes such as hot emissions can penetrate an inversion. ALOHA 5.0 does not treat the case of positively buoyant plumes or inversion penetration.

in a similar manner to the ground reflection. The reflecting surface visualization showing the required **image sources** is sketched in Figure 3.3.

$$g_z(x,z:h_s,h_i) = \frac{1}{\sqrt{2\pi}\sigma_z}\left\{\exp\left[-\frac{1}{2}\left(\frac{z-h_s}{\sigma_z}\right)^2\right] + \exp\left[-\frac{1}{2}\left(\frac{z+h_s}{\sigma_z}\right)^2\right]\right\} \tag{3.5}$$
$$+\sum_{n=1}^{J}\left\{\exp\left[-\frac{1}{2}\left(\frac{z-2nh_i-h_s}{\sigma_z}\right)^2\right] + \exp\left[-\frac{1}{2}\left(\frac{z+2nh_i-h_s}{\sigma_z}\right)^2\right]\right.$$
$$\left.+\exp\left[-\frac{1}{2}\left(\frac{z-2nh_i+h_s}{\sigma_z}\right)^2\right] + \exp\left[-\frac{1}{2}\left(\frac{z+2nh_i+h_s}{\sigma_z}\right)^2\right]\right\}$$

where J is the number of reflecting pseudo-sources for the downstream distance.

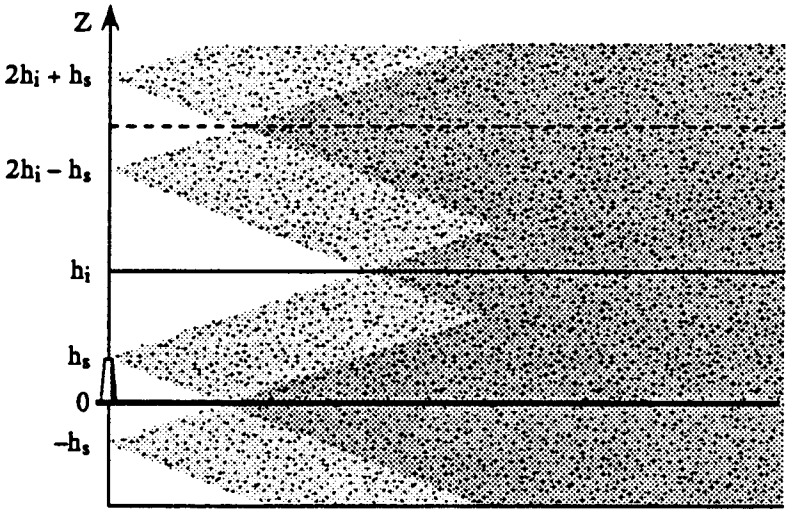

Figure 3.3: Visualization of the inversion and ground as reflecting surfaces for the diffusing plume.

After some distance downstream, the boundary layer is considered to be fully mixed. Typically this condition occurs when J is less than three. When $\sigma_z(x) \geq 2h_i$, (3.5) is simplified to

$$g_z = \begin{cases} h_i^{-1} & \text{if } 0 \leq z \leq h_i \\ 0 & \text{otherwise} \end{cases} \tag{3.6}$$

3.2.3 The Ground Source

A user selection of a direct source (Sec. 2.2) allows for non-zero source elevation. Otherwise, ALOHA concerns itself only with ground emissions, $h_s = 0$. In this case,

$$g_z(x,z;0) = \frac{2}{\sqrt{2\pi}\sigma_z}\left\{\exp\left[-\frac{1}{2}\left(\frac{z}{\sigma_z}\right)^2\right]\right. \tag{3.7}$$
$$\left.+\sum_{n=1}^{J}\left\{\exp\left[-\frac{1}{2}\left(\frac{z-2nh_i}{\sigma_z}\right)^2\right] + \exp\left[-\frac{1}{2}\left(\frac{z+2nh_i}{\sigma_z}\right)^2\right]\right\}\right\}$$

ALOHA 5.0 is interested in life-threatening ground-level concentrations where $z = 0$. At ground level, equation (3.7) is simplified by setting $z = 0$. The maximum concentration occurs on the centerline where $g_y = 1$.

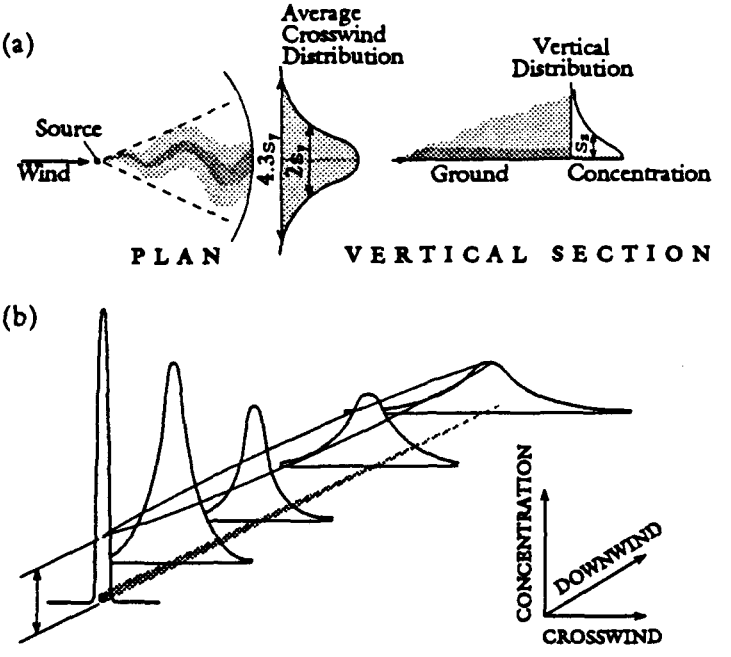

Figure 3.4: Ground-based source emission. (a) Plan and profile views. Historically the plume width is defined as $4.3\sigma_y$ where the concentration is one-tenth the central value. Likewise the plume height is $2.15\sigma_z$ (From Pasquill and Smith, 1983) (b) A sketch showing the spread of the concentration at ground level with downwind direction.

3.3 Determination of $\sigma_y(x)$ and $\sigma_z(x)$

ALOHA must estimate $\sigma_y(x)$ and $\sigma_z(x)$ using simple inputs and in the absence of research-grade instrumentation. The user can select one of two methods to estimate the dispersion parameters:

1. **Stability-Class Method.** This method requires manual input of time, wind speed, wind direction, ground roughness, stability class, and cloud index. Solar insolation is computed from given time and location information. These are used to compute σ_y and σ_z.

2. **σ_θ Method.** σ_θ is the standard deviation of wind direction about its mean value. Measurements of σ_θ from a weather station are used to compute σ_y and σ_z. This method can be used only if an automatic weather station (SAM) is connected to the computer.

3.3.1 Stability Class Method

The discussion of Hanna et al. (1982) provides a good description of this classic method. The equations are based on certain field experiments with uniform terrain and distances less than

1 km. There is no observational evidence to justify use of the equations beyond 1 km, although it is done routinely.

The stability class ranges from A to F[3] as the surface layer varies from highly unstable to highly stable. Table 3.1 shows the original Pasquill types.

Table 3.1: Meteorological conditions defining Pasquill turbulence types.

A: Extremely unstable
B: Moderately unstable
C: Slightly unstable
D: Neutral
E: Slightly stable
F: Moderately stable

Surface wind speed, $m\,s^{-1}$	Daytime insolation			Nighttime conditions	
	Strong	Moderate	Slight	Thin overcast or $> \frac{4}{8}$	$\leq \frac{3}{8}$ cloudiness
<2	A	A–B	B		
2–3	A–B	B	C	E	F
3–5	B	B–C	C	D	E
5–6	C	C–D	D	D	D
>6	C	D	D	D	D

Table 3.2: Analytical expressions from Briggs (1973) for $\sigma_y(x)$ and $\sigma_z(x)$.

CLASS	σ_y (m)	σ_z (m)
Open-country Conditions		
A	$0.22x(1+0.0001x)^{-\frac{1}{2}}$	$0.20x$
B	$0.16x(1+0.0001x)^{-\frac{1}{2}}$	$0.12x$
C	$0.11x(1+0.0001x)^{-\frac{1}{2}}$	$0.08x(1+0.0002x)^{-\frac{1}{2}}$
D	$0.08x(1+0.0001x)^{-\frac{1}{2}}$	$0.06x(1+0.0015x)^{-\frac{1}{2}}$
E	$0.06x(1+0.0001x)^{-\frac{1}{2}}$	$0.03x(1+0.0003x)^{-1}$
F	$0.04x(1+0.0001x)^{-\frac{1}{2}}$	$0.016x(1+0.0003x)^{-1}$
Urban Conditions		
A–B	See Note 1 below	$0.24x(1+0.001x)^{-\frac{1}{2}}$
C		$0.20x$
D		$0.14x(1+0.0003x)^{-\frac{1}{2}}$
E–F		$0.08x(1+0.0015x)^{-\frac{1}{2}}$ (note 2)

Note 1: By recommendation from the ALOHA Review Committee (May 1990), the open-country values for σ_y are used in urban conditions.
Note 2: The coefficient for E-F, urban conditions, was incorrectly given in Briggs (1973) as 0.00015. This was corrected by Briggs (1991).

ALOHA asks the observer for stability class, wind speed, and cloud cover on a scale[4]. Users can access Table 3.1 through the on-line help option as an aid in selecting stability class. Certain combinations of wind speed and insolation are very unlikely and ALOHA alerts the user when they select one of the "forbidden" combinations. The Pasquill turbulence classes are shown in Figure 3.5 as a function of Monin-Obukhov length, L, and aerodynamic roughness, z_0 (Golder, 1972). L is a scale height where thermal production or suppression of turbulence equals

[3]Occasionally one sees a G class to fill in the spaces in Table 3.1. There is no strong justification for doing this and ALOHA does not.

[4]ALOHA requests cloudiness on a 0–10 scale. When algorithms require another scale, such as 0–8, an interpolated value is computed.

mechanical production (Sec. 4.3.2). ALOHA uses stability class D when the sky is completely overcast regardless of wind speed or time of day.

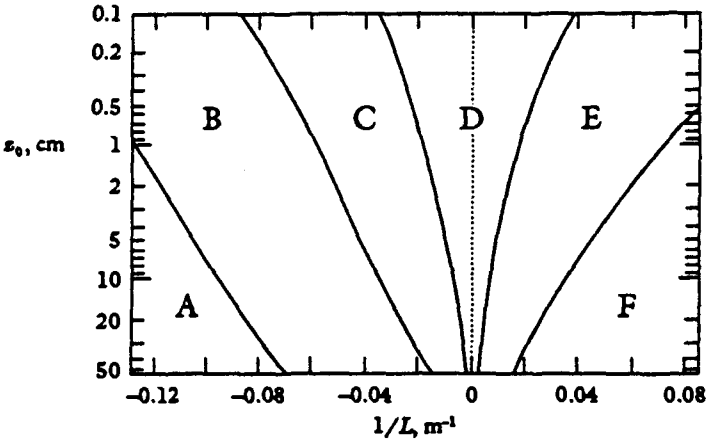

Figure 3.5: Stability classes designate ranges of turbulence. See discussion below.

Once a stability class has been identified, the dispersion parameters are calculated using empirical equations. The observed variation of $\sigma_y(x)$ and $\sigma_z(x)$ over surfaces with different roughnesses was simplified by Briggs (1973) (see also Hanna et al., 1982) and resulted in the relationships given in Table 3.2.

In 1990, an ALOHA technical review committee pointed out that the original Briggs coefficients did not account for the averaging times in the different data sets from which they were derived. Rural coefficients were derived from the Prairie Grass data with three-minute averages and the urban coefficients were derived from the St. Louis data which used one-hour averages. When the dispersion coefficients were corrected for this difference, the curves were identical. Thus, ALOHA 5.0 uses only the rural coefficients.[5]

3.3.2 σ_θ Method and the SAM Weather Station

The SAM weather station

The σ_θ method of determining the dispersion parameters requires input from an external meteorological station. ALOHA software is designed to interface to a portable weather station it refers to as a SAM (Station for Atmospheric Measurements). The SAM samples wind speed and wind direction at a a rate of one sample each two seconds. The station either is aligned to north or uses a compass to correct each wind measurement from relative to true geographic coordinates. Wind speed and direction are converted to u and v wind vector components and, in addition, wind direction is converted to unit-vector coordinates, $\hat{x}$ and $\hat{y}$. Components u and $\hat{x}$ are aligned

[5]Briggs (1991) noted that his analytical solution for σ_y is based on Pasquill's (1961) curves, and has an averaging time of three minutes. He chose three minutes because longer-term averages include larger-than-local effects. He did not make a distinction between rural and urban formulations. In any case, he recommended that his new formulations for σ_y be implemented. That recommendation is under consideration for the next versions of ALOHA.

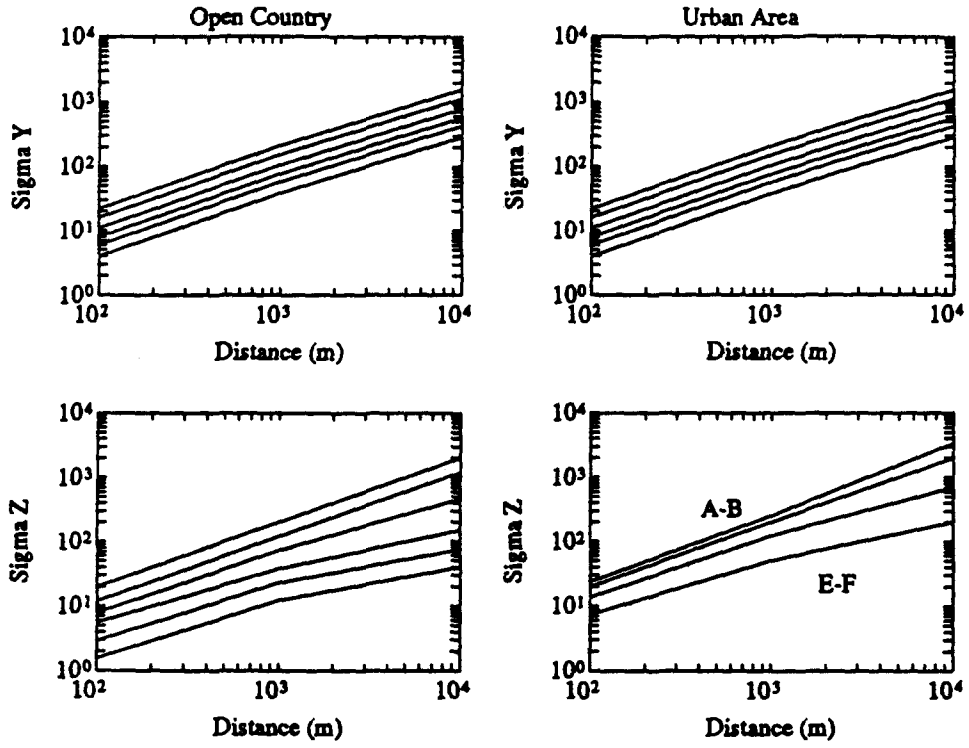

Figure 3.6: Plot of Briggs dispersion coefficients (Briggs, 1973) as shown in Table 3.2. The plots on the left are for open country, $z_0 = 0.1$ m. The plots on the right are representative of urban conditions, $z_0 \approx 1$ m. The curves represent stability classes A–F from top to bottom respectively.

to east and v and $\hat{y}$ are aligned to north. Unit vectors are averaged and the averages, X and Y respectively are converted to estimates of σ_θ. Manufacturers may use different methods to compute the sigmas, but the methods described by Yamartino (1984) are recommended.

$$\epsilon^2 = 1 - (X^2 + Y^2) \tag{3.8}$$

$$\sigma_\theta = \arcsin(\epsilon)\,[1.0 + b\epsilon^3] \tag{3.9}$$

where $b = (2/\sqrt{3}) - 1 = 0.1547$.

The SAM station computes five-minute running averages of measured quantities and transmits a data line each 30 seconds. A data line is formatted as a comma-delimited free field in the form

```
<cr><lf>ID,VS,VD,SD,TA,SP,WD,TI,B,CHK
```

where <cr><lf> are the carriage and line feed characters for alignment, ID is the station identification number, VS is the vector mean wind speed ($m\,s^{-1}$), VD is the vector mean wind direction (°true), SD is the standard deviation in the wind direction (deg), TA is the average air temperature (°C), SP is the instantaneous wind speed ($m\,s^{-1}$), WD is the instantaneous wind direction (°true), TI is the instantaneous air temperature (°C), B is the weather station battery voltage (volts), and CHK is a checksum computed as the arithmetic sum of the ASCII decimal values of all characters in the string including the carriage return and line feed characters.

σ_θ Method of Determining Pasquill Stability Class

When measurements of σ_θ are available, the Pasquill stability classes are determined by methods in U.S. Environmental Protection Agency (1987, pages 6-27 to 6–30). The method involves looking up information in Tables 3.3 and 3.5, shown below. According to EPA (ibid) users of the method below will select the correct stability class 50% of the time and will miss by less than one class more than 90% of the time.

The procedure uses the following definitions. The measurement height, Z_m, is 10 m, and the assumed roughness coefficient, z_0, is 0.15 cm. The height and roughness can be corrected, but measurements must be taken in the range $2 \leq Z_m \leq 10$ m. Nighttime is the period from one hour before sunset to one hour after sunrise. The averaging period for mean wind and σ_θ must be in the range 3–60 minutes. It is essential that the mean values are relatively constant in time during the sampling period. The SAM averaging period of 5 minutes meets these criteria and is short enough that the stationarity assumption is generally valid. Typically, the SAM measurement height is 2 m.

If the site roughness differs from 0.15 m, the limits of σ_θ in Table 3.3 must be corrected. For a given value of surface roughness, the measured values of σ_θ in Table 3.3 are corrected by the equation

$$\sigma'_\theta = (\sigma_\theta)_m \left(\frac{z_0}{0.0015}\right)^{0.2} \tag{3.10}$$

where σ'_θ is the corrected value, $(\sigma_\theta)_m$ is the measured value, and z_0 is the roughness for the terrain in meters. Examples of roughness lengths for different terrains are given in Table 3.4 (Wieringa, 1980).

Table 3.3: Initial estimate of stability class for measured σ_θ. Ranges of σ_θ are for $z_0 = 0.15$ m and measurement height, $Z_m = 10$ m. Use (3.10) and (3.11) respectively for different conditions.

INITIAL CLASS	σ_θ RANGE
A	$22.5 \leq U < 90^*$
B	$17.5 \leq U < 22.5$
C	$12.5 \leq U < 17.5$
D	$7.5 \leq U < 12.5$
E	$3.8 \leq U < 7.5$
F	$0 \leq U < 3.8$

* When measurements of σ_θ approach 90°, the measurement is suspect and the site or the equipment must be examined.

After correcting for roughness, a correction for the measurement height is made. If the measurement height, Z_m, is different than 10 m, a correction is applied. The equation for this is

$$\sigma_\theta = \sigma'_\theta \left(\frac{Z_m}{10}\right)^{-p} \tag{3.11}$$

where σ_θ is the finally corrected value for use in Table 3.3 and Z is the actual measurement height. The exponent $p = [0.06, 0.15, 0.17, 0.23, 0.38, 0.38]$ for stability classes A–F respectively.

Table 3.4: Terrain classification in terms of z_0.

TERRAIN TYPE	z_0 (m)
Open sea, fetch at least 5 km	0.0002
Open flat terrain, grass, few isolated obstacles	0.03
Low crops, occasional large obstacles, $x'/h > 20$ •	0.10
High crops, scattered obstacles, $15 < x'/h < 20$	0.25
Parkland, bushes, numerous obstacles, $x'/h > 10$	0.5
Regular, large, obstacle coverage (suburb, forest)	0.5–1.0

• x' = typical distance to upwind obstacle
h = height of obstacle

Table 3.5: Wind speed correction for final stability class. Use with Table 3.3.

Daytime

INITIAL CLASS	U_{10} (m s^{-1})	FINAL CLASS
A	$0 \le U_{10} < 3$	A
	$3 \le U_{10} < 4$	B
	$4 \le U_{10} < 6$	C
	$6 \le U_{10} < \infty$	D
B	$0 \le U_{10} < 4$	B
	$4 \le U_{10} < 6$	C
	$6 \le U_{10} < \infty$	D
C	$0 \le U_{10} < 6$	C
	$6 \le U_{10} < \infty$	D
D,E,F	any	D

Nighttime

INITIAL CLASS	U_{10} (m s^{-1})	FINAL CLASS
A	$0.0 \le U_{10} < 2.9$	F
	$2.9 \le U_{10} < 3.6$	E
	$3.6 \le U_{10} < \infty$	D
B	$0.0 \le U_{10} < 2.4$	F
C	$2.4 \le U_{10} < 3.0$	E
	$3.0 \le U_{10} < \infty$	D
C	$0.0 \le U_{10} < 2.4$	E
	$2.4 \le U_{10} < \infty$	D
D	any	D
E	$0.0 \le U_{10} < 5.0$	E
	$5.0 \le U_{10} < \infty$	D
F	$0.0 \le U_{10} < 3.0$	F
	$3.0 \le U_{10} < 5.0$	E
	$5.0 \le U_{10} < \infty$	D

Table 3.5 provides a correction to the stability class based on the 10-m wind speed, U_{10}. In general, for $2 \le U_m \le 10$, the correction of U_m to U_{10} is small and other factors contribute much larger errors. Hence, U_m can be used directly.

3.4 Time-Varying Source as a Sequence of Clouds

The source module software produces a time-dependent, point-source emission approximation as a sequence of five point-source emissions, each with constant emission rate for a finite time. The time intervals are selected to represent the actual source curve and to reproduce faithfully the peak emissions. With this digitization scheme, the model must keep track of five separate gas clouds and the concentration at any point is simply a summation of the concentrations from all the clouds.

In this section we discuss a model of a single gas cloud, and then we extend the model to the full case of five clouds. A sketch of one case where three gas clouds are emitted is shown

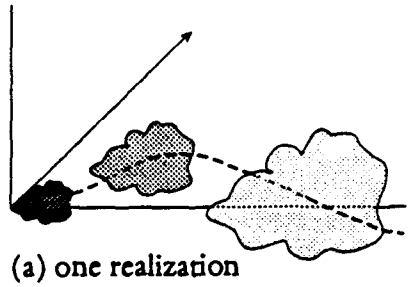

(a) one realization

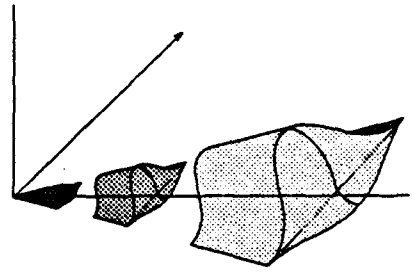

(b) ensemble average

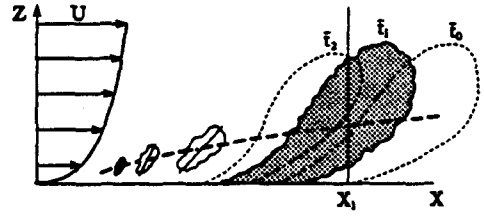

(c) effects of vertical shear

Figure 3.7: Diffusion of a series of gas clouds released at ground level. (a) An instantaneous realization of three clouds. (b) The ensemble mean of the cloud behavior. (c) Diffusion of a series of clouds in shear flow (Wilson, 1981, page 490)

in Figure 3.7: (a) Snapshot of the three clouds at the moment when the third emission has been completed; (b) The ensemble (one-hour) average for three clouds has a centerline along the x-axis and exhibits dispersion in all three directions; and (c) An x-z cross-section through the three clouds. The dashed cloud is produced by setting $\sigma_x = \sigma_x(x_1)$, $\sigma_y = \sigma_y(x_1)$, and $\sigma_z = \sigma_z(x_1)$ over the entire x length of the cloud. x_1 is the center point of the cloud.

The effect of surface wind shear is to bend the plume in a forward direction. The combination of vertical mixing motion with wind shear strongly enhances the along-wind dispersion of the gas.

3.4.1 Puff Dispersion

The mathematical derivation for the gas cloud model used in ALOHA 5.0 is provided by Palazzi et al. (1982). An infinitesimal puff of gas with mass dM is emitted with a mass flow rate of Q over a time dt. The differential equation for an infinitesimal portion of the source release is

given by the classical equation for the concentration of a puff.

$$dC(x,y,z,t) = \frac{Q(t)}{U}\, g_x(x,t)\, g_y(x,y)\, g_z(x,z)\, dt \tag{3.12}$$

where $g_y(x,y)$ and $g_z(x,z)$ are defined in Equations (3.2) to (3.6). In the original formulation, the speed U is the velocity of the puff centroid (center of mass). ALOHA substitutes the mean wind speed, U_{10} with little induced error.

Downwind, x-dispersion of the puff is present and is given by

$$g_x(x,t) = \frac{1}{\sqrt{2\pi}\sigma_x(x)} \exp\left[-\frac{1}{2}\left(\frac{(x-U_{10}t)}{\sigma_x(x)}\right)^2\right] \tag{3.13}$$

The x-spreading defines a puff whose center moves downwind at speed U_{10}, and whose volume increases in all three directions.

A gradient of mean wind in the vertical direction (wind shear) strongly enhances x-dispersion. As discussed by Wilson (1981b), two processes contribute to σ_x and the combination is given by

$$\sigma_x^2 = \sigma_{xs}^2 + \sigma_{xt}^2 \tag{3.14}$$

where σ_{xs} is the dispersion induced by the combined vertical mixing and advection by mean vertical wind shear, and σ_{xt} is the dispersion induced by turbulent spread. Wilson's relationship for σ_x in the constant-stress, logarithmic region near the ground leads to large values of σ_x. Above approximately one meter, the wind speed gradient is relatively small, and ALOHA follows the suggestions of Beals (1971) and Palazzi (1982) and uses values of $\sigma_x \approx \sigma_y$ (Figure 3.8).

3.4.2 Cloud Dispersion from a Release of Finite Duration

A cloud is formed when the gas is released at rate Q for a finite time duration of $(0 \le t \le t_r)$. Equation (3.12) is integrated over the release time assuming σ_x, σ_y and σ_z are constant over the span of the cloud.

$$C(x,y,z,t) = \begin{cases} \frac{\chi}{2}\left[\mathrm{erf}\left(\frac{x}{\sigma_x\sqrt{2}}\right) - \mathrm{erf}\left(\frac{(x-Ut)}{\sigma_x\sqrt{2}}\right)\right] & (t \le t_r) \\ \frac{\chi}{2}\left[\mathrm{erf}\left(\frac{x-U(t-t_r)}{\sigma_x\sqrt{2}}\right) - \mathrm{erf}\left(\frac{x-Ut}{\sigma_x\sqrt{2}}\right)\right] & (t_r < t < \infty) \end{cases} \tag{3.15}$$

where $\chi(x,y,z) = (Q(t)/U)\, g_y(x,y)\, g_z(x,z)$ is the equation for a classical Gaussian plume as defined by (3.2)–(3.5). The 10-meter wind, U_{10}, is used for the centroid wind speed, U.

Equation (3.15) implies that the centroid of the cloud moves with the wind speed, U, and that the dispersion parameters are constant over the entire cloud. These are questionable approximations and warrant further investigation.

3.5 CAMEO vs. ALOHA 5.0 Models

CAMEO uses a steady-state Gaussian model in its scenarios options stack. Plume predictions made by CAMEO differ from ALOHA steady-state Gaussian plumes in urban release cases. The

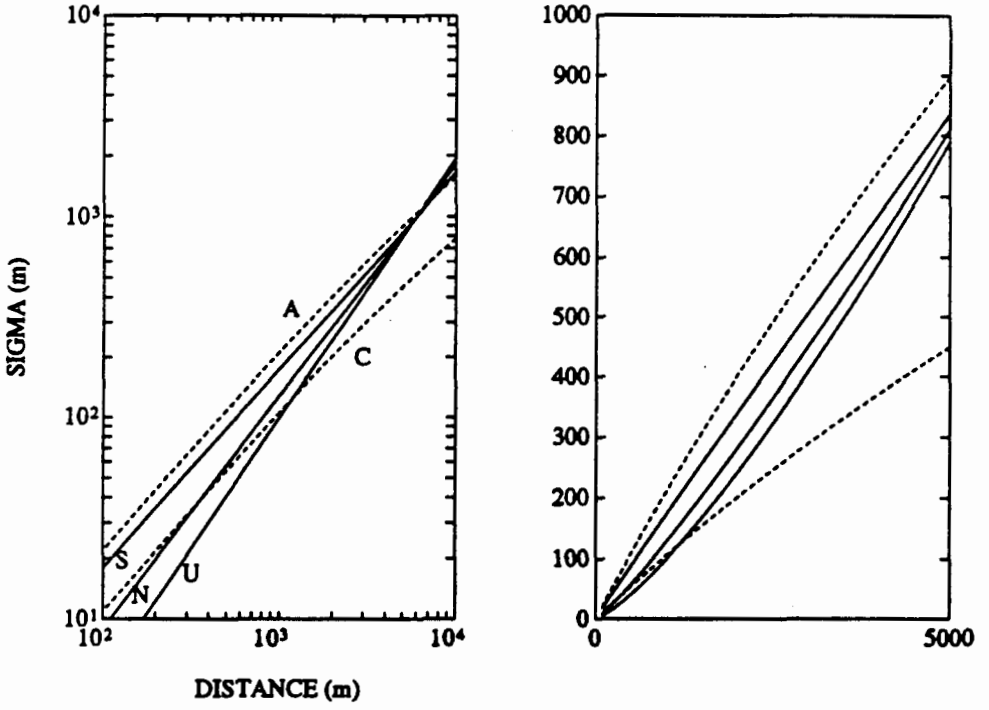

Figure 3.8: Graph of σ_z for stable, neutral, and unstable boundary layers from Beal (1971). The dashed lines are curves for σ_y for classes A and C from Figure 3.6 (urban and open country values are the same). The same data are shown as log-log and linear plots.

difference is a result of ALOHA's use of rural Briggs' coefficients for both rural and urban cases (see Table 3.2, page 49) and CAMEO's use of the original values.

The result of changing ALOHA is that for urban conditions, ALOHA predicts a longer plume than CAMEO. The difference in the length between ALOHA and CAMEO plumes is dependent on boundary-layer stability. Under class A it is less than 10% longer usually, but under class F it can be almost double the CAMEO output.

Mathematical Symbols

A–F	stability classes for the turbulent boundary layer (none)
b	parameter used in the computation of σ_y from vector averages. (none)
C	contaminant concentration ($\mathrm{kg\ m^{-3}}$)
C_l	cloudiness index, $\{0, 1, \ldots, 10\}$ (none)
g_x	Gaussian dispersion function in the x direction ($\mathrm{m^{-1}}$)
g_y	Gaussian dispersion function in the y direction ($\mathrm{m^{-1}}$)
g_z	Gaussian dispersion function in the z direction ($\mathrm{m^{-1}}$)
h_i	height of the inversion (m)
h_s	height of the source above the ground (m)
h'_s	effective stack height as a result of lofting of a buoyant plume (m)
J	integer number of image sources to be considered at x as a result of ground-inversion trapping (none)
L	Monin-Obukhov length (m)
n	summation index (none)
p	exponent in the correction of dispersion coefficients for measurement height (none)
Q	source emission strength ($\mathrm{kg\,s^{-1}}$)
t	time (s)
U	mean wind speed in the x direction ($\mathrm{m\,s^{-1}}$)
U_{10}	mean wind measured at a standard height of 10 m ($\mathrm{m\,s^{-1}}$)
U_m	mean wind speed measured at an arbitrary height, Z_m ($\mathrm{m\,s^{-1}}$)
u, v, w	instantaneous wind speed components in the x, y, z directions ($\mathrm{m\,s^{-1}}$)
u', v', w'	turbulent wind speeds in the x, y, z directions ($\mathrm{m\,s^{-1}}$)
x	the horizontal distance downstream (m)
$\hat{x}$	eastward component of the unit vector from vane measurement (none)
X	unit vector average in the east direction (none)
y	the horizontal distance perpendicular to the plume axis (m)
$\hat{y}$	northward component of the unit vector from vane measurement (none)
Y	unit vector average in the north direction (none)
z	vertical distance above the ground (m)
z_0	the turbulent roughness length (m)
Z_m	measurement height of a weather station (m)
ϵ	parameter used in the computation of σ_θ from measurements (-)
σ_x	downwind dispersion parameter used for puff formulations (m)
σ_y	the cross-wind dispersion parameter (m)
σ_z	the vertical dispersion parameter (m)
σ_θ	the standard deviation in horizontal wind direction (deg)
σ'_θ	roughness-corrected standard deviation in horizontal wind direction (deg)
$(\sigma_\theta)_m$	estimate of σ_θ from measurements at Z_m (deg)
χ	2-D Gaussian plume concentration ($\mathrm{kg\,m^{-3}}$)
$(.)_\tau$	the τ-minute average of a quantity (none)

Chapter 4

Heavy Gas Dispersion

4.1 General Comments

Most hazardous industrial materials produce a cloud that is heavier than the ambient air. Industrial gases and liquefied energy gases (LEG) are stored, handled, and shipped in large quantities and have attracted attention because of the magnitude of the potential hazards in cases of accidental releases. Recent terrible accidents are the dioxin release in Seveso Italy, the methyl isocyanate release in Bhopal, India in 1984, and liquefied petroleum gas explosions in Mexico City in the same year. There are over 100 analytical or numerical models currently available that describe the dispersion of dense gases (Britter, 1989). ALOHA 5.0 includes an adaptation of the DEGADIS heavy-gas dispersion model (Havens and Spicer, 1985; Spicer and Havens, 1989) because of the general acceptance of DEGADIS, and the extensive testing that was carried out by the authors. DEGADIS is an adaptation of the Shell HEGADIS model described by Colenbrander (1980, 1983) and it incorporates some techniques used by van Ulden (1974, 1983). The ALOHA user can choose to use either a Gaussian or a heavy-gas dispersion model. If ALOHA sees that the release is sufficiently dense (see Sec. 4.2.3), it will treat the release as a case of heavy gas dispersion unless prevented by the user.

ALOHA-DEGADIS incorporates simplifications which speed up computations and reduce the amount of input data that would not typically be available in an emergency situation:

1. **Ground releases only.** The original momentum jet model for elevated sources (Ooms, 1974) is not included, and ALOHA-DEGADIS assumes that all spills originate at ground level.

2. **Simplified equations.** The mathematical approximation procedures used for solving the model's equations are faster, but more approximate than those used in DEGADIS.

3. **Approximations for non-steady sources.** When the source strength varies in time, ALOHA-DEGADIS solves the equations for a series of short, steady releases.

4. **Footprint approximation.** The iterative solutions required for DEGADIS are too time-consuming on an ordinary personal computer and, hence, footprint contours are based on a continuous release of the peak source strength. This and other approximations are discussed in detail in Sec. 4.6.1.

4.2 Examples of Transient and Continuous Releases

Cloud behavior depends primarily on the ambient wind speed, U, and the cloud density. The density difference between the gas cloud and the ambient air is represented by the density ratio $\Delta = (\rho - \rho_a)/\rho_a)$, and the buoyancy force is proportional to the **reduced gravity**, $\hat{g} = g\Delta$. (See equation (4.3).) In the case of heavy gases, $\Delta > 1$ and the ambient turbulent mixing is suppressed.

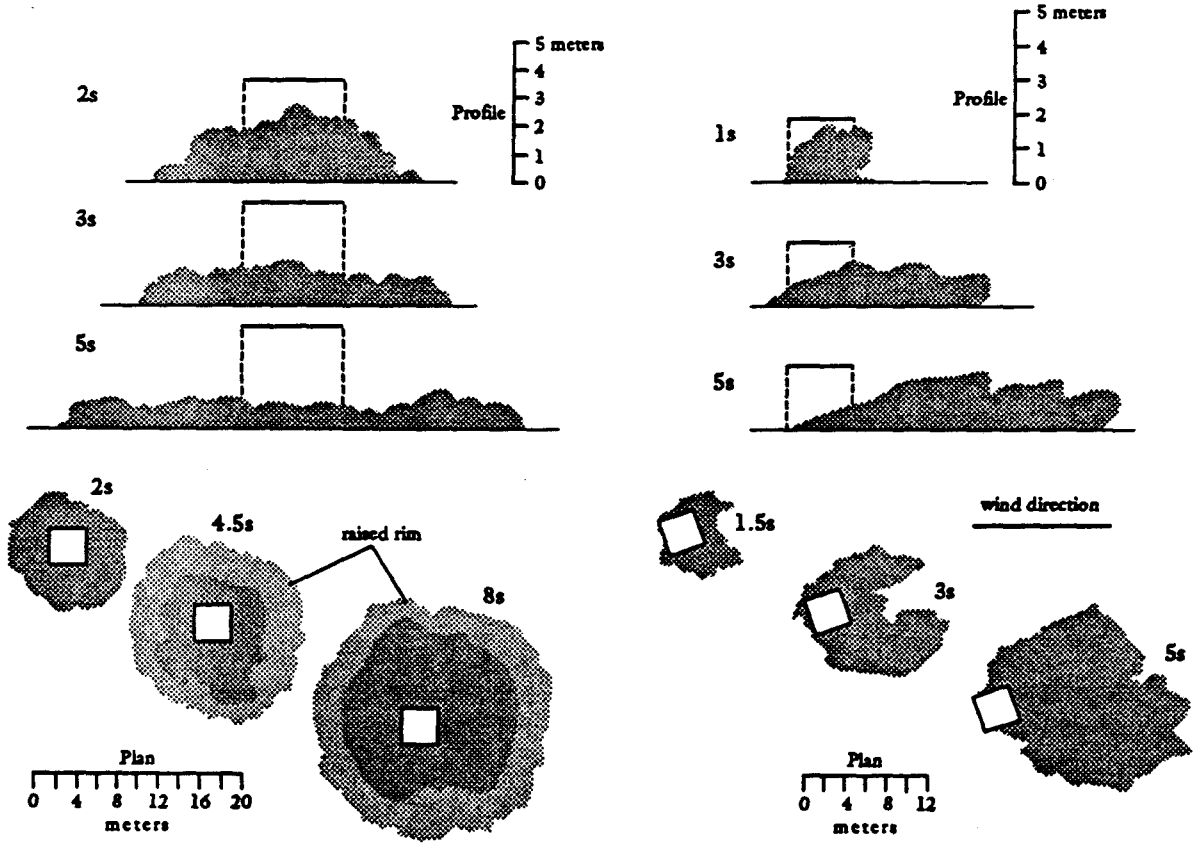

Figure 4.1: Sketches of the release of 40 m^3 of Freon-12 in (a) calm and (b) windy conditions on a level surface in Porton Downs, England. (from Picknett, 1981)

Three stages in a heavy gas release are (Havens and Spicer, 1985):

1. **Buoyancy-Dominated Dispersion.** This is the near-source region where the buoyancy forces, the inertial forces, and the ambient air motions all contribute to the development of the cloud. The initial heavy cloud will "slump" over the ground and spread as an expanding vortex ring called a **head**. A useful rule of thumb is that in the process it will entrain approximately ten times its original mass of ambient air, i.e. the density ratio is reduced by a factor of ten. This stage occurs quickly, so that the advection by ambient wind is neglected. At the end of this stage, a thin **blanket** is formed.

The buoyancy-dominated regime evolves through three overlapping sub-stages: (i) *Slumping*, where the strong, buoyancy-dependent spreading forces are balanced by counter-flow of the ambient fluid. This phase occurs in a few seconds. (ii) *Buoyancy-inertial phase*, where the buoyancy spreading forces are balanced by inertial forces. Extreme cloud dilution occurs in this phase as a spreading "head" which entrains ambient fluid (Figure 4.2). (iii) *Viscous phase*, where buoyancy forces are balanced by viscous forces. Turbulent mixing is suppressed and the dilution rate is greatly reduced. Because almost all the entrainment occurs in the buoyancy-inertial phase, this physical process was closely modeled in DEGADIS.

2. **Stably Stratified Shear Flow.** In this region, buoyancy forces and ambient flow determine the plume development. The dispersion process can be described as a stably stratified cloud embedded in the mean wind flow. The cloud remains thin and spreads laterally as it is advected downwind. The stable density profile in the cloud suppresses turbulence, and turbulent fluctuations in the cloud are less than ambient levels. Air is entrained into the spreading cloud through the edges and, primarily, through the top

3. **Passive Turbulent Dispersion.** Cloud dilution continues until its excess density has a negligible effect on the dispersion and natural levels of turbulence return. The gas becomes a passive contaminant.

4.2.1 Transient Releases

Transient heavy gas releases provide a clear picture of the rapid and complex buoyancy-dominated stage of a release. Current knowledge of the behavior of heavy gas has benefited from three experiments in which the initial gas shape was in the form of a "top hat" (Raj, 1982): (a) Porton Downs: 42 experiments with 40 m^3 releases of Freon-12 (Picknett, 1981; Figure 4.1). Tests were conducted on flat and sloping ground and in neutral to unstable stratifications. (b) Thorny Island, where 2000 m^3 of freon-nitrogen mixture were released (McQuaid, 1984); and (c) Havens and Spicer (1985) released 2-m^3, top-hat clouds of Freon-12 in an enclosed environment.

The entire buoyancy-dominated flow stage occurs in a few seconds (Figure 4.1) and any drift of the cloud by mean wind advection is neglected. The effects of large-scale convective mixing are also negligible. The Porton Downs blanket was almost fully formed in eight seconds with a 4.7 $m\,s^{-1}$ wind. Flow perturbations around the structure were quickly erased so the blanket was almost identical to the calm-air example with the exception of a small downwind drift. The downwind drift of the cloud depends on the entrainment of momentum from ambient air into the cloud. Typically, the downwind translation of the centroid of the cloud is about $0.5\,U_{10}$.

As the rapidly spreading cloud forces itself under the ambient atmospheric boundary layer, shear at the ground and at the top of the cloud creates a vortex ring at the forward edge of the cloud (Britter, 1989). This head is a region of high shear and considerable entrainment of ambient air (Figure 4.2). The advancing head is stabilized by vortex stretching as it expands, and some of the mixed fluid is left behind to provide a substantially diluted cloud. Eventually the leading-edge vortex weakens and adopts a classical, gravity-head form.

Figure 4.3 shows the growth and dissipation of a cloud of cold Freon-12 which evaporated quasi-instantly from a puddle. During the first few seconds, expansion caused intensive mixing with the air and resulted, after 5 sec, in $\Delta = 1.25$. The boundary layer was neutral, $U_{10} = 3$ $m\,s^{-1}$, $z_0 = 0.05$ m, and $u_* = 0.25$ $m\,s^{-1}$(van Ulden, 1974).

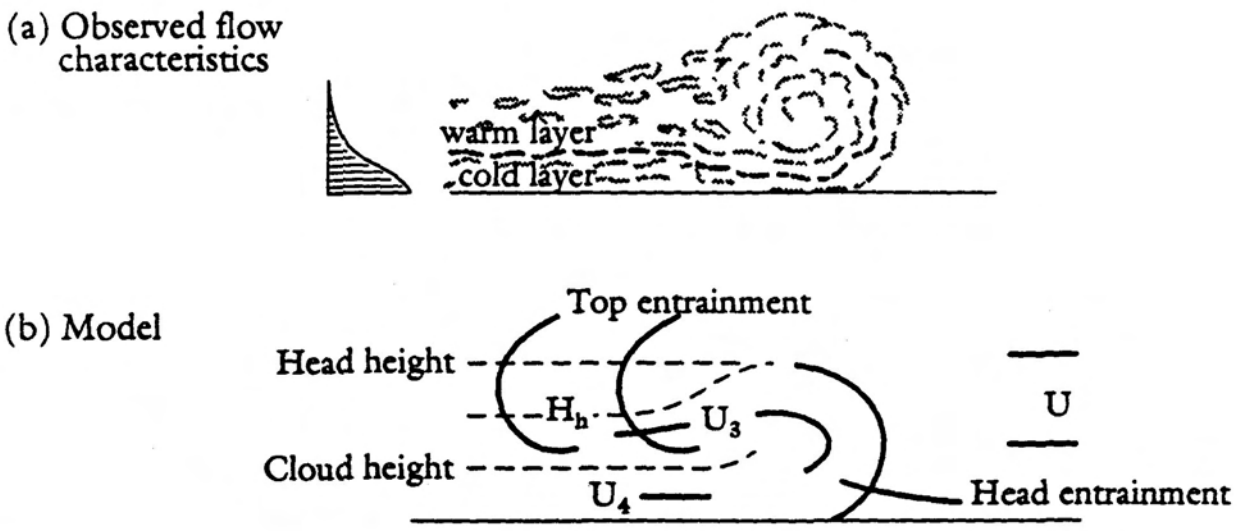

Figure 4.2: Observed and modeled descriptions of the head of a steady gravity current. The flow acts to redistribute the mass consistent with a thin, nearly flat cloud. The peak of the front is cut off and re-entrained, aided by negative buoyancy. (Adapted from Fanneløp and Jacobsen, 1984 and Havens and Spicer, 1985.)

4.2.2 Continuous Releases

Observations in the laboratory and in the field show a wide, flat plume downwind of the source, and in the case of low U or large Δ, the plume extends upwind of the source and can be wider than the physical source size. The extent of the cloud upwind and to the sides of the source has not been well defined (Britter, 1989). Ambient flow will limit the upwind spread and ensure that all material will be carried downwind. In some cases, a gravity-current head is formed and in other situations of a deeper surface layer, the gravity-current head will collapse to form a salt-wedge counterflow as in certain estuaries.

The major stages in the development of a heavy cloud release (Figure 4.4) are identical to a near-instantaneous release. In the stable shear-flow dispersion region, the ambient turbulence is reduced and the stable density gradient can lead to a cloud that spreads considerably and thins out.

Measured concentrations in dense gas plumes show similar characteristics: (a) sharp, well-defined edges in the gravity-flow region, (b) lateral concentration profiles approach Gaussian shape in the passive region, (c) near exponential variation in vertical concentration profiles, (d) density difference reduces mixing between the plume and the air and causes the plume to become spread and thin. (e) the resulting larger surface area provides more area for entrainment and plume dilution. The last two characteristics—reduced mixing and increased mixing area—result in the surprising fact that, beyond the near field, measured, ground-level, heavy-gas concentrations along the plume axis are predicted well by Gaussian models.

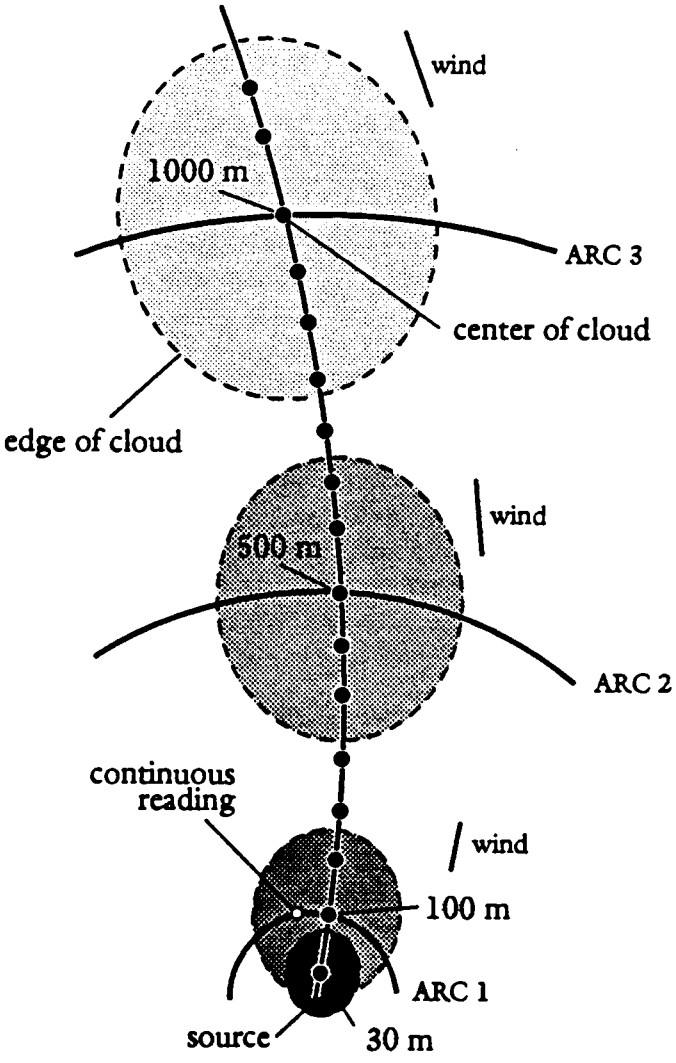

Figure 4.3: Progress of a cloud of cold Freon-12 which evaporated quasi-instantly from a puddle. Adapted from van Ulden (1974).

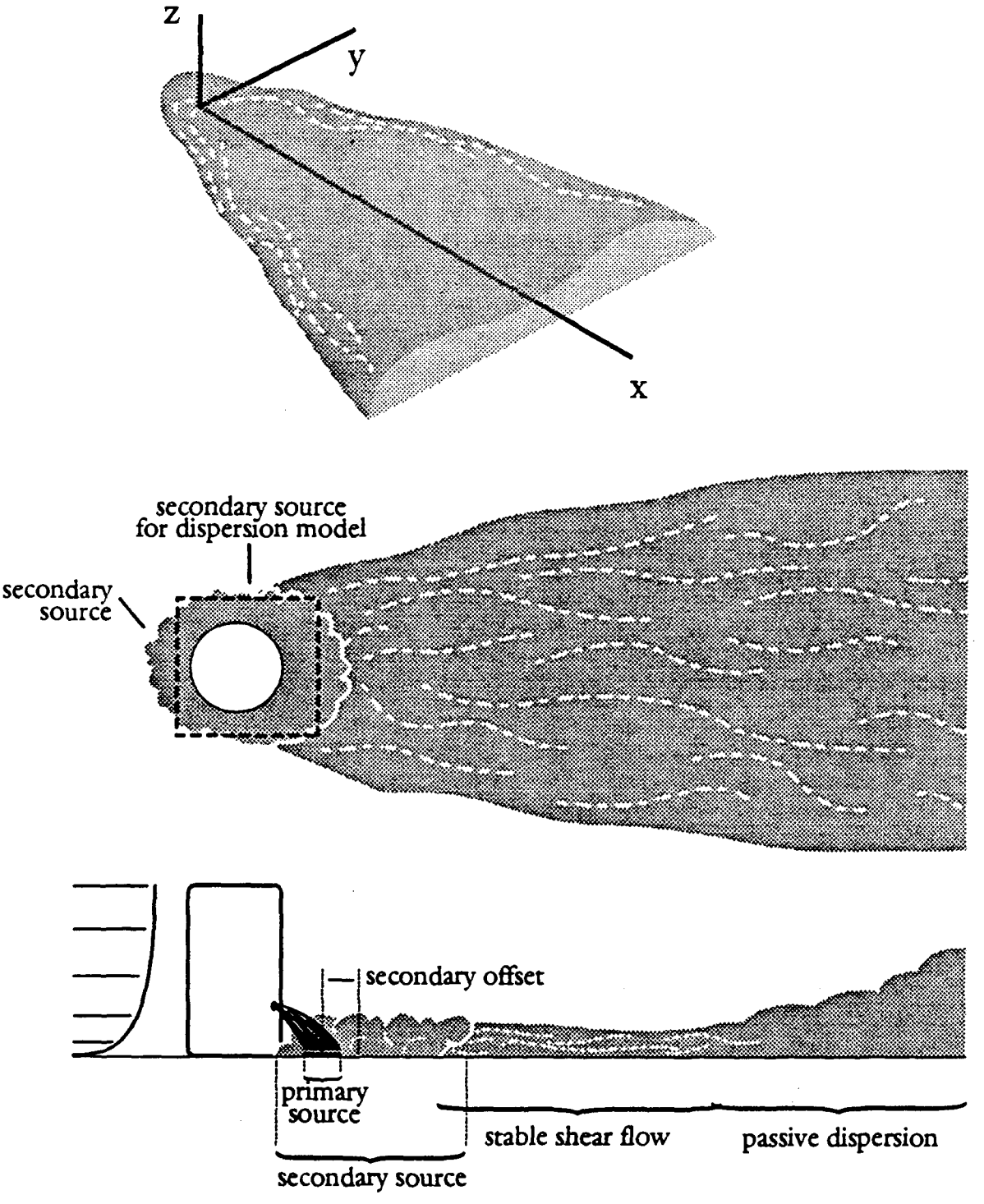

Figure 4.4: The major stages of a heavy gas cloud. Profile view of a near-continuous release into a surface layer wind shear. (a) The source as defined in Chapter 2 can be a near-instantaneous release, a continuous release, a puddle, or a leaking tank or pipe. (b) a stable stratified shear flow region quickly forms with subdued vertical dispersion and enhanced horizontal dispersion compared to a passive gas. (c) After considerable dilution, ambient turbulence dominates the mixing processes and the dispersion is well described by passive (Gaussian) dispersion formulations.

4.2.3 Criteria for Heavy Gas vs. Gaussian Modeling

A slightly heavy gas may not be able to overcome the ambient advection and turbulence, and so can be modeled as a passive gas with little error. A small release into a strong wind or highly convective atmosphere, or a release over a large source area may be considered effectively passive.

Spicer and Havens (1989) use the friction Richardson's Number as the criterion for passive or non-passive dispersion.

$$\mathrm{Ri}_C = \frac{\hat{g}_0 H}{u_*^2} \leq 1 \tag{4.1}$$

where $\hat{g}_0$ is the initial reduced gravity of the source gas, H is a characteristic height for the source, and u_* is the friction velocity of the ambient air flow and is discussed on page ??. DEGADIS uses observations from a water tunnel to approximate $u_* = U_{10}/16$. When Ri_C is less than 1, the gas is considered to be passive and, unless instructed otherwise, ALOHA will compute dispersion using the Gaussian dispersion model.

Determination of the characteristic cloud height depends on the type of source discharge. For an instantaneous release of volume, V_0, the source height is given by $H = V_0/A_0$, where A_0 is the ground area of the source. For a continuous or semi-continuous discharge with volume flow rate $\dot{V}_0$ $\mathrm{m^3\,s^{-1}}$, the characteristic height is given by $H = \dot{V}_0/U_{10}D$, where D is the scale dimension of the source.

The above equations indicate the importance of the ambient wind speed. In the case of a continuous discharge, a doubling of the wind speed is equivalent to a 8-times increase in release volume.

4.2.4 Primary and Secondary Source

Many possible sources are described in Chapter 2. Each of the source types (evaporating puddle, instantaneous release, etc.) has a known or computed size. For heavy gas modeling, the actual chemical release source is called the **primary source** and it is assumed that it is circular with radius R_p.

With lower winds and/or more dense gases, the gas will spread around the primary source forming a **secondary source** or **blanket** which approximates as a circular blanket with radius R_b. The **maximum amount** of contaminant that can be taken into the atmosphere is called the **maximum atmospheric takeup rate** and is represented by $Q_{*max}(t)$ with units of $(\mathrm{kg\,s^{-1}\,m^{-2}})$, and if the primary release rate exceeds Q_{*max}, then the heavy gas blanket forms. (The source input for ALOHA-DEGADIS is discussed in Sec. 4.4.) Any down-wind displacement of the secondary source from the primary source is neglected.

The size and density of the blanket is computed by a balance of mass and thermodynamics (Sec. 4.4) and this result is an input to the dispersion model discussed in Sec. 4.5. The heavy gas dispersion model in rectangular coordinates needs a rectangular source, and a square secondary source with the same area is assumed: $2B = \sqrt{\pi} R_b$. B is the **secondary source half-width.** If the primary source release rate is less than Q_{*max}, the released gas is taken up directly by the atmosphere and dispersed downwind.

4.3 Fluid Dynamic Approximations and Simplifications

This section describes the parameters used to describe the complex dynamic and thermodynamic processes in a heavy gas cloud.

4.3.1 Density and Reduced Gravity

Colenbrander (1980) and Colenbrander and Puttock (1983) distinguish between several different densities related to the dispersing gas cloud. Ambient air density, $\rho_a(x, y, z)$ is a function of height. The ambient conditions are assumed to be horizontally homogeneous. In his dispersion model description, Colenbrander treats the air density at ground level, $\rho_a(0)$, and the density at the same altitude as the cloud top, $\rho_a(H_{eff})$ separately, but ALOHA-DEGADIS uses a constant average density, $\rho_a(x) = \rho_a(x, 0)$.

Inside the cloud, the centerline concentration of contaminant at ground level, along the downwind axis, is $c_c(x)$. The The density of the gas mixture in the cloud is $\rho(x)$. The density anomaly, Δ, and reduced gravity are important cloud parameters:

$$\Delta(x) = (\rho(x) - \rho_a(x))/\rho_a(x) \tag{4.2}$$

$$\hat{g}(x) = g\,\Delta(x) \tag{4.3}$$

The density of the cloud, ρ, must be computed from thermodynamic relations. We assume adiabatic mixing of the contaminant and the ambient air, and for an ideal gas mixture

$$\left(\frac{\rho(x) - \rho_a}{c_c(x)}\right) = \text{constant} \tag{4.4}$$

where $\rho(x)$ is the mean density of the cloud at position x, and $c_c(x)$ is the centerline contaminant concentration.

The specific heat of the mixture of contaminant and ambient air is given by

$$c_{pm}(x) = c_c(x)c_{pc} + (1 - c_c(x))\,c_{pa} \tag{4.5}$$

where the specific heats of the air and the contaminant are known.

The gas constant of the air-contaminant mixture is given by

$$R_m(x) = c_c(x)R_c + (1 - c_c(x))\,R_a \tag{4.6}$$

where R_c is the gas constant of the contaminant and R_a is the gas constant for the ambient atmosphere, including the effects of humidity of the air.

Given the cloud mixture gas constant, cloud can be computed by

$$\rho(x) = \frac{P_a}{R_m(x)T_c(x)} \tag{4.7}$$

where T_c is the temperature in the cloud.

4.3.2 The Ambient Wind Profile

The behaviour of the atmosphere near the ground depends critically on the sign of the mean, vertical density gradient. The **surface sublayer** is the lower part of the boundary layer above the roughness obstacles, where the flow is relatively unaffected by viscosity and the structure of individual obstacles, and by Coriolis force (Brutsaert, 1982, provides a good review.). This region typically extends up to 10 m and contains most ground-released heavy gas dispersion.

The wind profile in the surface sublayer is approximated by the relation

$$U(x,z) = \frac{u_*}{k}\left[\ln\frac{z+z_0}{z_0} + \psi\left(\frac{z}{L(x)}\right)\right] \tag{4.8}$$

where $U(x,z)$ is the mean wind at height z and downwind position x; u_* is the local friction velocity; $k = 0.4$ is the von Kármán constant; z_0 is the local roughness length[1]; $L(x)$ is the Obukhov length and $\psi(z/L)$ is a function of the non-dimensional height z/L.

The non-dimensional height $\zeta = (z/L)$ is a measure of the stability of the sublayer at height z, and L is approximately the height where mechanical production of turbulent energy equals production of energy by buoyancy flux:

$$L = -\frac{T}{g}\frac{u_*^3}{k\overline{w'T'}} \tag{4.9}$$

where T is the characteristic temperature of the boundary layer, and $\overline{w'T'}$ is the vertical heat turbulent heat flux. We take L to be constant everywhere.

It should be noted that all surface sublayer formulations are based on horizontally homogeneous, stationary conditions which are not present in heavy gas releases. Nevertheless, the formulations provide a reasonable view of the interdependence of the terms and are a useful starting place for engineering approximations. Hence, in practice, $U(x,z) = U(z)$ and $L(x) = L$.

When the atmosphere is neutral (Stability class D), then $\zeta = 0$, and the profile is a simple log function. In convective situations (Stability classes C–A), $\zeta < 0$ and the surface layer is characterized by thermal plumes merging into thermals on the scale of the boundary layer height, 1 km. In stable surface layers, $\zeta > 0$, and turbulence is suppressed. The functional relationship of $\psi(\zeta)$ depends on the sign of ζ.

Empirical equations for $\psi(\zeta)$ for unstable, neutral, and stable surface sublayers are (Businger, 1973)

$$\psi(\zeta) = \begin{cases} 2\ln(1+a)/2 + \ln(1+a^2)/2 - 2\arctan a + \pi/a & \zeta < 0 \\ 0 & \zeta = 0 \\ -4.7\zeta & \zeta > 0 \end{cases} \tag{4.10}$$

where $a = (1-15\zeta)^{1/4}$.

[1] In his paper, Colenbrander (1980) uses z_R for the roughness length, and z_0 for the reference height in the power-law approximation profile (below). Havens and Spicer (1985) follow this lead. However, this convention is exactly opposite to current literature and it is opposite to the nomenclature followed in the rest of this document.

Empirical equations relating L to the surface roughness for the Pasquill stability classes are as follows:

$$L = \begin{cases} -11.4\, z_0^{0.10} & \text{Class A} \\ -26.0\, z_0^{0.17} & \text{Class B} \\ -123\, z_0^{0.30} & \text{Class C} \\ \infty & \text{Class D} \\ 123\, z_0^{0.30} & \text{Class E} \\ 26.0\, z_0^{0.17} & \text{Class F} \end{cases} \tag{4.11}$$

Power-law Approximation to the Wind Profile

Mathematical manipulations are simplified if the logarithmic wind profile, (4.8), is replaced by a power function of height (Brutsaert, 1982, pg 63),

$$U(z) \approx U_R\,(z/z_R)^n \tag{4.12}$$

where $U(z)$ is the mean wind speed at height z, z_R is a reference height, U_R is the mean wind speed at z_R, and n is the power law exponent.

The dispersion results are highly sensitive to exponent, n. DEGADIS matches the profile from (4.8)–(4.11) for the given ambient conditions to (4.12) for the best estimate of n. For Pasquill stability classes A–F, typical values of $n = \{0.108,\ 0.112,\ 0.120,\ 0.142,\ 0.203,\ 0.253\}$ for $z_0 = 15$ cm. We select $z_R = 10$ m and $u_R = U_{10}$.

4.4 The Primary and Secondary Sources

The total mass of the developing blanket is

$$M_b(t) = \pi R_b(t)^2 H_b(t) \rho(t) \tag{4.13}$$

where $R_b(t)$ is the blanket radius, $H_b(t)$ is the blanket height, and $\rho(t)$ is the overall mean density of the blanket. M_b, R_b, H_b, and ρ are unknowns.

The rate of change in the blanket mass depends on the entrainment of air and contaminant into the cloud:

$$\frac{\mathrm{d}M_b}{\mathrm{d}t} = \frac{E(t)}{w_{c,p}(t)} + Q_{w,s}(t) + Q_a(t) - \pi R_b(t)^2 \left[\frac{Q_{*max}(t)}{w_c(t)}\right] \tag{4.14}$$

where $E(t)$ is the contaminant evolution rate from the primary (liquid) source; $w_{c,p}(t)$ is the contaminant mass fraction in the primary source; $Q_{w,s}(t)$ is the entrainment rate from water if the spill occurs over water; $Q_a(t)$ is the entrainment rate into the air above the blanket; $Q_{*max}(t)$ is the maximum take up flux, the largest possible takeup rate; and $w_c(t)$ is the mass fraction of contaminant in the developing cloud. The term $Q_{w,s}$ applies only if the spill is over water and otherwise it is zero. For ALOHA-DEGADIS it is neglected. Equation (4.14) introduces new unknowns: $Q_a(t)$, $Q_{*max}(t)$, and $w_c(t)$. The terms $E(t)$ and $w_{c,p}(t)$ depend on the primary source and are provided as external parameters.

In the final phases of the developing cloud, (humid) air entrainment is primarily through the top, and its rate is given by

$$Q_a(t) = \frac{(2\pi R_b(t) H_b(t))\, \rho_a(t)\, (\epsilon u_f(t))}{(\hat{g}(t) H_b(t)/u_f(t)^2)} \tag{4.15}$$

where ϵ is the entrainment rate coefficient at the front of the cloud, u_f is the rate of advance of the cloud front

$$u_f(t) = \mathrm{d}R_b(t)/\mathrm{d}t \tag{4.16}$$

The total contaminant in the source blanket is

$$M_c(t) = w_c(t) 2\pi R_b(t)^2 H_b(t) \rho(t) = w_c(t) M_b(t) \tag{4.17}$$

and its rate of change is

$$\frac{\mathrm{d}M_c(t)}{\mathrm{d}t} = E(t) - \pi R_b(t)^2 Q_{*max}(t) \tag{4.18}$$

The amount of air in the source blanket

$$M_a(t) = w_a(t) 2\pi R_b(t)^2 H_b(t) \rho(t) = w_a(t) M_b(t) \tag{4.19}$$

and its rate of change is

$$\frac{\mathrm{d}M_a(t)}{\mathrm{d}t} = \frac{E(t)}{w_{c,p}(t)} \left[\frac{1 - w_{c,p}(t)}{1 + q_a}\right] + \frac{Q_a(t)}{1 + q_a} - w_a(t)\, (\pi R_b(t)^2)\, \frac{Q_{*max}(t)}{w_c(t)} \tag{4.20}$$

where q_a is the absolute humidity, the ratio of water density to dry air density.

The total energy in the cloud is

$$U_b(t) = \pi h_b(t) R_b(t)^2 H_b(t) \rho(t) \tag{4.21}$$

where $U_b(t)$ is the total energy in the cloud and $h_b(t)$ is the mean enthalpy (energy per unit mass) for the blanket. and the rate of change in it is

$$\frac{\mathrm{d}U_b(t)}{\mathrm{d}t} = \frac{h_s(t) E(t)}{w_{c,p}(t)} + h_a Q_a(t) - \pi h_b(t) R_b(t)^2 \left[\frac{Q_{*max}(t)}{w_c(t)}\right] + \pi R_b(t)^2\, F_{Hs}(t) \tag{4.22}$$

where $F_{Hs}(t)$ is the surface heat flux.

4.5 ALOHA-DEGADIS Dispersion Model

The heavy gas dispersion model in DEGADIS is almost identical to the the similarity model proposed by Colenbrander (1980) (Figure 4.5).

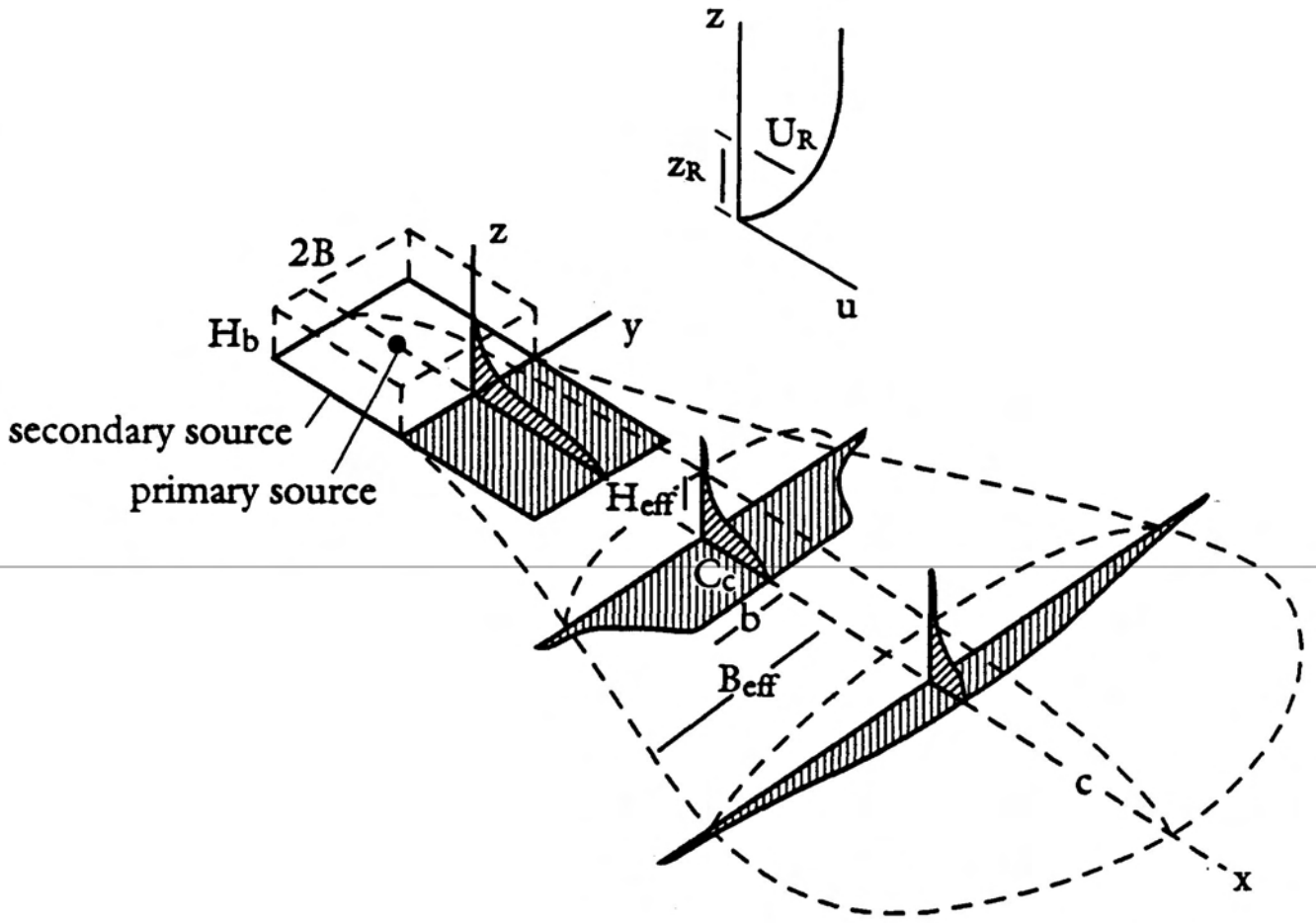

Figure 4.5: The plume model proposed by Colenbrander (1980)

The plume is assumed to be composed of (i) a horizontally homogeneous core of width $2b$ which has vertical dispersion, and (ii) Gaussian-shaped edges.

$$c(x,y,z) = \begin{cases} c_c(x)\exp\left(-\left(\frac{|y|-b(x)}{S_y(x)}\right)^2 - \left(\frac{z}{S_z}\right)^{1+n}\right) & |y| > b(x) \\ c_c(x)\exp\left(-\left(\frac{z}{S_z}\right)^{1+n}\right) & |y| \le b(x) \end{cases} \tag{4.23}$$

Four variables in (4.23) are functions of x and must be computed for each downwind step.

$c_c(x)$ the centerline ground-level concentration

$S_y(x)$ the lateral dispersion parameter

$S_z(x)$ the vertical dispersion parameter

b the half-width of the homogeneous core section

In the discussion to follow, a coupled set of empirical parametric equations will be presented. This set of equations must be solved simultaneously at each step in the x direction.

4.5.1 The Effective Cloud Width, Height, and Velocity

Empirical formulations for the plume/cloud dispersal require a cloud height parameter. The **effective cloud height**, H_{eff}, is based on the centerline concentration of contaminant in the form

$$H_{eff}(x) = \frac{1}{c_c(x)}\int_0^\infty c(x,0,z)\,\mathrm{d}z \tag{4.24}$$

The effective cloud height, from (4.24), is

$$H_{eff}(x) = \frac{S_z(x)}{1+n}\Gamma\left(\frac{1}{1+n}\right) \tag{4.25}$$

where $\Gamma(1/(1+n))$ is the Gamma function. This term will appear several times in the development below and will be written simply as Γ.

We define an **effective cloud width** by the sum of the constant concentration central core, $b(x)$ and the tail-off region on each side,

$$B_{eff}(x) = b(x) + \frac{\sqrt{\pi}}{2}S_y(x) \tag{4.26}$$

The lateral spread of the cloud is modeled by a Froude number representation as

$$\frac{\mathrm{d}B_{eff}}{\mathrm{d}x} = C_E\Gamma\left(\frac{Z_R}{S_z(x)}\right)^n\left[\frac{\hat{g}H_{eff}(x)}{U_R^2}\right]^{1/2} \tag{4.27}$$

where C_E is a constant. At some x downwind, $b(x) \to 0$ and the cloud width is defined by $S_y(x)$. The cloud initially spreads under the influence of $\hat{g}$, then, as the cloud is diluted and $S_z(x)$ grows, the core area diminishes to zero, at which point the heavy gas effects cease.

The **effective cloud velocity** in the plume is the concentration-weighted mean of the wind speed:

$$U_{eff}(x) = \frac{\int_0^\infty c(x,0,z)\,U\,dz}{\int c(x,0,z)\,dz} = \left(\frac{S_x(x)}{Z_R}\right)^n \frac{U_R}{\Gamma} \tag{4.28}$$

4.5.2 Richardson number, Ri_*

The **Bulk Richardson Number** is defined as follows:

$$\mathrm{Ri}_*(x) = \frac{\hat{g}(x)\,H_{eff}(x)}{u_*^2} \tag{4.29}$$

where $H_{eff}(x)$ is defined in (4.24) and (4.25). Experiments show that in continuous releases the plume has well-defined sharp edges when $\mathrm{Ri}_* > 1$ and lateral concentration profile approaches a Gaussian shape when $\mathrm{Ri}_* < 1$.

4.5.3 Corrections to Ri_* for Heat Flux

When the surface temperature under the plume, T_s, is greater than the mean temperature of the cloud, $T_c(x)$, a positive heat flux reduces the cloud stability. In this case, Ri_* is corrected in the form

$$\mathrm{Ri}'_*(x) = \mathrm{Ri}_*(x)(u_*/\sigma_w)^2 \tag{4.30}$$

where σ_w is a root-mean-square (rms) vertical velocity at the top of the gas cloud. The ratio (σ_w/u_*) at the top of the cloud is estimated by

$$\frac{\sigma_w}{u_*} = \left[1 + \mathrm{Ri}_T^{2/3}\right]^{1/2} \tag{4.31}$$

where the bulk temperature Richardson number is given by

$$\mathrm{Ri}_T = g\left[\frac{T_s - T_c}{T_c}\right]\frac{H_{eff}}{u_* U_R}\left[\frac{Z_R}{H_{eff}}\right]^n \tag{4.32}$$

Equation 4.32 introduces a new unknown, the cloud temperature, T_c. A cloud energy balance must be added to the equation set in order to estimate this term.

4.5.4 Heavy Gas Dispersion Coefficients

The two-dimensional diffusion equations represent a balance between the downwind gradient in concentration and either the vertical or the lateral turbulent diffusion. By separation of variables:

$$U\frac{\partial c(x,y,z)}{\partial x} = \frac{\partial}{\partial z}\left(K_z\frac{\partial c}{\partial z}\right) \tag{4.33}$$

$$U\frac{\partial c(x,y,z)}{\partial x} = \frac{\partial}{\partial y}\left(K_y\frac{\partial c}{\partial y}\right) \tag{4.34}$$

The equations are solved using (4.12) and the empirical approximations of

$$K_z(x,z) = \frac{ku_*z}{\phi(\mathrm{Ri}'_*(x))} \tag{4.35}$$

$$K_y(x) = K_0 U B_{eff}(x)^{\gamma_1} \tag{4.36}$$

where γ_1 is a constant, K_0 is a dimensionless constant ($= n^{(1-\gamma_1)}$), and $\phi(\mathrm{Ri}_*)$ is a stability factor given by

$$\phi(\mathrm{Ri}'_*) = 0.88 + 0.099\mathrm{Ri}'^{1.04}_* + 1.4 \times 10^{-25}\mathrm{Ri}'^{5.7}_* \qquad \mathrm{Ri}'_* \geq 0 \tag{4.37}$$

Equations 4.12, 4.30, 4.23, 4.33, and 4.35 are solved to yield the similarity form of the dispersion equation in the x-z plane:

$$\frac{\mathrm{d}}{\mathrm{d}x}\left[\left(\frac{U_R Z_R}{1+n}\right)\left(\frac{S_z(x)}{Z_R}\right)^{1+n}\right] = \frac{ku_*(1+n)}{\phi(\mathrm{Ri}'_*)} \tag{4.38}$$

4.5.5 Mass and Energy Balance

The mean density of the cloud gas mixture depends on the $c_c(x)$ and the temperature, T_c. These are approximated from a combined mass and energy balance for a differential slice with thickness $\mathrm{d}x$, width of B_{eff}, and height H_{eff}.

The mass balance at x is given by $(\rho U_{eff} H_{eff} B_{eff})$ and

$$\frac{\mathrm{d}}{\mathrm{d}x}\left[\rho U_{eff} H_{eff} B_{eff}\right] = \frac{\rho_a k \sigma_w (1+n)}{\phi(\mathrm{Ri}'_*(x))} B_{eff}(x) \tag{4.39}$$

When the surface temperature, T_s is greater than the cloud temperature, T_c, then Ri_* is corrected with (4.30)–(4.32) and the cloud temperature is a new dependent variable, $T_c(x)$. The temperature of the cloud will change as heat is added to the cloud by flux of sensible heat from the ground, F_H. The added energy density of the cloud, D_h, in ($\mathrm{J\,kg^{-1}}$) computed from

$$D_h(x) = c_{pg}(x)\left(T_c(x) - T_c(0)\right) \tag{4.40}$$

The energy budget for a transverse slice of the cloud is

$$\frac{\mathrm{d}}{\mathrm{d}x}[D_h \rho U_{eff} H_{eff} B_{eff}] = F_{Hs} B_{eff}/\delta_L \tag{4.41}$$

where F_{Hs} is the surface heat flux under the cloud, and δ_L is an empirical constant.

When the core width $b = 0$, the energy balance becomes

$$\frac{\mathrm{d}}{\mathrm{d}x}[D_h \rho U_{eff} H_{eff}] = F_H/\delta_L \tag{4.42}$$

4.5.6 Final Solution

The set of 14 equations (4.2), (4.3), (4.7), (4.12), (4.23), (4.25), (4.26), (4.27), (4.28), (4.29), (4.30) if required, (4.37), (4.38), (4.39), and (4.41) or (4.42) must be solved simultaneously for

the 14 dependent variables $c_c(x)$, $\rho(x)$, $\Delta(x)$, $\hat{g}(x)$, $T_c(x)$, $H_{eff}(x)$, $\mathrm{Ri}'_*(x)$, $\sigma_w(x)$, $b(x)$, $S_y(x)$, $S_z(x)$, $U_{eff}(x)$, $\phi(\mathrm{Ri}'_*)$, and finally $c(x,y,z)$.

Input parameters for each dispersion case are ρ_a, g, P_a, R_m, R_c, R_a, Z_R, U_R, z_0, u_*, k, L, the stability class, and T_s.

The required empirical constants are C_E, the empirical constants in (4.37).

4.6 Computational Details

4.6.1 Approximations for a Time-Dependent Source

In order to calculate and display a plume footprint in the short time available during an emergency response, the ALOHA-DEGADIS module has been simplified in two ways. In these two respects, this module differs from the full DEGADIS model. The user should be aware of these differences and their implications for plume modeling. When a series of finite source steps are fed to the ALOHA-DEGADIS module, the module will overpredict footprint size in two ways: *only the largest source step is considered, and the selected release rate is assumed to be continuous.* That is, the duration of the release is ignored. Hence, the briefer the release, and the greater the fastest release rate relative to rates calculated for other source steps, the more the module will overpredict the size of the footprint. The module will overpredict the least when a release is of long duration, and of constant, or nearly constant rate.

These simplifications were required to speed plume calculations. The alternative to this method of calculation would be to compute concentrations over a grid of points, then to contour the footprint. Such a calculation method would require solving the heavy gas equations between 30 and 100 times, slowing plume calculation by an equivalent factor.

Note that when the user requests calculations of concentration and dose for a particular location, the concentration equations are solved for this point only, and none of the above approximations are made. For such a case, the heavy gas module and the full DEGADIS model produce similar estimates. An important side effect of the difference between producing a heavy gas footprint and producing a concentration and dose estimate for a single location is that for scenarios in which overprediction occurs, concentrations at a point within a footprint may remain well below the level of concern.

KEY POINT: The heavy gas footprint should be used as an initial conservative screening of the potential threat area. Specific points of interest should then be checked with the concentration and dose calculations.

4.7 Comparisons with DEGADIS

ALOHA-DEGADIS has been, and continues to be, verified by comparisons to field experiments, the original DEGADIS model, and other reference models. As part of the verification process, the authors of both models reviewed each model's code and computations line-by-line (Havens, 1990).

Estimates made by ALOHA-DEGADIS and DEGADIS for a series of release scenarios were also compared. Using a fractional factorial experimental design (Cochran and Cox, 1957), a set of 24 test scenarios was prepared. Eight DEGADIS input variables—stability class, wind

speed, spill size, release duration, gas density, ground roughness, chemical-ground temperature difference, the coefficients of the equation of state, and level of concern—were varied in the 24 scenarios in order to span the expected variability within model parameters. We believe that these factors are the most important influences on concentration estimates made by DEGADIS.

For the 24 cases, the correlation between the estimates of concentration and downwind distance made by the two models was 0.997. For steady-state, continuous release cases, ALOHA-DEGADIS tended to predict a longer distance than was predicted by the full DEGADIS model. ALOHA-DEGADIS footprints averaged 10% longer than those predicted by DEGADIS. For short-term releases, the arrival time of the peak concentration at a given location downwind and the maximum value of the peak were also examined. Arrival times predicted by ALOHA-DEGADIS were slightly later than those predicted by DEGADIS, although the correlation between estimates made by each model was 1.0. ALOHA-DEGADIS predicted downwind movement of gas clouds to average about 9% slower than the travel rate predicted by DEGADIS. ALOHA-DEGADIS predicted maximum concentrations that exceeded DEGADIS estimates by an average of 8%; the correlation between maximum concentration estimates made by the two models was 0.994%.

These results demonstrate that the ALOHA-DEGADIS model, which completes calculations considerably faster than DEGADIS, is consistently slightly more conservative than DEGADIS. It can be expected to produce peak concentration estimates for a given point that are usually about 10% greater than estimates made by the full DEGADIS model.

Mathematical Symbols

A_0 characteristic area for the primary source (m^2)
B secondary source half-width (m)
B_{eff} effective half width of the heavy-gas plume (m)
C_E constant used in the computation of B_{eff} (none)
c_c centerline concentration of contaminant (kg/,m^{-3})
c_p specific heat at constant pressure ($J\,kg^{-1}\,K^{-1}$)
c_{pa} specific heat at constant pressure of air ($J\,kg^{-1}\,K^{-1}$)
c_{pc} specific heat at constant pressure of contaminant ($J\,kg^{-1}\,K^{-1}$)
c_{pw} specific heat at constant pressure of water ($J\,kg^{-1}\,K^{-1}$)
D_h energy density in the cloud ($J\,kg^{-1}$)
$E(t)$ contaminant primary source rate ($kg\,s^{-1}$)
F_{Ha} surface heat flux ($W\,m^{-2}$)
g acceleration of gravity ($m\,s^{-1}$)
$\hat{g}$ reduced gravity, $g(\rho - \rho_a)/\rho_a$ ($m\,s^{-1}$)
$\hat{g}_0$ reduced gravity at the primary source ($m\,s^{-1}$)
H characteristic height of the primary source (m)
H_b blanket height or characteristic release depth of cloud (m)
H_{eff} effective cloud height (m)
h_a enthalpy of air ($J\,kg^{-1}$)
h_b mean blanket enthalpy ($J\,kg^{-1}$)
h_E enthalpy of source mass flow ($J\,kg^{-1}$)
h_L layer average enthalpy ($J\,kg^{-1}$)
h_s enthalpy of primary source ($J\,kg^{-1}$)
h_w enthalpy of water ($J\,kg^{-1}$)
k von Kármán constant, 0.4 (none)
L Obukhov mixing length (m)
M_a total mass of the air in the cloud (kg)
M_b total mass of the cloud (kg)
M_c total mass of contaminant in the cloud (kg)
n exponent in the wind profile power-law formula. (none)
Q_a mass rate of air entrainment into the cloud ($kg\,s^{-1}$)
$Q_{w,a}$ mass rate of water into the cloud ($kg\,s^{-1}$)
Q_* atmospheric mass takeup flux ($kg\,m^{-2}\,s^{-1}$)
Q_{*max} maximum atmospheric mass takeup flux ($kg\,m^{-2}\,s^{-1}$)
q_a absolute humidity of the ambient air (kg(water)/kg(dry air))
R_a gas constant for air ($Pa\ m^3\,kg^{-1}\,K^{-1}$)
R_b secondary source (blanket) radius (m)
R_c gas constant for a contaminant ($Pa\ m^3\,kg^{-1}\,K^{-1}$)
R_m gas constant for an air-gas mixture ($Pa\ m^3\,kg^{-1}\,K^{-1}$)
R_p primary source radius (m)
Ri_C Critical Richardson number for passive/heavy gas (none)
Ri_T Richardson number based on cloud temperature. (none)
Ri_* cloud bulk Richardson number. (none)
Ri'_* Ri_* modified for convective turbulence. (none)
S_y, S_z heavy-gas plume dispersion parameters (m)
T characteristic temperature in the cloud (K)
T_c temperature in the cloud (K)
U characteristic mean wind speed ($m\,s^{-1}$)
U_b total internal energy in the blanket (J)
U_R mean wind speed at the reference height, z_R. ($m\,s^{-1}$)
U_{10} mean wind speed at the standard height of 10 m. ($m\,s^{-1}$)
u_* friction velocity of the ambient air. ($m\,s^{-1}$)
u_f cloud front velocity ($m\,s^{-1}$)
u', v', w' turbulent pertubation velocities ($m\,s^{-1}$)
V_0 characteristic volume of the primary source (m^3)
w_a mass fraction of air in the cloud gas mixture ($kg\,kg^{-1}$)
w_c mass fraction of contaminant in the cloud ($kg\,kg^{-1}$)
$w_{c,p}$ mass fraction of contaminant in primary source ($kg\,kg^{-1}$)
$\overline{w'T'}$ vertical turbulent heat flux ($m\,K\,s^{-1}$)
x, y, z coordinates for the plume model (m)
Z_R Reference height for the wind power-law approximation. (m)
z_0 surface roughness length scale (m)
Δ density enhancement in heavy gas mixture (none)
ϵ frontal entrainment coefficient (0.59)
κ_g molecular diffusivity of the contaminant gas ($m^2\,s^{-1}$)
$\psi(z/L)$ Stability correction to the logarithmic wind profile. (none)
$\phi(z/L)$ stability correction for eddy mixing coefficient (none)
ρ density of air-gas mixture in the cloud ($kg\,m^{-3}$)
ρ_a air density ($kg\,m^{-3}$)
σ_w root-mean-square turbulent vertical velocity ($m\,s^{-1}$)
ζ non-dimensional height,$= z/L$ (none)

Chapter 5

Infiltration

5.1 General Comments

It is generally recognized that a well-insulated house or building provides excellent protection against a toxic cloud of finite time duration (Wilson, 1987). Assuming the infiltration rate is small and that the air inside is always well-mixed, the building acts like a low-pass filter and an electrical R-C filtering circuit offers an excellent analog.

The infiltration time constant is the time required after a step-increase in the outside concentration of a gas for the concentration inside to reach 63% of the step difference. This number can vary from 1 to 0.1 hours depending on the building tightness, the wind, and the inside-outside temperature difference. The wind blowing against a building creates pressure differences and these drive infiltration and exfiltration depending on the direction of the pressure gradient. Temperature differences create a pressure gradient and thus enhance the infiltration process.

Because of the extreme variability in weather and building types, ALOHA must make some broad generalizations. Sherman (1980, 1984) studied 196 houses and found that an effective leakage area ((5.3) below) is 0.00059 times the area of the house. ALOHA uses this figure and assigns an average house floor area of 160 m^2 (1722 ft^2). An average building ceiling height of 2.5 m is taken for a single-story house and 5 m is used for a two-story building. A reasonable approximation of inside temperature is 20°C. It is assumed that all leakage occurs evenly over the structure and that there is no difference between floor and ceiling leakage.

The subject is not closed and new theories on infiltration continue to emerge (Engelmann, 1990).

5.2 Theory

We assume that the outside and inside concentrations are uniform and that environmental conditions are stationary in time. A balance of inflow and outflow of the chemical is described by the equation

$$\frac{dc_i(t)}{dt} = (c_o(t) - c_i(t))/\tau_E \tag{5.1}$$

where $c_i(t)$ is the inside concentration, $c_o(t)$ is the outside concentration, and τ_E is the infiltration time constant.

The infiltration time constant was defined in Sec. 5.1 as an analog to a low-pass filter. This parameter can be specified by the user during setup but, more than likely, an emergency responder will not have that information and it must be approximated.

5.2.1 Estimating τ_E

An algorithm by Sherman (1980) was adapted for estimating τ_E from a few input parameters. The basic assumption is that $\tau_E \propto (|P_i - P_o|)^{-1/2}$ where P_i is the pressure inside and P_o is the pressure outside. Often the **exchange rate**, $E_x = \tau_E^{-1}$, is referred to in place of the time constant. Pressure differences are caused by dynamic pressure effects from the wind flow around the building and from the temperature difference which is called the **stack effect**. The stack effect causes infiltration primarily through the floor and ceiling while the wind effect causes leakage primarily through the walls.

The exchange time constant depends on infiltration from temperature differences, Q_s, and from wind loading, Q_w. When Q_s and Q_w are computed, the exchange constant is computed by

$$\tau_E = E_x^{-1} = \frac{V_s}{\sqrt{Q_s^2 + Q_w^2}} \tag{5.2}$$

where V_s is the total structure volume ($= HA_{floor}$.

The temperature-induced infiltration is given by Grimsrud et al. (1983),

$$Q_s = A_e f_s \sqrt{|\Delta T|} \tag{5.3}$$

where Q_s ($\mathrm{m^3\,s^{-1}}$) is the volume inflow rate, A_e is the effective leakage area, f_s is the stack parameter ($\mathrm{m\,s^{-1}\,K^{-1}}$), and $\Delta T = T_i - T_o$. The absolute value of ΔT is used so the equations work properly at positive or negative temperature differences.

As discussed in Sec. 5.1, ALOHA uses $A_e = 0.00059 A_{floor}$ with $A_{floor} = 160\ \mathrm{m^2}$.

The stack parameter, f_s, is estimated from the formula

$$f_s = \frac{1 + R/2}{3}\left[1 - \left(\frac{X}{2 - R}\right)^2\right]^{3/2}\sqrt{\frac{gH}{T_i}} \tag{5.4}$$

where R is the ratio of vertical to total leakage, X is the difference between floor and ceiling leakage, H_s is the structure height, and T_i is the uniform internal temperature.

ALOHA sets $X = 0$. Leakage is assumed to occur uniformly over the structure, and we assume the structure is square with floor area A_f and height H.

The ratio R is computed by the equation

$$R = \frac{2A_{floor}}{A_{total}} \tag{5.5}$$

However, ALOHA uses a constant value of $R = 0.5$.

The infiltration from wind loading is approximated by

$$Q_w = A_e f_w U \tag{5.6}$$

where A_e is the defined in (5.3), f_w is the wind parameter, and U is the mean wind speed evaluated at the building height using the stability class and the power-law profile as described in Sec. 4.3.2.

If the building is located in a sheltered position, the wind effect is reduced. Sheltering is represented by the coefficient of f_w,

$$f_w = C_{sh}(1 - R)^{1/3} \tag{5.7}$$

where R is defined in (5.4) and

$$C_{sh} = \begin{cases} 0.24 & \text{sheltered} \\ 0.32 & \text{unsheltered} \end{cases} \tag{5.8}$$

5.2.2 Computation Notes

Equation (5.1) is solved by numerical integration using a trapezoidal algorithm (Press et al., 1988). The time series of c_0 is maintained by ALOHA for the selected coordinates of the building.

To demonstrate the importance of the various terms in the infiltration model, the following test situation is used.

$$\begin{aligned} c_o(t) &= \begin{cases} 0 & t < 0 \\ 100 & t \geq 0 \end{cases} \\ A_{floor} &= 160 \ \text{m}^2 \\ H_s &= 2.5 \ \text{m} \\ T_i &= 20 \ ^\circ\text{C} \\ T_o &= 10 \ ^\circ\text{C} \\ U &= 10 \ \text{m s}^{-1} \\ A_e &= 0.00059 A_{floor} \ \text{m}^2 \\ R &= 0.5 \\ X &= 0 \\ \text{exposure} &= \text{unsheltered} \end{aligned}$$

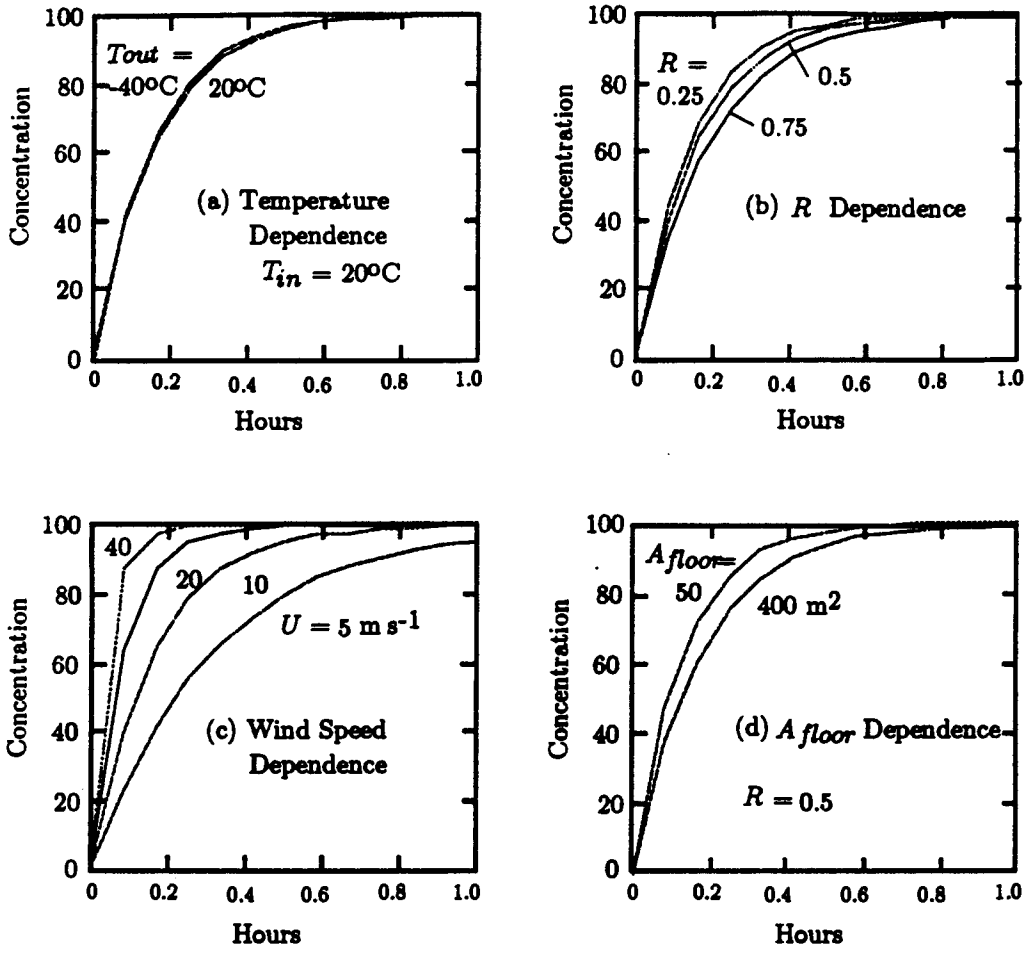

Figure 5.1: Examples of infiltration based on the base conditions. (a) As inside-outside temperature differences vary from -40°C to 0°C the time constant holds nearly constant at 0.18 hr. (b) The leakage ratio, R, can vary from 0–1 depending on the leakage through the floor and roof compared to the side walls. Typical values range from 0.5–0.9 and the differences in infiltration are slight. ALOHA holds a constant $R = 0.5$. (c) The wind can vary from 4 to 40 $m\,s^{-1}$ and the effect on the infiltration rate is reduced by 0.3 hr to 0.04 hr. (d) The floor area can vary from 50–400 m^2 and the effect on infiltration is small.

Mathematical Symbols

A_e	effective leakage area (m^2)
A_{floor}	floor area of the building (m^2)
c_i	inside concentration ($kg\,m^{-3}$)
c_o	outside concentration ($kg\,m^{-3}$)
C_{sh}	sheltering coefficient (none)
f_s	stack parameter ($m\,s^{-1}\,K^{-1}$)
f_w	sheltering coefficient (none)
E_z	exchange coefficient (s^{-1})
H	height of the building (m)
P_i	pressure inside a building (Pa)
P_o	pressure outside a building (Pa)
Q_s	infiltration rate due to temperature differences ($m^3\,s^{-1}$)
Q_w	infiltration rate due to wind loading ($m^3\,s^{-1}$)
R	ratio of vertical to total leakage (none)
t	time (s)
T_i	inside temperature (K)
T_o	outside temperature (K)
U	mean wind speed at ten meters height ($m\,s^{-1}$)
V	total structure volume (m^3)
X	difference between floor and ceiling leakage (none)
ΔT	inside-outside temperature difference (K)
τ_E	infiltration time constant (s)

Chapter 6

ALOHA References

American Association of Railroads. 1986. *Emergency Handling of Hazardous Materials in Surface Transportation.* Washington, D.C.: AAR, Bureau of Explosives. 800 pp.

American Institute of Chemical Engineers. 1989. *Workbook of Test Cases for Vapor Cloud Source Dispersion Models.* New York: Amer. Inst. Chem. Engrs. Center for Chemical Process Safety. 122 pp.

Arthur D. Little Inc. 1988. *CHEMS-PLUS (Enhanced Chemical Hazard Evaluation Methodologies) Reference Manual, Ver 1.0.* Cambridge, MA: Arthur D. Little. 106 pp.

Arya, S. Paul. 1988. *Introduction to Micrometeorology.* San Diego: Academic Press, Inc. (ISBN: 0-12-064490-8). 307 pp.

Atkins, P.W. 1990. *Physical Chemistry, Fourth Edition.* San Diego: W.F. Freeman Hall (ISBN: 0-7167-2073-6). 995 pp.

Beals, Gordon A., Maj U.S.A.F. 1971. *Guide to Local Diffusion of Air Pollutants.* Scott AFB, IL: Technical Rept 214, U.S. Air Force, Air Weather Service. 83 pp.

Bean, H. (ed). 1971. *Fluid Meters: Their Theory and Application, 6th ed..* New York: Am Soc Mech Engr. 272 pp.

Bell, R. 1978. Isopleth Calculations for Ruptures in Sour Gas Pipelines. *Energy/Processing/Canada, Vol. 71, No. 4*, pp. 36–39.

Belore R. and I. Buist. 1986. *A Computer Model For Predicting Leak Rates of Chemicals From Damaged Storage and Transportation Tanks.* Canada: Report EE-75, Environment Canada. 45 pp.

Blevins, R.D. 1985. *Applied Fluid Dynamics Handbook.* New York: Van Nostrand Reinhold (ISBN:0-442-21296-8). 558 pp.

Box, G.E.P., W.G. Hunter, and J.S. Hunter. 1978. *Statistics for Experimenters, An Introduction to Design, Data Analysis, and Model Building.* New York: John Wiley & Sons. 653 pp.

Box, G.E.P. and S. Bisgaard. 1987. The scientific context of quality improvement. A look at the use of scientific method in quality improvement. *Quality Progress, Vol. 20, No. 6*, pp. 54–61.

Briggs, G.A. 1973. *Diffusion Estimation for Small Emissions.* ATDL Contribution File No. 79. Atmospheric Turbulence and Diffusion Laboratory. 85 pp.

Briggs, G.A. 1991. Personal communication, March 1991.

Brighton, P.W.M. 1985. Evaporation from a plane liquid surface into a turbulent boundary layer. *Jour. Fluid Mech., Vol. 159*, pp. 323–345

Brighton, P.W.M. 1990. Further Verification of a Theory for Mass and Heat Transfer from Evaporating Pools. *Journal of Hazardous Materials, Vol. 23*, pp. 215–234

Briscoe, F. and P. Shaw. 1980. Spread and Evaporation of Liquid. *Progress in Energy and Combined Science, Vol. 6, No. 2*, pp. 127–140.

Britter, Rex E. 1989. Atmospheric dispersion of dense gases. (J.L. Lumley, M. van Dyke, and H.L. Reed, eds) *Annual Rev. Fluid Mech., 21*, pp. 317–344.

Britter, R.E. and J. McQuaid. 1988. *Workbook on the Dispersion of Dense Gases.* HSE Contract Research Report No. 17/1988. Sheffield, Gr. Britain: Health and Safety Executive, 129 pp. (29 non-paginated figures).

Brutsaert, W. 1982. *Evaporation into the Atmosphere.* Boston: D. Reidel (ISBN: 90-277-1247-6). 299 pp.

Businger, J.A. 1973. Turbulence transfer in the atmospheric surface layer. *Workshop on Micrometeorology.* D.A. Haugen, ed., Boston: American Meteorological Society. pp. 67–100.

Carslaw, H.S. and J.C. Jaeger. 1959. *Conduction of Heat in Solids.* London: Oxford University Press. 510 pp.

Chatwin, P.C. 1991. New Research on the Role of Concentration Fluctuations in Useful Models of the Consequences of Accidental Releases of Dangerous Gases. *International Conference and Workshop on Modeling and Mitigating the Consequences of Accidental Releases of Hazardous Materials* . New York: American Institute of Chemical Engineers, pp. 334–340.

CRC (Chemical Rubber Co.). 1970. *Handbook of Chemistry and Physics, 50th Edition* Cleveland, OH: Chemical Rubber Co. various pagings.

Cochran, William G. and Gertrude M. Cox. 1957. *Experimental Designs, 2nd ed.*. New York: John Wiley and Sons. 611 pp.

Colenbrander, G.W. 1980. *A Mathematical Model for the Transient Behavior of Dense Vapor Clouds.* Basel, Switzerland: 3rd International Symposium on Loss Prevention and Safety Promotion in the Process Industries.

Colenbrander, G.W. and J.S. Puttock. 1983. *Dense Gas Dispersion Behavior: Experimental Observations and Model Developments.* Harrogate, England: International Symposium on Loss Prevention and Safety Promotion in the Process Industries.

Danner, R.P. and T.E. Daubert. 1985. *Data Compilation Tables of Properties of Pure Compounds.* New York: DIPPR/AIChE. 1v. (various pagings).

Danner, R.P. and T.E. Daubert. 1987. *Manual for Predicting Chemical Process Design Data: Data Prediction Manual* (with hand-written corrections). New York, NY: DIPPR/AIChE, 1v. (loose leaf).

Daubert, T.E. and R.P. Danner. 1989. *Physical and Thermodynamic Properties of Pure Chemicals.* New York, NY: Design Institute for Physical Property Data, AIChE, Hemisphere Publ. Co., four volumes.

Deacon, E.L. 1973. Geostrophic Drag Coefficients. *Boundary Layer Meteorology., Vol. 5, No. 4*, pp. 321–340.

Eberhard, W.L., W.R. Moninger, and G.A. Briggs. 1988. Plume Dispersion in the Convective

Boundary Layer. Part I: CONDORS Field Experiment and Example Measurements. *Journal of Applied Meteorology., Vol. 27, No. 5*, pp. 599–616.

E.I. Du Pont De Nemours 1989. *TRACE II Software.* Westlake Village CA: E.I. DuPont De Nemours. 222 pp.

Engelmann, Rudolf J. 1990. *Effectiveness of Sheltering in Buildings and Vehicles for Plutonium.* U.S. Dept of Energy report DOE/EH-0159T UC-160. 48 pp.

Fackrell, J.E. and A.G. Robins. 1982. Concentration fluctuations and fluxes in plumes from point sources in a turbulent boundary layer *J. Fluid Mech. Vol. 117*, pp. 1–26

Fannelop, T.K. and Ø. Jacobsen. 1980. Gravitational spreading of heavy gas clouds instantaneously released. *Journal of Applied Mathematics and Physics (ZMAP)., Vol. 14, No. (none)*, pp. 769–777.

Fauske, H.K. 1985. Flashing Flow: Some Practical Guidelines for Emergency Releases. *Plant/Operations Progress, Vol. 4, No. 3*, pp. 132–134.

Fauske, H. and M. Epstein. 1988. Source Term Considerations in Connection with Chemical Accidents and Vapor Cloud Modelling. *Proc. Intl. Conf. on Vapor Cloud Modeling.* New York: Center for Chemical Process Safety, Amer. Inst. Chem. Engrs. pp. 251–273.

Fisher, H.G., H.S. Forrest, S.S. Grossel, J.E. Huff, A.R. Miller, J.A. Noronha, and B.J. Tilley. 1989. *The Design Institute for Emergency Relief Systems (DIERS) Project Manual, Version IV.* 345 East 47th Street, New York 10017: American Institute of Chemical Engineers.

Fox, D.G. 1984. Uncertainty in air quality monitoring. *Bull. Meteor. Soc., Vol. 65, No. 1*, pp. 27–36.

Frouin, Robert, David W. Lingner, and Catherine Gautier. 1989. A Simple Analytical Formula to Compute Clear Sky Total and Photosynthetically Available Solar Irradiance at the Ocean Surface. *Jour. Geophys. Res., Vol. 94, No. C7*, pp. 9731–9742.

Golder, D. 1972. Relations Among Stability Parameters in the Surface Layer. *Boundary-Layer Meteor., Vol. 3, No. 1*, pp. 47–58.

Goldwire Jr., H.C., T.G. McRae, G.W. Johnson, D.L. Hipple, R.P. Koopman, J.W. McClure, L.K. Morris, and R.T. Cederwall. 1985. *Desert Tortoise Series Data Report 1983 Pressurized Ammonia Spills.* Report UCID-20562, Lawrence Livermore National Laboratory, Contract No. W-7405-ENG-48 (also available from U.S. Dept of Commerce, NTIS, Springfield VA 22161). 244 pp.

Grimsrud, D., M. Sherman, and R. Sonderegger. 1983. *Calculating Infiltration: Implications for a Construction Quality Standard.* Lawrence Berkely Laboratory, Report LBL-9416. 31 pp.

Grolmes, M.A. and J.C. Leung. 1984. Scaling Considerations for Two-Phase Critical Flow. *Multiphase Flow and Heat Transfer III. Part A.* eds: T.N. Veziroglu and A.E. Bergles pp. 549–563.

Hanna, Steven R. and David Strimaitis. 1989. *Workbook of Test Cases for Vapor Cloud Source Dispersion Models.* New York: Center for Chemical Process Safety of the American Institute of Chemical Engineers (ISBN: 0-8169-0455-3). 122 pp.

Hanna, Steven R., Gary A. Briggs, and Rayford P. Hosker, Jr. 1982. *Handbook on Atmospheric Diffusion.* Report DOE/TIC-11223 , U.S. Dept of Energy, Technical Information Center (also available from NTIC as DE82002045(DOE/TIC-11223). 102 pp.

Havens, J. and T. Spicer. 1985. *Development of an Atmospheric Dispersion Model for Heavier-*

than-Air Gas Mixtures, Vol I. Report CG-D-22-85, U.S. Coast Guard. 158 pp.

Havens, J. 1990. NOAA DEGADIS Evaluation Report letter from University of Arkansas, Fayetteville. 3 pp.

Havens, Jerry and Tom Spicer. 1990. *LNG Vapor Dispersion Prediction with the DEGADIS Dense Gas Dispersion Model.* Topical Report (April 1988–July 1990) Chicago: Gas Research Institute. 32 pp.

Henry, R.E. and H.S. Fauske. 1971. The Two-Phase Critical Flow of One-Component Mixtures in Nozzles, Orifices, and Short Tubes. *Journal of Heat Transfer, May 1971*, pp. 179–187.

Huff, J.E. 1985. Multiphase Flashing Flow in Pressure Relief Systems. *Plant/Operations, Vol. 4, No. 4*, pp. 191–199.

Hunt, J.C.R. and A.H. Weber. 1979. A Lagrangian statistical analysis of diffusion from a ground-level source in a turbulent boundary layer. *Quart. Jour. Roy. Met. Soc., 105*, pp. 423–443.

Kawamura, P. and D. MacKay. 1985. *The Evaporation of Volatile Liquids.* Univ. of Toronto Depts. of Chem. Eng. and Appl. Chem.: TIPS Report EE-59, Environment Canada. 54 pp.

Kawamura, Peter I. and Donald Mackay. 1987. The Evaporation of Volatile Liquids. *Journal of Hazardous Materials, Vol. 15*, pp. 343–364

Kunkel, B.A. 1985. *Development of an Atmospheric Diffusion Model for Toxic Chemical Releases.* Hanscom AFB, MA: Air Force Geophysics Laboratory Environmental Research Paper 939, AFGL-TR-85-0338 (also available from NTIS AD-A169 135). 34 pp.

Leung, J.C. 1986. A generalized correlation for one-component homogeneous equilibrium flashing choked flow. *AIChE Journal, Vol. 32, No. 10*, pp. 1743–1746.

Leung, Joseph C. and Hans K. Fauske 1987. Runaway System Characterization and Vent Sizing Based on DIERS Methodology. *Plant/Operations Progress, Vol. 6, No. 2*, pp. 77–83.

Leung, J.C. and M.A. Grolmes 1987. The Discharge of Two-phase Flashing Flow in a Horizontal Duct. *AIChE Journal, Vol. 33, No. 3*, pp. 524–527.

Leung, J.C. and M.A. Grolmes. 1988. A Generalized Correlation for Flashing Choked Flow of Initially Subcooled Liquid. *AIChE Journal, Vol. 34, No. 4*, pp. 688–691.

Leung, Joseph C. 1990. Two-phase flow discharge in nozzles and pipes—a unified approach. *J. Loss Prev. Process Ind., Vol. 3 (January)*, pp. 27–32

Lyman, W.J., W.F. Reehl, and D.H. Rosenblatt. 1982. *Handbook of Chemical Estimation Methods.* New York: McGraw-Hill. 874 pp.

McQuaid, J. 1984. Large Scale Experiments on the Dispersion of Heavy Gas Clouds. *Atmospheric Dispersion of Heavy Gases and Small Particles*, Symposium, Delft, Aug 29–Sept 2, 1983 (eds. G. Ooms and H. Tennekes). New York: Springer-Verlag. pp. 129–138.

NOAA (National Oceanic and Atmospheric Administration), Hazardous Materials Response Group and U.S. Environmental Protection Agency, Chemical Emergency Preparedness and Prevention Office. 1990a. *ALOHA™ 5.0, Areal Locations of Hazardous Atmospheres for the Apple Macintosh Computer.* Washington, D.C.: National Safety Council. 178 pp.

NOAA (National Oceanic and Atmospheric Administration), Hazardous Materials Response Group and U.S. Environmental Protection Agency, Chemical Emergency Preparedness and Prevention Office. 1990b. *CAMEO™ 3.0 for the Apple Macintosh Computer.* Washington, D.C.: National Safety Council. 235 pp.

Oke, T.R. 1978. *Boundary Layer Climates.* New York: Methuen and Co. 372 pp.

Ooms, G., A.P. Mahieu, and F. Zelis. 1974. *The Plume Path of Vent Gases Heavier than Air.* First International Symposium on Loss Prevention and Safety Promotion in the Process Industries, (C.H. Buschman, ed.), Amsterdam: Elsevier Press.

Palazzi, E., M. De Faveri, G. Fumarola, and G. Ferraiolo. 1982. Diffusion from a steady source of short duration. *Atmospheric Environment, Vol. 16, No. 12*, pp. 2785–2790.

Pasquill, F. 1976. *Atmospheric Dispersion Parameters in Gaussian Plume Modelling: Part II. Possible Requirements for Change in the Turner Workbook Values.* Report EPA-600/4-760306, U.S. E.P.A. 55 pp.

Pasquill, F. and F.B. Smith. 1983. *Atmospheric Diffusion, 3rd Edition.* New York: Halstead Press 437 pp.

Perry, R.H., D.Green, and J.O. Maloney (eds). 1984. *Perry's Chemical Engineer's Handbook, 6th Edition.* New York: McGraw-Hill (IBSN: 0-07-049479-7). 2336 pp.

Picknett, R.G. 1981. Dispersion of dense gas puffs released in the atmosphere at ground level. *Atmospheric Environment, Vol. 15, No. 2*, pp. 509–525.

Press, William H., Brian P. Flannery, Saul A. Teukolsky, and William T. Vetterling 1988. *Numerical Recipes in C.* Cambridge/New York: Cambridge University Press (IBSN: 0-521-35465-X). 735 pp.

Raj, P.K. 1982. *Heavy Gas Dispersion—a State-of-the-Art Review of the Experimental Results and Models.* Belgium: Heavy Gas Dispersal Lecture Series, 1982–83. Von Karman Institute. 73 pp.

Raj, P.K. and J.A. Morris. 1987. *Source Characteristics and Heavy Gas Dispersion Models for Reactive Chemicals.* Burlington MA: Technology & Management Systems, Inc. 48 pp.

Raphael, J.M. 1962. Prediction of temperature in rivers and reservoirs. *Journal of the Power Division.* American Society of Chemical Engineers. pp. 157–165.

Reid, R.C., J.M. Prausnitz, and B.C. Poling. 1987. *The Properties of Gases and Liquids.* McGraw-Hill. 741 pp.

Sawford, B.L., C.C. Frost, and T.C. Allan. 1985. Atmospheric boundary-layer measurements on concentration statistics from isolated and multiple sources. *Boundary Layer Meteorology, Vol. 31, No. 3*, pp. 249–268.

Sawford, B.L. 1985. Concentration statistics for surface plumes in the atmospheric boundary layer. *Seventh Symposium on Turbulence and Diffusion* Boston MA: American Meteorology Soc. pp. 323–326.

Shapiro, A. H. 1953. *The Dynamics and Thermodynamics of Compressible Fluid Flow, Vol I.* New York: John Wiley & Sons. 647 pp.

Sherman, M.H. 1980. *Air Infiltration in Buildings.* University of California: Ph.D. Dissertation, also Lawrence Berkeley Laboratory Report LBL-9162. 1v. various foliations

Sherman, M., D. Wilson, and D. Kiel. 1984. *Variability in Residential Air Leakage.* Lawrence Berkeley Laboratory, Report LBL-17587. 25 pp.

Singh, Jasbir, Leslie Cove, and Mark McBride. 1990. Loss of contaminant—some practical aspects in consequence prediction. *Jour. Loss Prev. Process Ind., 1990, Vol. 3, January*, pp. 146–149

Smith, F.B. 1965. The role of wind shear in horizontal diffusion of ambient particles. *Quart. Jour. Roy. Met. Soc., 91*, 318-329

Smith, M.E. 1984. Review of the attributes and performances of 10 rural diffusion models. *Bull. Meteor. Soc., Vol. 65, No. 1*, pp. 27–36.

Spicer, T. and J. Havens. 1989. *User's Guide for the DEGADIS 2.1 Dense Gas Dispersion Model* Cincinnati OH: Report EPA-450/4-89-019, U.S. Environ. Protection Agcy. 1v. (various pagings).

Streeter, V. L. and E.B. Wylie. 1985. *Fluid Mechanics.* McGraw-Hill. 586 pp.

Sutton, O.G. 1932. A Theory of Eddy Diffusion in the Atmosphere. *Proc. Roy. Soc. (London), Ser A., Vol. 135*, pp. 143–165

Thibodeaux, L.G. 1979. *Chemodynamics: Environmental Movement of Chemicals in Air, Water, and Soil.* New York: John Wiley and Sons. 501 pp.

Turner, D. Bruce. 1970. *Workshop on Atmospheric Dispersion Estimates.* U.S. Dept of Health, Education, and Welfare, Public Health Service, Report PB-191 482 (also available through NTIS, Springfield, VA). 84 pp.

Turner, D. and Lucille W. Bender. 1986. *Description of UNAMAP (Version 6).* Springfield VA: National Technical Information Service. 13 pp.

U.S. Coast Guard 1985. *Chemical Hazard Response Information System (CHRIS)—Hazardous Chemical Data.* Washington, D.C.: U.S. Coast Guard, U.S. Government Printing Office. 2265 pp.

U.S. Department of Transportation. 1984. *1984 Emergency Response Guide Book.* Neenah Wisconsin: JJ. Keller & Assoc. 91 pp.

U.S. Department of Transportation. 1989. *Handbook of Chemical Hazard analysis Procedures. (ARCHIE Manual).* Washington, DC: U.S. Department of Transportation, U.S. environmental Protection Agency, and Federal Emergency Management Agency. Publications Office. 251 pp.

U.S. Environmental Protection Agency. 1986. *Chemical Profiles—Chemical Emergency Preparedness Program.* Washington, D.C.: U.S. EPA, U.S. Government Printing Office 1458 pp.

U.S. Environmental Protection Agency. 1987. *On-Site Meteorological Program Guidance for Regulatory Modeling Applications.* Washington, D.C.: Report EPA-450/4-87-013, U.S. Environmental Protection Agency. 174 pp.

van Ulden, A.P. 1974. On the Spreading of a Heavy Gas Released Near the Ground. *First International Loss Prevention Symposium, Delft, The Netherlands, May 1974.* Amsterdam: Elsevier Scientific Publ. Co. pp. 28–30.

van Ulden, A.P. 1983. *A New Bulk Model for Dense Gas Dispersion: Two-Dimensional Spread in Still Air.* Delft, The Netherlands: I.U.T.A.M. Symposium on Atmospheric Dispersion of Heavy Gases and Small Particles.

Wieringa, J. 1980. Representativeness of wind observations at airports. *Bull. Amer. Meteor. Soc., Vol. 61, No. 9*, pp. 962–971.

Wilson, D. 1979. *The Release and Dispersion of Gas from Pipeline Ruptures.* Alberta Environment Research Report, Contract 790686. 91 pp.

Wilson, D.J. 1981a. *Expansion and Plume Rise of Gas Jets from High Pressure Pipeline Rup-*

tures. Alberta Environment Research Report, Contract 810786 (reissued April 1986). 61 pp.

Wilson, D.J. 1981b. Along-wind diffusion of source transients. *Atmospheric Environment, Vol. 15,* pp. 489–495

Wilson, D.J. 1987. Stay indoors or evacuate to avoid exposure to toxic gas? *Emergency Preparedness Digest,14, No. 1,* pp. 19–24.

Wilson, D.J. 1989. Personal communication, letter dated 28 April, 1989, 3 pp.

Wilson, D.J. 1990a. *Model Development for EXPOSURE-1 and SHELTER-1: Toxic Load and Adverse Biological Effects for Outdoor, Indoor, and Evacuation Exposures in Dispersing Toxic Gas Plumes.* Alberta Canada: Report 73, University of Alberta, Department of Mechanical Engineering. 55 pp.

Wilson, D.J. and B.W. Zelt. 1990b. *Technical Basis for EXPOSURE-1 and SHELTER-1 Models for Predicting Outdoor and Indoor Exposure Hazards from Toxic Gas Releases.* Alberta Canada: Report 72, University of Alberta, Department of Mechanical Engineering. 50 pp.

Wilson, D.J. 1991. Accounting for Peak Concentrations in Atmospheric Dispersion. In *International Conference and Workshop on Modeling and Mitigating the Consequences of Accidental Releases of Hazardous Materials.* New York: American Institute of Chemical Engineers, 385–395

Wyngaard, John C. 1985. Large-eddy simulation in small-scale meteorology. *Seventh Symposium on Turbulence and Diffusion* Boston MA: American Meteorology Soc. pp. 339–341.

Yamartino, R.J. 1984. A comparison of several "single-pass" estimators of the standard deviation of wind direction. *Journal of Climate and Applied Meteor., Vol. 23, No. 9,* pp. 1362–1366.

Zelt, B.W. and D.J. Wilson. 1990. *User's Manual for EXPOSURE-1 and SHELTER-1 Software for Toxic Gas Exposure Hazard Estimates.* Alberta Canada: Report 74, Univ. of Alberta Dept. Mech. Engr., Alberta Occupational Health and Safety Research Grant 86-62-RB. 25 pp.

Index